Natural disturbance regimes in the Biosphere Reserve Nevados de Chillán – Laguna del Laja

Master thesis

Thomas Häfelfinger
Davos, 24.07.2015

Supervisors :
Dr. Peter Bebi

Dr. Alejandro Casteller

SLF

WSL

ETH
Eidgenössische Technische Hochschule Zürich
Swiss Federal Institute of Technology Zurich

Table of content

List of illustration and tables

Abstract

Natural hazards endanger infrastructure and human lives in many parts of the world. Historical events are often poorly documented and information about spatial and temporal patterns are missing. In order to design detailed hazard maps and asses future risk, accurate information about the frequency and spatial extent of disturbances is necessary. This master thesis aimed at working towards a hazard maps and improved knowledge on forest-avalanche interactions for the region of Nevados de Chillán (Chile), an area undergoing fast economic development but where only few information about natural hazards exist.

After detecting and delineating different disturbances with remote sensing data, forest structure and age distribution of avalanche and debris flow disturbed forest stands as well as undisturbed control stands were investigated. Collected tree-ring data allowed to reconstruct spatial and temporal patterns of debris flows and avalanches. These information are combined with avalanche simulations to define release areas of avalanches. Avalanches with a return period of 10 and 100-year were simulated with the new forest module of the avalanche simulation software RAMMS to show and quantify the protective effect of forests against avalanches. Avalanches are the most frequent and nowadays spatially most important disturbance regime in the area. Avalanches and debris flows lead to a reduction of canopy density, tree density and age of the forest. However, no such influence could be detected with regard to tree diameter. Tree heights are reduced in avalanche disturbed forests significantly, but increased in forests disturbed by debris flow compared to not disturbed forests. Trees provide valuable information about the event history. Avalanche and debris flow events occur particularly frequent, most intensively in 1995 and 2000 with detected avalanches and debris flows in many tracks. The combination of avalanche simulations with dendrogeomorphic information can provide relatively reliable information on potential release areas for avalanches. For tracks without specific dendrogeomorphic information, release areas were based on avalanche simulations, existing pictures, observations and the interpretation of flow directions and the runout extent. Comparing avalanche events with a return period of 10 and 100-year revealed that more avalanches reach the road with a higher pressure and flow height. Also the spatial extent of these rare events is larger. Simulations without forests showed that forest reduces the impact pressure and flow height on the road and walking path, as well reduce the spatial extent of the runout. Scenarios with additional afforestations suggest that such measures would contribute to lower maximum pressures and reduced avalanche frequencies on transportation lines, but cannot avoid that avalanches reach the road. In areas where information about past avalanches is missing, the combination of avalanche simulations with dendrochronological methods is helpful for the assessment of the risk and should be tested in other afforested areas in the world.

1 Introduction

1.1 Research gap

In mountain areas, human settlements and infrastructure are commonly endangered by natural disturbances like avalanches, debris flows, rockfalls and landslides. Disturbances are poorly documented in many areas of the world and no data about historic events is available (e.g. Casteller et al., 2008). Information about the spatio-temporal pattern of disturbances is necessary for the reconstruction of historic events (Stoffel and Bollschweiler, 2008). The documentation of geomorphic processes and their related natural disasters is important for risk assesments (Stoffel and Huggel, 2012). The same holds true for the present study in Nevados de Chillán, Chile. A unique place in South America where poorly documented disturbances - in this case especially avalanches - broadleaved forest as a effective risk reduction and protection measurement are present, as well as endangered human infrastructure and settlement occur in the same place.

This study is part of the EPIC-project[1], which is being implemented by the International Union for Conservation of Nature (IUCN) and several local partners. The project is funded by the International Climate Initiative (ICI) of the German Federal Ministry for Environment, Nature Conservation, Building and Nuclear Safety (BMUB). The goal of the project is to show how healthy ecosystems can help to improve livelihood resilience and contribute to reduce impacts of natural hazards. In addition, the project aims at demonstrating how improved ecosystem management can reduce the risk of disasters and help to adapt to climate change (Cordero et al., 2014). A further goal is to analyze and quantify the empirical and economic value of the ecosystem for climate change adaptation and risk reduction. Depending on the research site, the focus lies on a different hazard. In Chile the main focus is on avalanches and how protective forests can be used for cost-effective avalanche risk management. A further aim of the project is to develop management strategies for different mountain forest ecosystems to reduce the risk of natural disasters (Cordero et al., 2014).

An important function of forests in mountainous regions is to protect infrastructure and people against natural hazards (Brang et al., 2006). Forests have an important protective function against avalanches. Avalanches can break tree stems, as well as uproot and overturn trees (de Quervain, 1978; Bartelt and Stöckli, 2001). For large avalanches (> 60000 m^3), which start far above the treeline, forests have only a marginal influence on the kinetic energy and runout extent of the avalanche (Bartelt and Stöckli, 2001; Teich et al., 2012). In the case of small (5000-25000 m^3) to medium sized (25000-60000 m^3) avalanches however, forests can extract snow from the avalanche through depositon of snow behind trees and increase friction parameters. The breaking of trees results in a reduction of kinetic energy. These processes reduce the speed of avalanches and contribute to stop the avalanche, which can shorten the

[1] EPIC stands for Ecosystems Protecting Infrastructure and Communities.

runout extent (Feistl et al., 2015). Forest parameters, such as stand composition, structure, stem density, wooden debris and ground vegetation influence the spatial extent of small and medium sized avalanches (Teich et al., 2012). Apart from slowing down and stopping avalanches, forests stabilize the snowpack in potential release areas and thus help to prevent avalanche initiation (Bebi et al., 2009). For the protection of infrastructure and settlements against avalanches, forests are the cost-efficient protection measure (Olschewski et al., 2012). Besides of the protective function of forest against natural hazards, trees are a natural archive of past events and provide valuable information about the spatial and temporal extent of past geomorphic processes.

1.2 Dendrogeomorphology

Dendrogeomorphology is the research of geomorphic processes through growth anomalies in trees (Alestalo, 1971). This research field arose in the 1970s and is under permanent advancement (e.g. Alestalo, 1971; Shroder, 1978; Butler, 1987; Stoffel and Bollschweiler 2008). Dendrogeomorphology is a widely accepted approach to describe the historical occurence of geomorphic processes (e.g. Stoffel et al., 2013; Stoffel and Corona, 2014). The approach was already used in the Patagonian Andes for several tree-ring studies to detect past avalanche activity. Studies focusing on broadleaved species became more popular over the last years (e.g. Mundo et al., 2007; Casteller et al., 2008; Arbellay et al., 2010; Casteller et al., 2011; Arbellay et al., 2013). A “process-event-response”-concept is the basis of this research (Shroder, 1978). Trees show specific responses[2] and can react to geomorphic processes in the following way. The partial removal of bark and wood-penetrating injuries cause a local destruction of the cambium (Lundström et al., 2009). Trees react to injuries by compartmentalizing the wounds (Shigo, 1984) and start to produce callus tissues to overgrow the wounds with cambium cells (Schweingruber, 2001). The reactions of trees are typically caused by the impact of broken trees and rocks, which are incorporated in the avalanche (Burrows and Burrows, 1976). Tilting and inclination of a stem can be caused by landslide activity or the induced pressure from material deposition of mass movement processes. Also the activity of avalanche snow and debris flow material can lead to tilting and bending of trees (Lundström et al., 2007, 2008). To regain their vertical position, broadleaved species produce tension wood (Westing, 1965) whereas conifers react with the formation of compression wood. The tilting of stems is dependent on the size and flexibility of the tree species. The formation of reaction wood typically leads to an eccentric growth, which allows to date disturbance events. Growth reductions are caused by burying of tree stems with depositing material from debris flows, landslides, floods or dirty avalanches. It can reduce the annual growth of trees by limiting

[2] In this context the word respond is used as a reaction of trees to geomorphic processes. The following information is based on studies for avalanches, floodings, landslides, rockfall and debris flows. In the context of dendrogeomorphic research the following remarks contain findings for broadleaved species as well as for conifers. This study focus on the detection of past avalanches and debris flows in broadleaved species.

water and nutrients supply due to the reduced activity of the roots (e.g. Hupp et al., 1987; Friedmann et al., 2005) or pressure on the cambium (Rubner, 1910). Removal of branches or decapitation of trees by geomorphic processes leads to a radial growth suppression of trees (Stoffel and Corona, 2014). The elimination of neighboring trees can result in a growth release of the survivor trees, which profit of less light competition and more available resources like water and nutrients (e.g. Bollschweiler and Stoffel 2010, Corona et al., 2012). Mass movement processes can eliminate entire forest stands. These destruction dates and the germination ages of new generations of trees in bare surfaces are also used to date disturbances (e.g. Winter et al., 2002; Bollschweiler et al., 2008; Reardon et al., 2008). Tracheid and vessel anomalies in the wood induced by wounds are characterized by smaller and more frequent vessels. No differences between injured and uninjured rings can be found for fiber and parenchyma cells (e.g. Arbellay et al., 2010; Arbellay et al., 2013). For mass movement processes, scars (injuries) are the most common growth disturbance (Stoffel et al., 2013). Additionally, growth releases and reductions were valuable for detecting past disturbance events. These responses of trees to disturbances can also be caused by processes like browsing, anthropogenic or climate disturbances. To be sure that these responses are caused by geomorphic processes, the study site has to be carefully analyzed for the occurance of geomorphic processes (Stoffel and Corona, 2014).

1.3 Aim of study and research questions

This study analyses the event history of avalanches and debris flows, which can reach the street and human settlements in Nevados de Chillán. In this and other studies (Casteller et al., 2008; Casteller et al., 2011) these dendrochronological investigations are combined with numerical models to reconstruct avalanche events. The simulation software RAMMS (Rapid Mass Movements) calculates mass movements in a three-dimensional terrain (Christen et al., 2010). In earlier times, the effect of forests in avalanche simulations was taken into account through increasing friction parameters (Bartelt and Stöckli, 2001). Nowadays, the new RAMMS version with the forest module considers also (i) the detrainment of snow, (ii) avalanche power reduction through tree destruction and (iii) variable friction parameters of different forest types (Feistl, 2015). In the study area and in many other parts in the southern Andes there is a lack of information about input parameters for avalanche simulations, like snow heights, precise location and size of release areas (Leiva et al., 2007). To overcome these restrictions, different avalanche simulations were done and adapted to define appropriate release areas. The results of avalanche simulations are combined with dendrogeomorphic information. To combine avalanche simulations with dendrochronological information about runout distance, the maximum pressure has to be defined in which trees respond to avalanches. Tiri (2009) showed that broken and uprooted trees were exposed to impact pressures up to 400 kPa. With larger

diameters at breast height[3], the chance to break or uproot trees is smaller. In the literature, critical pressure forces for a tree to break are specified for flow avalanches with 10-50 kPa and for powder snow avalanches between 3-5 kPa (Margreth, 2008). To detect past events and to show how ecosystems can help to reduce the impact of natural disturbances the following research questions are answered:

Question 1: What is the influence of avalanches and debris flows to the structure of forest?

Hypothesis 1.1: The canopy density is lower in forests which are influenced by avalanches and debris flows. Also the tree density is lower in forests where these natural disturbances play an important role.

Hypothesis 1.2: Trees in avalanche and debris flow tracks have a smaller DBH than trees in unaffected forests.

Hypothesis 1.3: The tree species distribution changes in tracks where avalanches or debris flows occur.

Hypothesis 1.4: Avalanches and debris flow events can destroy the forest. In that case the regrowth forest is younger than the unaffected forest.

Question 2: Scars and abrupt growth changes in the wood of trees indicate avalanche events.

Hypothesis 2.1: Avalanche years are clearly visible in the wood and happen frequently.

Question 3: How can potential release zones be defined based on topographical settings, historical records, simulation results and evidence from tree-ring samples?

Hypothesis 3.1: A sensitivitiy analysis with simulation results based on different RAMMS-input parameters (snow depth and release area) and a comparison with historical records and evidence from tree-ring samples allow to determine plausible release areas and RAMMS-input parameters.

Question 4: What is the influence of the forest on avalanche runouts?

Hypothesis 4.1: Forests can reduce the runout extent of avalanches.

Hypothesis 4.2: Afforestations can prevent avalanches.

[3] In the following the abbreviation DBH is used. Measured at 1.3 meter above the ground.

2 Material and methods

2.1 Investigation area

The investigation area is located in the Bíobío Region (VIII Region) of Chile and belongs to the northern part of Patagonia in the Central Chilean zone (Cordero et al., 2014). It is part of the Nevados de Chillán volcanic complex, which is located in the transition zone of the Biosphere Reserve Nevados de Chillán – Laguna del Laja. The Nevados de Chillán site has a high richness of wildlife and flora. The presence of the Patagonian huemul (*Hippocamelus bisulcus*) and other rare species, as well as the high genetic diversity leads to a high priority of conservation (UNESCO, 2011). The area is under high economic development (Pfanzelt et al., 2008). New constructions expose the infrastructure and settlements to natural disturbances and lead to endangering of parts of the native vegetation.

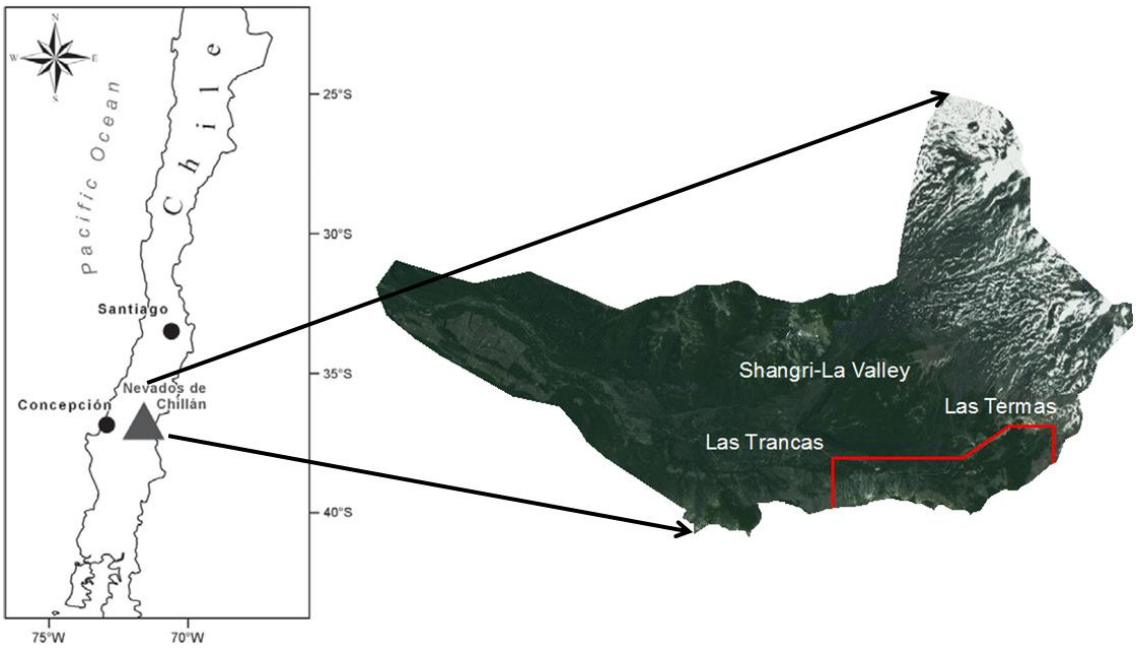

Figure 1: Location of the investigation area (adapted from Pfanzelt et al., 2008). The red line shows the area where disturbances can affect the road to Las Termas and where most analysis were done.

The investigation area is located in the following coordinates:

- East: 71°22'00" W, 36°52'34" S
- West: 71°37'48" W, 36°52'01" S
- North: 71°06'46" W, 36°21'25" S
- South: 71°25'52" W, 36°52'01" S

The investigation area inludes an area of 221 square kilometers. The lowest point is 744 m.a.s.l and the highest point is 2526 m.a.s.l. The investigation area is located between the temperate

and mediterranean macrobioclimates (Luebert and Pliscoff, 2006). The climate of Nevados de Chillán is characterized by dry summers and cold winters. Over 75% of the annual precipitation fall in the southern winter between April and September (Donoso, 1993).

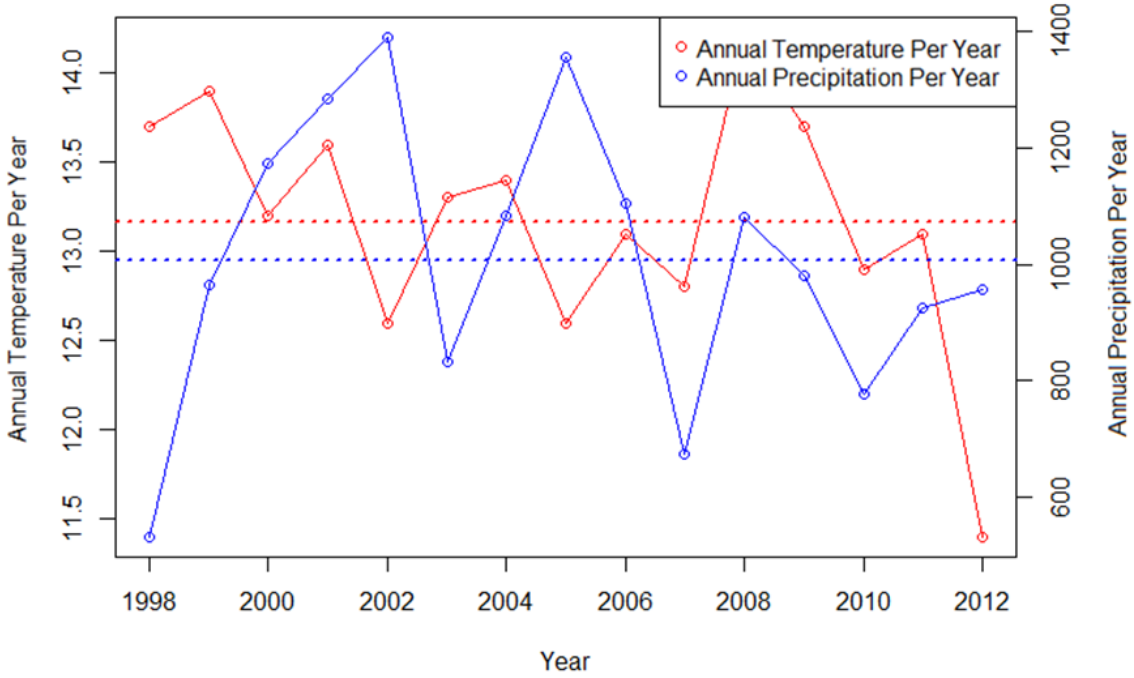

Figure 2: Weather data from station located at Las Trancas.

Climate data from a weather station located in Las Trancas show that mean annual precipitation between 1998 and 2012 was 1007 mm. The mean annual temperature in this time period was 13.2 degrees (Fig. 2)[4]. Specific data about snow heights and extreme snowfall events are missing. In the investigation area we can find a high diversity of geological substrates, which is caused by a high volcanic activity. The Nevados de Chillán volcano consists of the Cerro Blanco and Las Termas subcomplex, which were formed about 40000 years ago. In total there are 13 cones. The first recognized eruption was about 640000 years ago. The newest small eruptions occurred in 1973 and 2003. Due to the exposure of tourist facilities, the Nevados de Chillán volcano is categorised as one of the vulcanos with the highest damage potential in whole Chile (Dixon et al., 1999). Out of these multivariate geological substrates characteristic soils are formed. These soils are classified as inceptisols and are developed out of these volcanic products (Freiberg, 1984). The high diversity of geological substrates leads to different vegetation units. Pflanzelt et al. (2008) describes 11 different vegetation units in the region. In the main investigation area, where the analysed avalanche and debris flow tracks are located, the following vegetation units were found. Close to the riverbed in humid localities *Nothofagus dombeyi (Mirb.) Oerst.* forests can be found. The other parts of the forest are mixed forest stands with *Nothofagus dombeyi, Nothofagus pumilio (Poepp. & Endl.) Krasser and Nothofagus*

[4] The data was kindly provided by Departamento de Recursos Hídricos de la Facultad de Ingeniería Agrícola UdeC-campus Chillán, in English: Department of Water Resources of the Agricultural Engineering Faculty, University of Concepción-campus Chillán.

obliqua (Mirb.) Oerst.. The non-afforested part belongs to the *Chusquea culeou-Coirones* assemblage with the dominant representative species *Chusquea culeou Desvaux.* On the ridge some *Nothofagus pumillio* krummholz vegetation can be found.

2.2 Remote sensing analysis

For an overview of the disturbances in the investigation area, all disturbances were mapped with remote sensing data. According to other dendrogeomorphic studies, the identification of geomorphic processes starts with remote sensing data (Stoffel and Bollschweiler, 2008; Stoffel et al., 2013). The procedure of mapping natural disturbances via remote sensing data is divided in 2 stages:

1. First mapping before fieldwork: This step is based on the interpretation of aerial images (e.g. Bebi et al., 2001; Kulakowski et al., 2003; Veblen et al., 1994). The Google Earth image and the ArcGIS Basemap were the basis to map the visible disturbances. Further data exists, but were not used due to the bad resolution.
2. Second mapping after fieldwork: Out of field observations, information from local stakeholders, digital terrain model and newly generated drone images, new disturbance polygons were created and existing ones reshaped.

The fieldtrip was used for the detection and verification of different disturbances. Different site inspection and walks to the forest structure plots were used to detect new disturbances and verify the position of the already detected ones. Several GPS-points (model: GPSMAP® 64s) were taken to map the extent of runout zones and verify the spatial extent of the forest cover and settlements. Jaime Soto and Leandro Olivares from the company Geoespacio generated a high resolution aerial image and a digital terrain model with their drone. Further information from former field surveys and site inspections helped to draw different disturbances. It is distinguished between mud avalanches, debris flows, avalanches, landslides and rockfall disturbances with their criterias (Table 1). For the avalanche simulations and the survey of the investigation area, the forest extent and extent of settlements were also depicted. All spatial analysis and interpretation of aerial images was made in ArcMap 10.2 (ESRI, 2013). Additionally Google Earth images were used to display the information and as a basis for the interpretation of aerial images.

Table 1: Categories of disturbances, mapped settlements and forest extent in the investigation area.

Mud Avalanche	In this case avalanches are released due to hydrothermal activity of the ground and snow is mixed with the soil beneath (Dixon et al., 1999).
Debris Flow	It is defined as a rapid flow of saturated non-plastic debris in a steep channel (Jakob, Hungr, & Jakob, 2005).
Snow Avalanche	Avalanches are mass movements which transport snow from a release area to a runout (Föhn, 1993). Powder snow and wet snow avalanches are observed in the investigation area (Gustavo Aldea, personal communication, 25.02-8.03.2014)
Landslide	A landslide is defined as the movement of a mass of earth, rock or debris down a slope (Cruden, 1991).
Rockfall	Rockfall is defined as the falling of a newly detached mass of rock from a cliff or down a very steep slope (Colorado Geological survey, 2015).
Settlement	All houses and infrastructure (ski station, antenna, thermal spa and parking site) are summarized in the settlement layers. Objects, which are closer than 100 meters to each other are classed as a group.
Forest	Avalanche releases in forest gaps are possible. The critical length of forest gaps varies between 20 and 200 meters (Bebi et al., 2009). Single trees with a distance of more than 20 meter to each other are not considered as forest.

2.3 Fieldwork

The aim of the field trip from 12 to 25 February 2015 at Nevados de Chillán was the evaluation of the forest structure and collecting information about former and present disturbances. The forest age and structure was evaluated in specific plots. These plots were preselected before the fieldtrip in a specific target design: in each disturbance patch where forest occurs and also in each forest stand between two disturbances without signs of disturbances, a forest plot was created[5]. The plots were selected randomly in ArcMap 10.2 with the newly mapped forests and an existing disturbance map from previous fieldrips (ESRI, 2013).

[5] In the following the term “disturbed forest plot” is used for the forest structure plot with disturbances. For forest structure plots without disturbances the term “control plots” will be used.

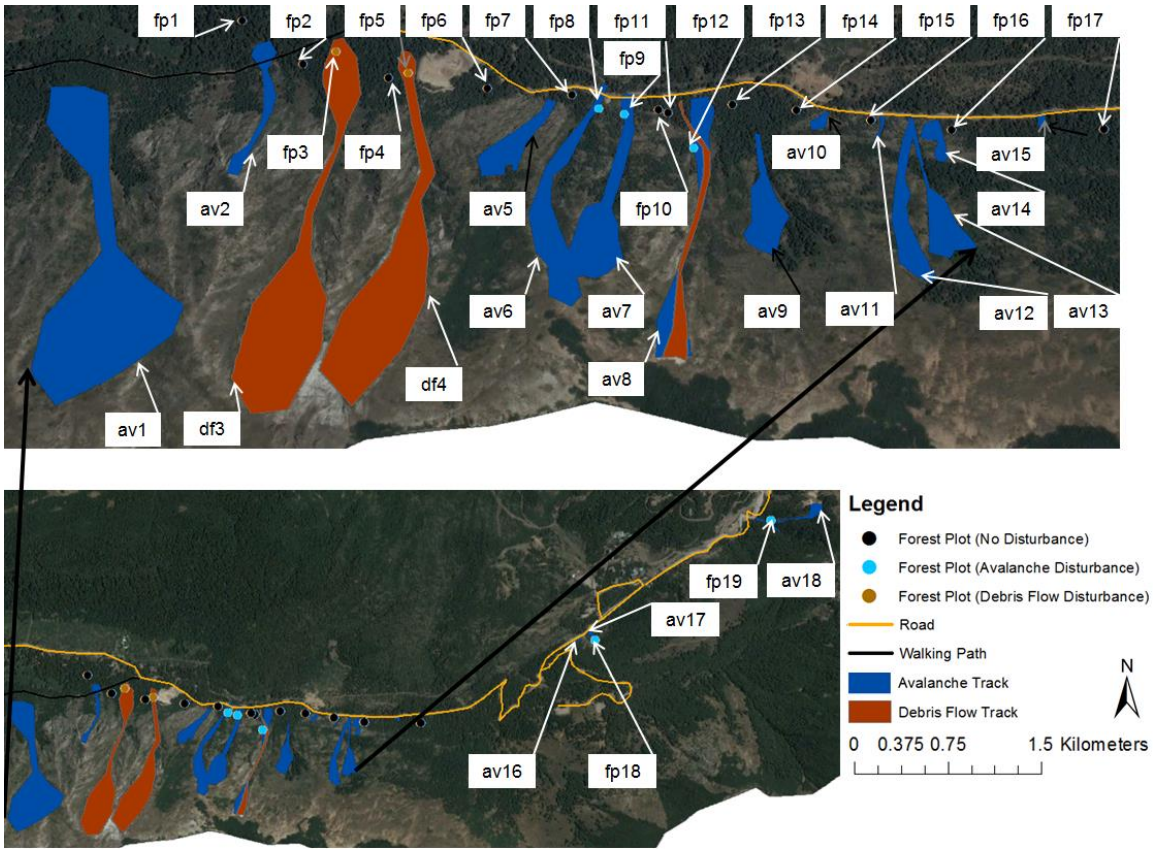

Figure 3: Location and labeling of forest plots and disturbance tracks after the remote sensing data work. The main settlement and tourist facilities are located between avalanche track 16 (av16) and avalanche tack 18 (av18).

For each forest structure plot a second possible position was selected in case the first point did not represent the area and their surrounding or if the first point was not accessible. These points were located with a GPS device (Model: GPSMAP® 64s) in the field. The following parameters with the specific categories were recorded in these forest structure plots (Table 2). The investigation area of each plot was a 10 meter radius of the center point. In some plots it was necessary to shrink the radius to 5 meters, because of on-site observed dense bamboo layer in the forest.

Table 2: Parameters and their categories for the description of forest plots.

Parameter	**Categories**
Terrain roughness	Qualitative descripition: flat, steep or broken
Canopy density of prevailing trees	10,20,30,40,50,60,70,80,90,100% According to Keller (2013) only trees from the prevailing layer were considered.
Shrub layer	1=bamboo, 2= no bamboo
Density of shrub layer	1=continous, 2=grouped, 3=dispersive
Height of shrub layer	In 0.5 meter steps
Slope angle	[°]

For each tree with a DBH > 8cm the following additional parameters were recorded (Table 3).

Table 3: Parameters and their categories for the recorded trees in the forest structure plots.

Parameter	**Categories**
Species	1=N.dombeyi, 2=N. obliqua, 3=N. pumilio, 4=Adesmia microphylla Hook. & Arn.
Diameter	[cm]
Height	[m]
Social status	1=dominant, 2=co-dominant, 3=supressed
Comments	Abnormalities like scars, broken stems etc.

Additionally to the forest structure parameters, at least 5 trees were cored in each plot to determine the age of the stands[6]. In disturbed forest plots, the increment cores were analysed to detect past events. All trees were selected randomly. For that, the number of trees, which had to be cored was estimated (for example: 15 trees estimated, for that every third tree had to be cored so that at least five trees were sampled). The first tree was normally located in the downslope direction and the sampling procedure continued clock-wise. Only one core per tree was taken. Increment corers from the company Haglöfs (width 0.5 cm) were used to core trees. Trees were typically cored in perpendicular direction to the slope at the DBH-level. In each plot, 4 pictures (north, east, south and west direction) were taken for the documentation.

During the previous fieldtrip in 2014 (25.02-8.03) trees were cored with a different sampling strategy. The aim of the 2014 fieldtrip was to reconstruct the spatial extent and temporal pattern of past snow avalanches and debris flow events. Trees which showed visible damage (scars, broken stems, broken branches and uprooted trees) of past disturbances were cored in this case[7]. Up to four cores per tree were obtained, depending on each particular tree. In cases where scars were visible on the trees, cores were obtained near the scars. Multiple cross-sections were taken at the height of the scar from selected dead trees with visible damage from past events. For each sampled tree, additional information was recorded such as DBH, height, social status, pictures and location of the scars along stems and branches. Because all these trees still have a protective function and reduce the risk for geomorphic processes, cores were extracted with an increment borer (Stoffel et al., 2006). Only from dead trees at a DBH-level some cross-sections were taken.

[6] Term “forest structure sampling strategy” is used in the text to describe this particular sampling strategy.
[7] Term “runout sampling strategy” is used in the text to describe this particular sampling strategy.

Table 4: Overview of collected tree-ring samples from the fieldtrips in 2015 and 2014.

Code	Sector	Cores [n]	Cross-sections [n]	Year of collection	Purpose
Fp 1	Unaffected forest	6	0	2015	Age measurement
Fp 2	Unaffected forest	5	0	2015	Age measurement
Fp 3	Debris flow runout	5	0	2015	Age measurement, disturbance history
Fp 4	Unaffected forest	5	0	2015	Age measurement
Fp 5	Debris flow runout	6	0	2015	Age measurement, disturbance history
Fp 6	Unaffected forest	5	0	2015	Age measurement
Fp 7	Unaffected forest	5	0	2015	Age measurement
Fp 8	Avalanche runout	5	0	2015	Age measurement, disturbance history
Fp 9	Avalanche runout	5	0	2015	Age measurement, disturbance history
Fp 10	Unaffected forest	6	0	2015	Age measurement
Fp 11	Unaffected forest	5	0	2015	Age measurement
Fp 12	Avalanche runout	4	0	2015	Age measurement, disturbance history
Fp 13	Unaffected forest	5	0	2015	Age measurement
Fp 14	Unaffected forest	5	0	2015	Age measurement
Fp 15	Unaffected forest	6	0	2015	Age measurement
Fp 16	Unaffected forest	5	0	2015	Age measurement
Fp 17	Unaffected forest	6	0	2015	Age measurement
Fp 18	Avalanche runout	6	0	2015	Age measurement, disturbance history
Fp 19	Avalanche runout	5	0	2015	Age measurement, disturbance history
Av 6	Avalanche runout	121	5	2014	Age measurement, disturbance history
Av 9	Avalanche runout	73	9	2014	Age measurement, disturbance history

All data from the forest structure plot were analyzed with the statistic software R (R Development Core Team, 2015). To test the significance of the results, a two-sample Wilcoxon test was performed, because the data do not have normal distribution. The non-parametric test classifies the data by their rank (Dalgaard, 2008). Specific adaptions have to be done in several parameters to have the same basis for comparison. The tree density illustrates the tree density per hectare. For the comparison individual slope angles and plot radii were removed. To have comparable standards, a flat area with a slope angle of 0° and an area of one hectare were computed. For the tree species distribution the percentage of each species per plot was calculated.

2.4 Dendrochronology work

These subchapters describe the procedure of detecting former disturbance events and the age of trees. The first chapter describes the preparation of the samples. Furthermore, the method to define the age of trees is explained, before the method to detect former avalanche and debris flow events is described.

2.4.1 Preparation of the samples

The following steps were performed to prepare the samples for further analysis. In the laboratory the samples were glued on a piece of wood, which was labeled with the respective sample code. Once the samples were dry, they were polished with five increasing granularities of sand papers (i.e. 100, 220, 320, 500, 600) until the ring borders were clearly visible. The next step was the counting of year rings. Due to the hard visibility of rings, ring borders were marked in many cases with a thin pencil line. Decades were marked with one dot, whereas every fifty (e.g. 1950) and hundred years (e.g. 1900) were drawn two and three dots, respectively (see examples in figure 4).

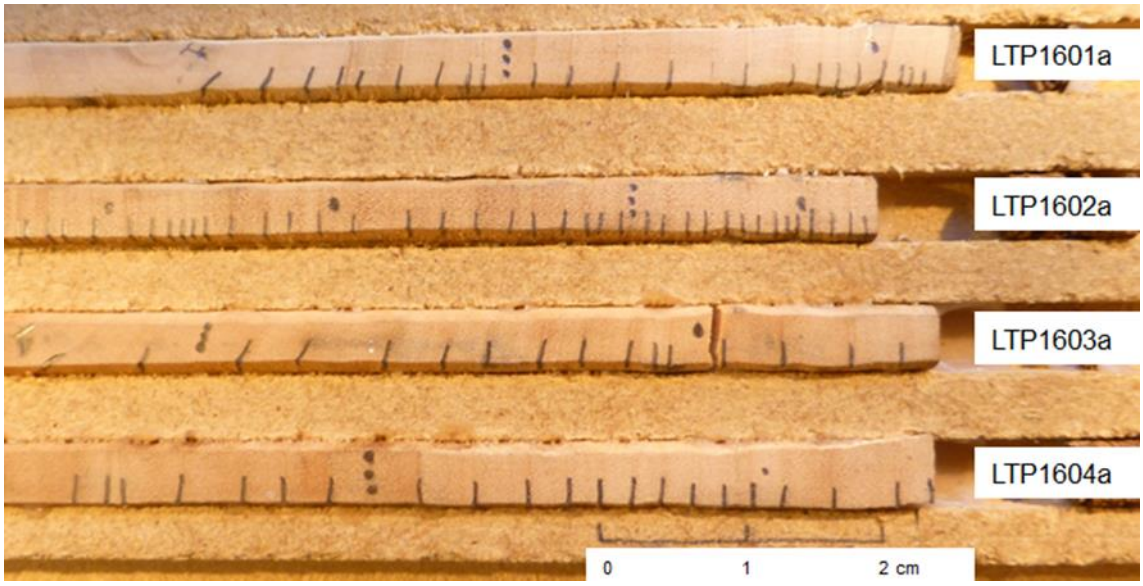

Figure 4: Example of marking dots in the cores from forest plot 12 (fp12). The bark is located in all cores on the right hand side. The pith is only visible in sample LTP1601a. The year 2000 (marked with three dots) is wide in all samples.

After polishing the cores from the control plots (fp1, fp2, fp4, fp6, fp7, fp8, fp13, fp14, fp15, fp16 and fp17) were ready to detect the age of trees. In all samples where former disturbance events should be detected the following step was necessary (fp3, fp5, fp8, fp9, fp12, fp 18 fp19, av6 and av9). Forest structure plot number 10 and 11 were used as a reference chronology and followed the same procedure. For the purpose of detecting past events, year-ring widths were measured with the measuring system LINTAB (RINNTECH, Germany). The rings were measured from bark to pith. For *Nothofagus* trees it was sometimes quite hard to recognize the year ring border. To be sure that the ring indicates the right calendar year, the software

COFECHA (Holmes, 1983) was used. It helps to detect assumed and missing rings. With this software it is possible that all cores are dated in the right way and the year rings indicate the correct year. Once conducted the previous steps of tree age determination, the samples were ready to determine the age of trees and the detection of former avalanche and debris flow events.

2.4.2 Procedure of detecting the age of trees

In all forest structure plots, the age of a core was counted to make statements over the age structure of the forest. In some cores the pith was missing. These missing rings had to be calculated. For that purpose, templates with circles of various diameters were used, to define the amount of missing rings to the pith (Bräker, 1981).

2.4.3 Procedure of detecting former events

In the past, different studies have used dendrogeomorphic analysis to reconstruct temporal patterns of snow avalanches (e.g. Casteller et al., 2008; Corona et al., 2012; Potter, 1969). Although a lot of dendrogeomorphic papers have been published in the last years and the applications of the method is well established, no standardization procedure with general thresholds exists (Butler and Sawyer 2008; Stoffel and Corona, 2014). A detailed list of investigations that used dendrochronology for the reconstruction of avalanche histories can be found in Corona et al. (2012). In our investigation, scars, growth releases and growth decreases were used for the tree-ring reconstruction of avalanches. In this procedure all cores were checked from pith to bark visually with the binocular to identify scars and abrupt growth changes. Growth reactions were grouped in three different categories (adapted from Dubé et al. (2004), Reardon et al. (2008) and Stoffel and Corona (2014)):

- class A: abrupt change in radial growth, strong impact where at least 5 rings are affected
- class B: abrupt change in radial growth, strong impact where one ring is affected
- class C: abrupt change in radial growth, weak impact where one ring is affected

All years were compared with the previous three to five years. An abrupt growth change was defined if the variation was larger than 50%. Additionally cell and color changes were registered, but not used to detect former events. A cell change was marked if there were unusual changes in the cell type and structure within the ring. Color changes are transitions between darker and brighter cells. The color changes between heartwood and sapwood is not mentioned.

Figure 5: Tree of cross-section LTA568 in avalanche track six (av6) to detect avalanche years. The white arrow indicates the scar.

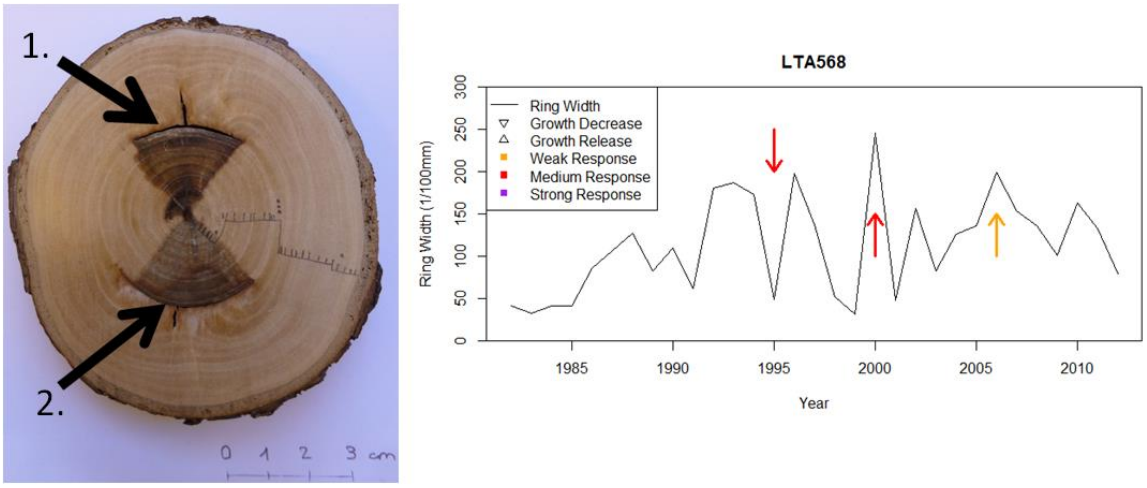

Figure 6: Example of a scar of cross-section LTA568. Arrow number one indicates a scar in the upslope direction, which is caused by transported material in the avalanche. For the scar in arrow number two, it is hypothesized that it was caused by another tree during tilting. The graph on the right side shows the ring width per year which is marked in the cross-section with a pencil. 1995 was a year with a medium growth decrease. The scars in the year 2000 indicate a medium growth release. In the year 2006 the tree responded to the avalanche with a medium growth release.

A literature research showed that in former studies the expert and indices approach were used for the reconstruction of avalanches using tree-rings. The expert approach is a semiquantitative analysis and is based on careful site selection (Stoffel and Corona, 2014). The selection of past events requires trees in the same spatial area, which show growth disturbances simultaneously. These growth disturbances are based on geomorphic activity (e.g. Stoffel et al., 2006; Bollschweiler et al., 2007). No fixed threshold of reacting trees is defined. The different cores are compared to each other and to define a disturbance year, also late event responses are

considered. In the expert approach, the comparison of scars and growth responses of trees in one plot and across all plots with the same disturbance allows to detect past disturbance events. The idea of the indices approach goes back to the work of Shroder (1978). An index value (It) is calculated on the base of the ratio between reacting and sampled trees (Butler and Sawyer, 2008). All years with an index value higher than a fixed threshold are identified as possible event years. For the comparison of the two approaches, in avalanche track 9 (av9) the calculations of the avalanche reconstruction are also made with the indices approach. The index value It is a ratio between responding and sampled trees (Corona et al., 2012).

$$It = \left(\sum_{i=1}^{n} (Rt) / \sum_{i=1}^{n} (At) \right) * 100 \quad (1)$$

R represents trees responding to a disturbance in year t. A is the number of sampled trees. The index values per year are displayed in a bar chart. The data from the growth responses are summarized in an event response histogram (Dubé et al., 2004; Reardon et al., 2008). The calculations are performed with the software R (R Development Core Team, 2015). Additionally to the index value a minimum number of responding trees has to be defined. The combination of the index value (It) and the minimum number of responding trees identifies past event years.
In all disturbed forest plots (fp3, fp5, fp8, fp9, fp12, fp 18 fp19) and runouts of avalanche track six and nine (av6 and av9), the expert approach is used to detect past avalanches.

Due to different different sampling strategies, it was necessary to apply slightly different procedures to detect the avalanche years. In disturbed forest plots where the forest structure sampling strategy was conducted, four to six different cores were extracted from different trees. In each plot, the disturbance history was reconstructed with the expert approach. An avalanche or debris flow year was defined if at least one of these growth disturbances were visible:

- one scar
- at least two growth responses with class C (also class A/B possible)
- one growth response with class A

Late growth responses up to several years after an event are also possible (Stoffel and Bollschweiler, 2008). This implies that also the growth responses of consecutive years have to be compared to the following years. With the visual inspection of the increment rings it was not possible to distinguish between different geomorphic processes. A detailed site inspection is necessary to define the processes which cause the disturbance (Stoffel and Corona, 2008). According to Stoffel et al. (2013) it is possible to distinguish snow avalanches and debris flow processes with the timing of the reaction. The reaction from snow avalanches can be found at the boundary of two rings. Debris flows, which occur normally in the summer, show reactions between the earlywood and latewood (Stoffel et al., 2006). In the investigation area it was not possible to distinguish between avalanche and debris flow events using tree-ring methods

because both processes occur typically in the same time period (winter), when most of the precipitation occurs.

In the runout of avalanche track 6 and 9 (av6, av9), where the runout sampling strategy was carried out, the reconstruction of the avalanche history was slightly different. In these tracks between one and four cores were taken per tree. To compare the responses of the different trees among each other, each tree needs the similar weigthed response. Trees with one core should show a similar weighted response as trees from which four cores per tree were extracted. For these trees with more than one core per tree, the same conditions as described for the forest plots above are determined to detect an avalanche year. There were years in which growth releases and decreases from different cores occur in the same year. In this case the signal with the higher classification was used (e.g. a strong response was preferred against a medium response). If there is only one core per tree, the following disturbances are necessary to determine an avalanche year:

- one scar
- one growth response with class A or B

Class C responses are only counted as an avalanche year if there is an avalanche year indicated from trees with more than one core. With these different conditions to detect an avalanche year it is possible to rank trees with one or more cores in the same way. In avalanche track 6 and 9 (av6 and 9) also several cross-sections were taken. The edge of a wound, where chaotic callus tissues has been built, can be used for dating past events.

To make sure that growth responses were caused by geomorphic disturbances and not by anthropogenic or climatic causes, the cores of the disturbance plots were compared with unaffected forest plots (plot 10 and 11 used as a master chronology). The comparison with unaffected trees allows to remove all growth responses, which are caused by the climate. To detect growth changes in unaffected trees from plots 10 and 11, two different approaches were used. The first approach was the same as described above, i.e., visual detection of scars and growth changes via the binocular. The same classification system as for the cores of the forest plots was used. Only if growth variations from the master chronology and the forest structure plot with disturbance go in the same direction (e.g., both have synchronic growth release), the reaction is defined by climate. The second method is based of the software IMPACT (Grissino-Mayer et al., 1997). The average of two rings before the investigated year divided by the average of two rings after the investigated year is calculated. If the threshold is higher than 150% or lower than 50%, ring width is influenced by a climate extreme. If these abrupt growth changes are influenced by a climate extreme, no disturbance events are possible in these years.

2.5 Avalanche simulations

The simulation software RAMMS is a two-dimensional software to calculate mass movement dynamics in a three-dimensional terrain (Christen et al., 2010). In practice, this tool is often used to predict the speed and mass of geophysical mass movements (Bartelt et al., 2013). Avalanches are calculated with the RAMMS avalanche module (RAMMS: AVALANCHE version 1.6.25 ©WSL/SLF) and the new forest applications.

2.5.1 Input paramters

Different input parameters have to be defined and adapted for the simulations. To specify the forest type, different parameters are necessary (Table 5). This information was obtained from the forest plot survey. If there is no forest plot nearby the track, the average of the 2 closest forest plots is calculated.

Table 5: Necessary information to specify the forest structure in each track. Avalanche track one has two different forest types. In all tracks the forest type is deciduous and beech trees are growing.

Track number	Crown coverage	Roughness	K-value code	DBH
1	0.6	2	N	21
1	0.7	2	N	50
2	0.5	2	N	21
3	0.9	2	J	39
4	0.2	2	Q	17
5	0.6	3	M	27
6	0.5	2	N	21
7	0.3	2	O	24
8	0.4	2	N	21
9	0.7	2	N	20
10	0.6	2	N	20
11	0.7	2	N	18
12	0.8	2	K	18
13	0.8	2	K	18
14	0.8	2	K	17
15	0.8	2	K	21
16	0.8	2	K	24
17	0.8	2	K	24
18	0.3	1	R	25
19	0.3	1	R	25

The detrainment coefficient K [kg m^{-1} s^{-2}] is calculated out of the forest type, crown coverage and roughness in the area. It represents the breaking power that a forest exerts on the avalanche flow (Feistl, 2015). The different values belong to a code which is implemented in

RAMMS. Information about snow height, snow density and erosion aspect of avalanches are not available for the study area. Due to the lack of information, several input parameters had to be adapted and tested in several simulations. Release areas are an important input parameter for avalanche simulations. In places with a lack of information about historic release areas, a GIS-analysis with topographic parameters (slope, aspect, confinement and distance to the next ridge) can be a valuable aid to define release areas (Maggioni and Gruber, 2003). In this case, the definition of the potential release areas was based on the interpretation of remote sensing data with the help of topographic parameters. From previous investigations, it is known that avalanches release in a terrain with slope angles between 30° and 60° (Salm, 1982; Munter, 1999). In this work, slope angle and aspect were the most important topographical parameters to define potential release areas. These release areas were the basis for the avalanche calculation in RAMMS. To cover extreme scenarios the largest possible release areas were drawn. A further input parameter which has to be adapted in several simulations is snow height. Several simulations with 10 and 100-year return periods were conducted. In addition, the friction value depends also on the return period, avalanche volume (release area, release height) and ground roughness. In this RAMMS version also the forest is taken into account. In different scenarios the avalanche volume and return period were adapted. Due to the lack of information about wind data, the wind load was set to zero. Out of these information, different friction values were calculated for open, channeled, gully and flat area slopes and also for forested areas. To have the same conditions in all tracks, the following parameters were not adapted and set as follows:

- Friction parameters Mu and Xi: These values have been calibrated in the Swiss Alps and are automatically computed in RAMMS. Due to the similar altitude range of the study area compared to Switzerland the standard elevation limits of 1500 and 1000 meter above sea level were adapted.
- In all simulations, numerical, random energy and miscellaneous parameters were placed at standard settings. Due to missing information also no erosion layers were used in the simulations.
- The snow density was set to 300 [kg /m^3].
- The erosion aspect was set to zero.
- The stopping threshold was defined at 7% of the total momentum. Simulations with different thresholds show that a value of 7% gives the most appropriate results.

2.5.2 Combination of avalanche simulations with additional information

In avalanche track 6 and 9 (av6 and av9) specific information about runout distances from past events were available. Trees which react to disturbances in the similar year were connected to runout zones and specific spatial patterns of different avalanche years were drawn. The aim was to combine the runout information from trees with runouts from avalanche simulations. Two

different approaches were tested to show how big the impact pressure has to be for trees, to show responses in the wood:

- 30 kPa-pressure approach: Trees respond to avalanches with flow pressures larger than 30 kPa.
- Tree destruction approach: The new RAMMS version is calculating areas, where trees break due to the high pressure. These calculations are based on the maximum pressure in a specific area, tree species and their DBH (Feistl, 2015). Here the assumption is that trees only respond in areas where tree break is possible.

To fulfill these different approaches with the runouts, simulations with different sizes of release areas and release heights were conducted. In avalanche tracks without information about the extent of the runout other methods were necessary. For that, in several simulations the extent and orientation of the release area was adapted until the avalanche flows in the right track and no forest without signs of disturbances was affected. All these simulations were made for 10-year return periods. According to local expert knowledge (Gustavo Aldea, personal communication, 25.02-8.03.2014), all these events occur frequently. For 100-year events it is possible that forests can be destroyed. Larger possible release areas are drawn for these events. Also here several simulations with different release height were done.

To show the effect of forests on avalanches, different simulations with and without forest were conducted. Additional afforestations should reduce the impact of avalanches. The different runout distances and extents from different scenarios were compared to each other. Also the pressure and flow height on the road or walking path were compared.

3 Results

The results chapter contains first an overview about all detected disturbances in the study area. In the chapter on the forest plots, all results about the influence of disturbances on the forest structure are presented. The results of the dendrochronological analysis show the age structure of the forest and also the disturbance history with their runouts. The results chapter ends with results from avalanche simulations in RAMMS and thus illustrates the crucial influence of forests on avalanches.

3.1 Natural disturbances in the study area

Considering the spatial extent, avalanches are the major source of disturbance in the study area (Table 6). Artificial avalanche releases in the ski resort are not considered. Potential rockfall areas are the second most frequent disturbance in the area (Fig. 26). The whole rockface between Shangri-La Valley and Las Trancas is declared as a possible rockfall area. Two different categories of landslides were detected. In the category “landslide”, areas with excavation or deposition of material for the newly built road are summarized. The category “landslide road” describes steep slopes along the road, which originate from the construction of the road. Human settlements and infrastructure are mostly endangered through avalanches followed by debris flows and landslides.

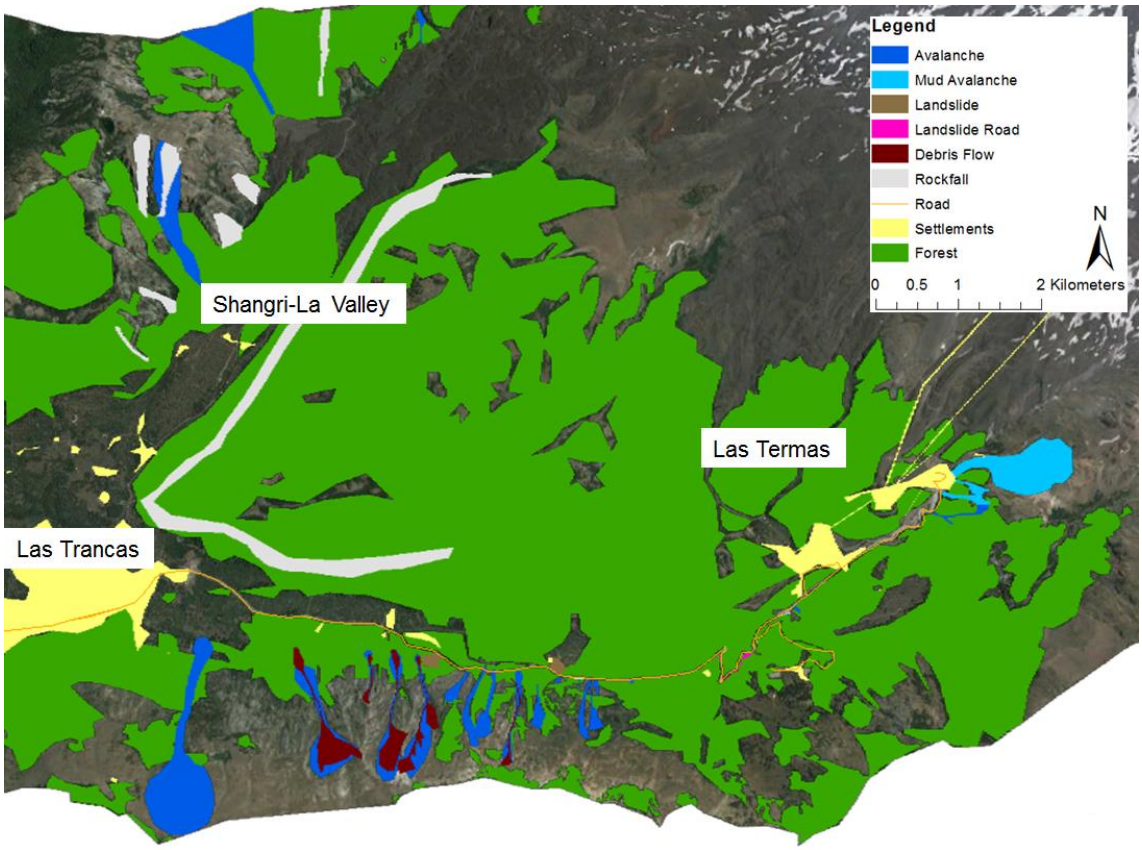

Figure 7: Mapped disturbances after the field trip in the investigation area.

Table 6: Percentage of different disturbances.

Process	Percentage per disturbance in whole area (defined in figure 7) [%]	Comparison per percentage per disturbance [%]
Mud Avalanche	0.0024	10.21
Debris Flow	0.0020	8.51
Avalanche	0.0235	100.00
Landslide	0.0003	1.28
Landslide Street	0.0001	0.43
Rockfall	0.0098	41.70

3.2 Forest structure in disturbed and control plots

Avalanches and debris flows influence the structure of the forest at our study site in Nevados de Chillán. Beside canopy density, disturbances also influence tree density, tree species distribution and also the tree height. Only the DBH show no clear influence of avalanches and debris flows.

Canopy densities of the investigated plots range between 20 and 90%. The average density of the canopy is 60%. There is a high variation in the canopy density of all plots (Fig. 8). The canopy density of control plots was never below 50%. A summary of the plots with the same

disturbance regime (Fig. 9) shows that disturbances lead in general to a reduction of the canopy density. The canopy density of plots with signs of debris flow disturbances is 9% lower than with no signs of disturbances. The reduction of the canopy density from not disturbed forests to avalanche disturbance forests is 18%. These results are however not significant (p-value > 0.05). As for the different types of disturbances, the canopy density of avalanche disturbances is lower than for debris flow disturbances. Considering the influence of disturbances to the tree density, slightly different results can be found.

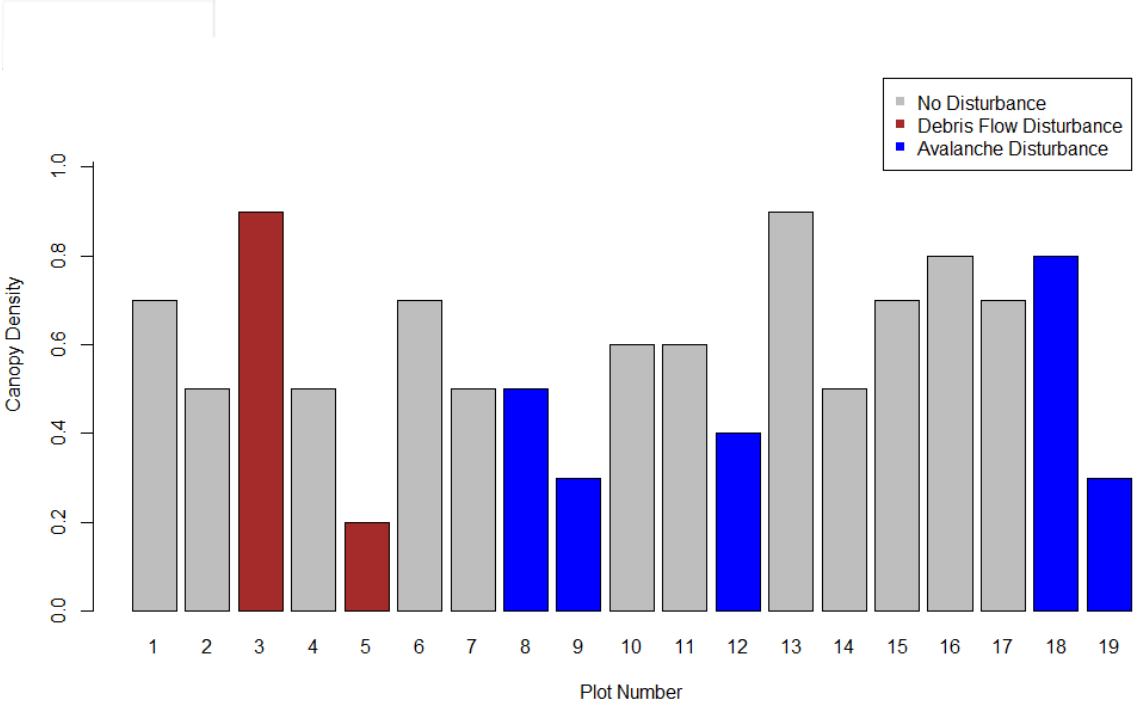

Figure 8: Canopy density distribution per plot.

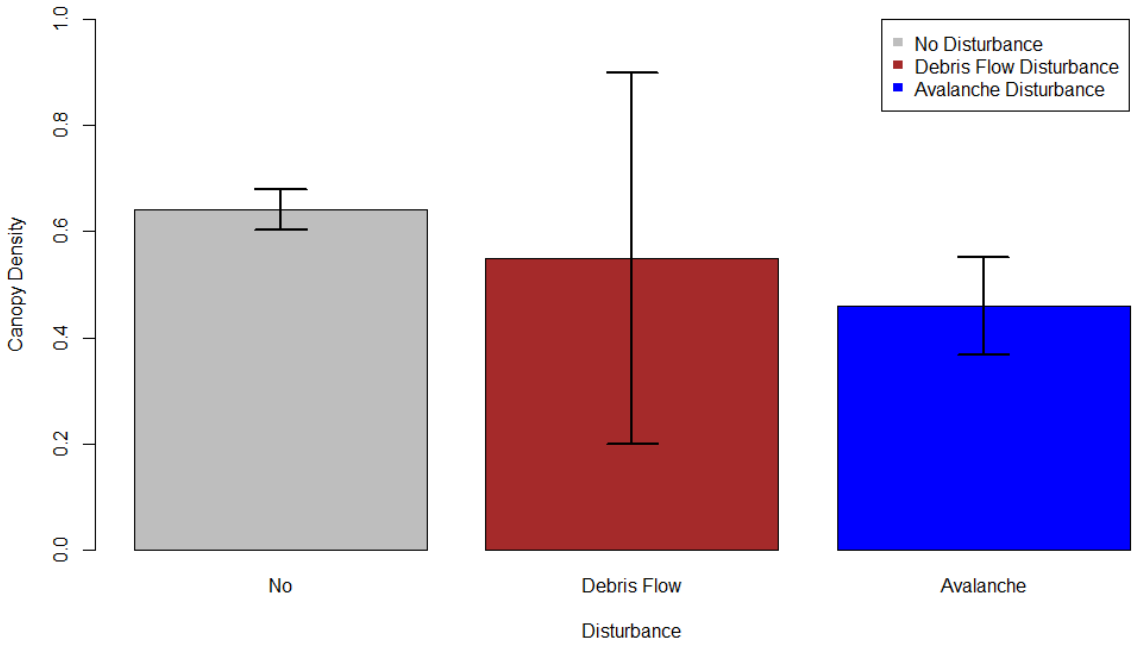

Figure 9: Canopy density distribution per disturbance.

Tree densities for plots without disturbances vary between 223 and 2410 trees per hectare. Plot numbers 13 to 16 all show densities with more than 1800 trees per hectare. All debris flow plots have a tree density below 1000 trees per hectare (Fig.10). With all different disturbances summarized, there is no significant difference (p-value>0.05) in the tree density per hectare if there were disturbances present in the forest or not (Fig. 11). Plots without disturbances have more trees per hectare than with disturbances. Slightly more trees per hectare can be detected in plots with avalanche disturbances than in plots with debris flow disturbances. The density of shrub layer has a different pattern. In 100% of the avalanche disturbance plots and 92% of the plots with no disturbances, the shrub layer is continuous. In debris flow plots the shrub layer is less dense.

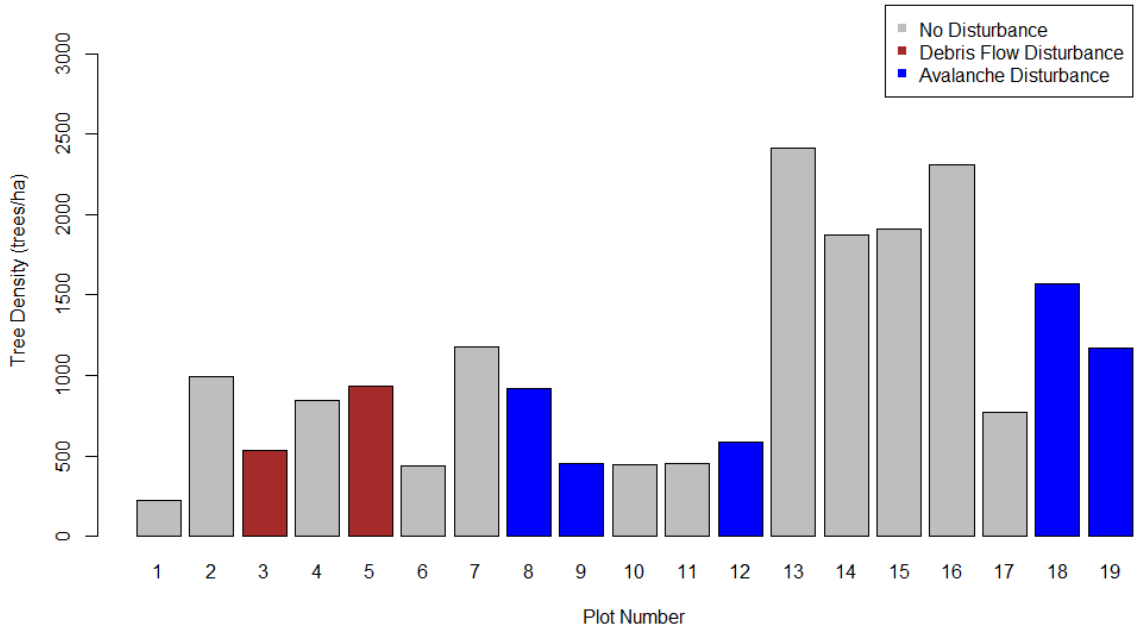

Figure 10: Tree density distribution per plot.

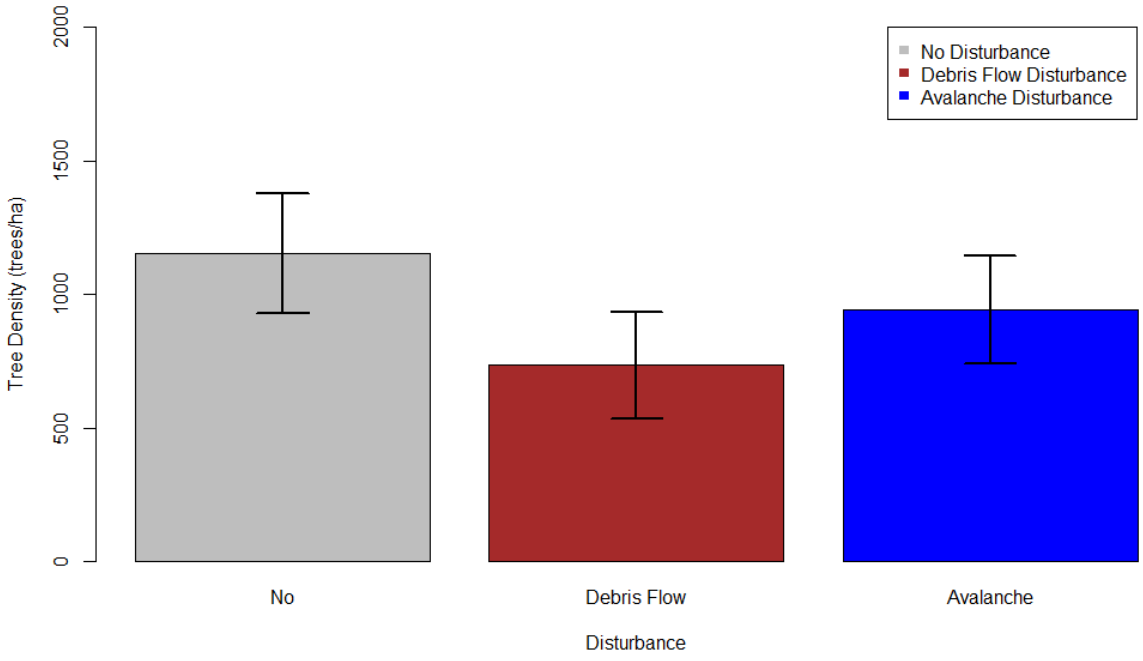

Figure 11: Canopy density distribution per disturbance.

The most common tree species in the forest of Nevados de Chillán is *Nothofagus obliqua* (Fig. 12). In the first three plots *Nothofagus dombeyi* is the most frequent species. There are two species which only occur in one plot, *Adesmia microphylla* is only growing in plot number 2 (3 individuals) and in plot number 19 we can only find *Nothofagus pumilio* (Fig. 12). *Nothofagus obliqua* is the most common species in all disturbance classes (87.3%, 65.5% and 75%) (Fig. 13). The highest percentage of *Nothofagus dombeyi* can be found in debris flow tracks

(34.52%). Except for plot 19, only *Nothofagus obliqua* trees are growing in avalanche tracks. In the shrub layer only bamboo is considered. In the majority of the plots where no disturbances occur, bamboo is growing (83%). Also in 75% of the avalanche plots, bamboo is the main shrub species. In all debris flow tracks bamboo is not found in the shrub layer. The last parameters where disturbances have an influence on the forest structure is tree height.

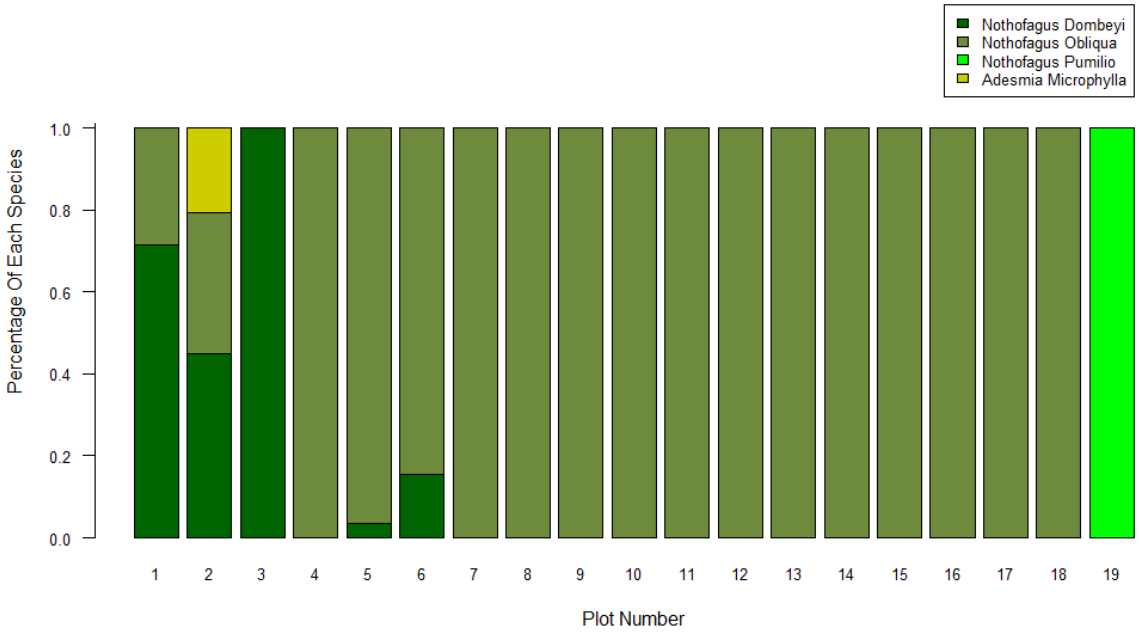

Figure 12: Tree species distribution per plot.

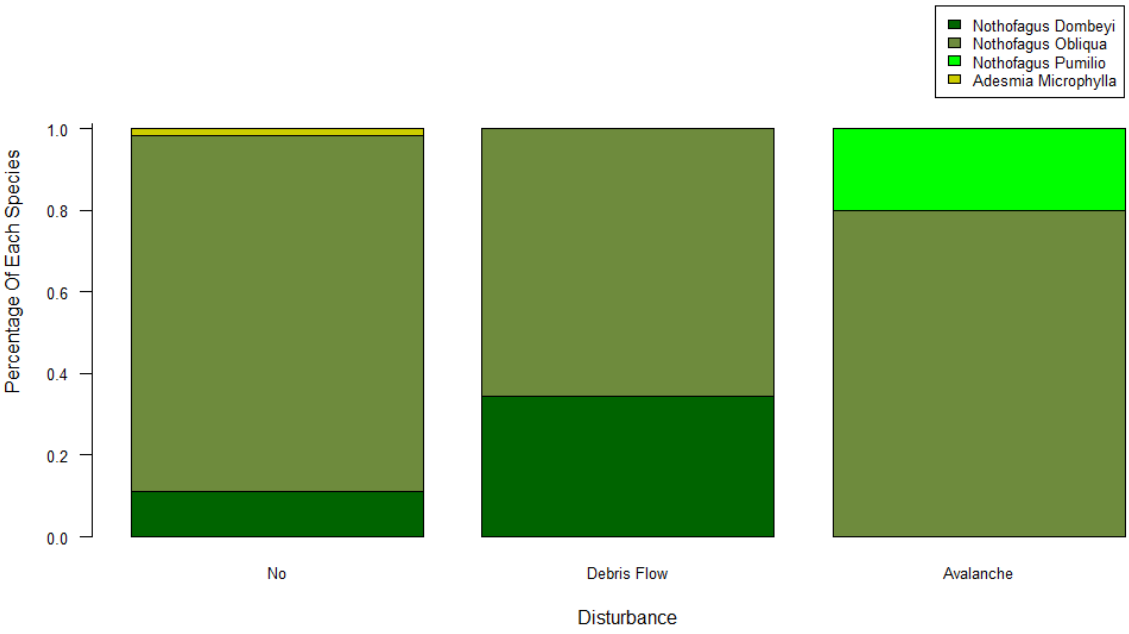

Figure 13: Tree species distribution per disturbance.

The mean height of trees per plot varies between 6 and 20 meters (Fig. 14). Plot number 1 and 3 have the highest average tree height with 19 and 20 meters, respectively. Tree height in areas where avalanche disturbances occurred, is significantly smaller (p-value=0.04) than for trees in

debris flow tracks and forest plots without disturbances. The height of the bamboo shrub layer varies between one and three meters. Between the plots where no disturbances occur and plots with avalanche or debris flow disturbances, no differences in the shrub height are visible (Fig 15).

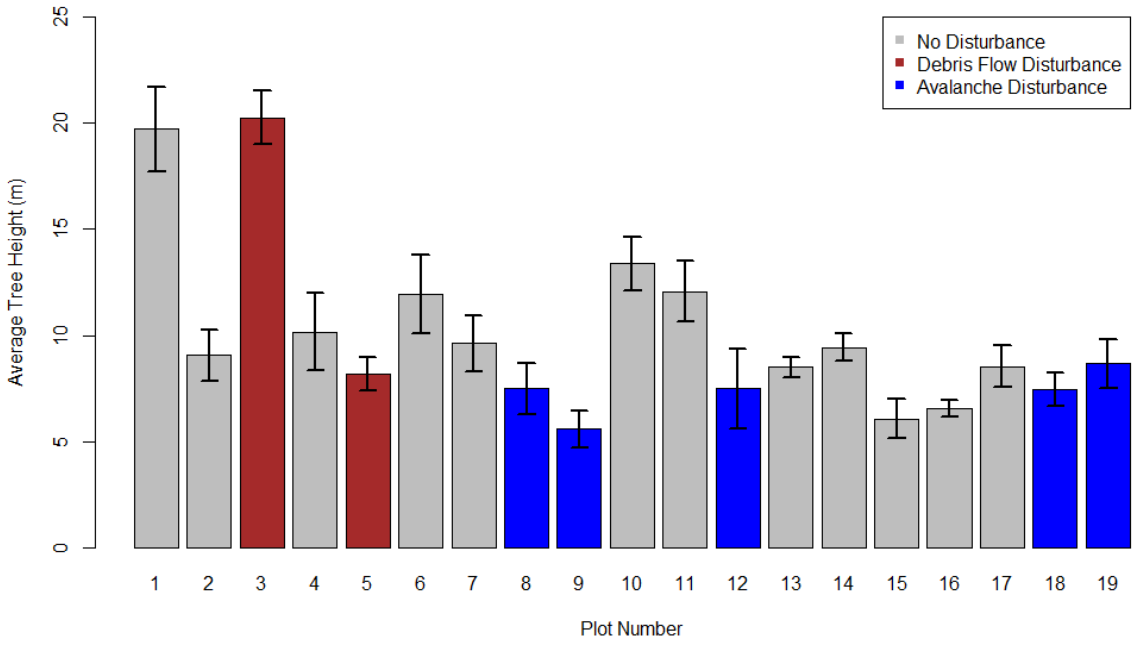

Figure 14: Tree height distribution per plot.

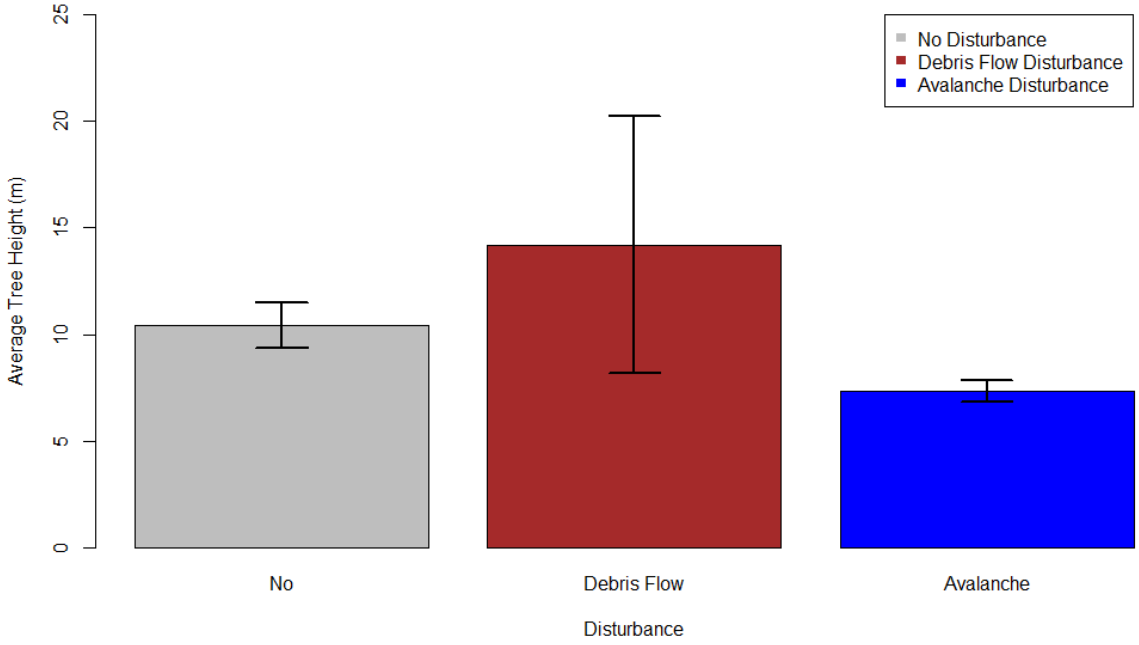

Figure 15: Tree height distribution per disturbance.

The DBH of plots with no disturbance varies between 17 and 50 centimeters (Fig. 16). Also the debris flow disturbances plots show big variations. The DBH from avalanche disturbance plots is quite constant and varies between 21 and 25 centimeters. Disturbances do not have significant influence on the DBH distribution (p-value=0.73).

The average DBH of trees in debris flow tracks is marginally higher than in tracks without disturbances or avalanche tracks (Fig. 17).

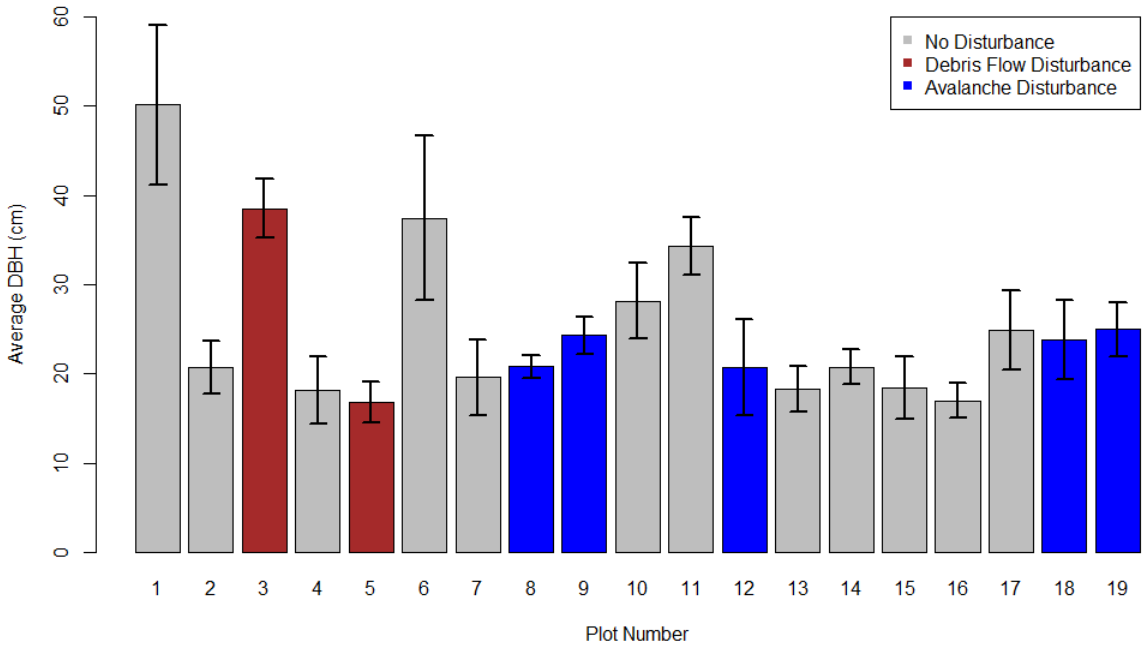

Figure 16: DBH distribution per plot.

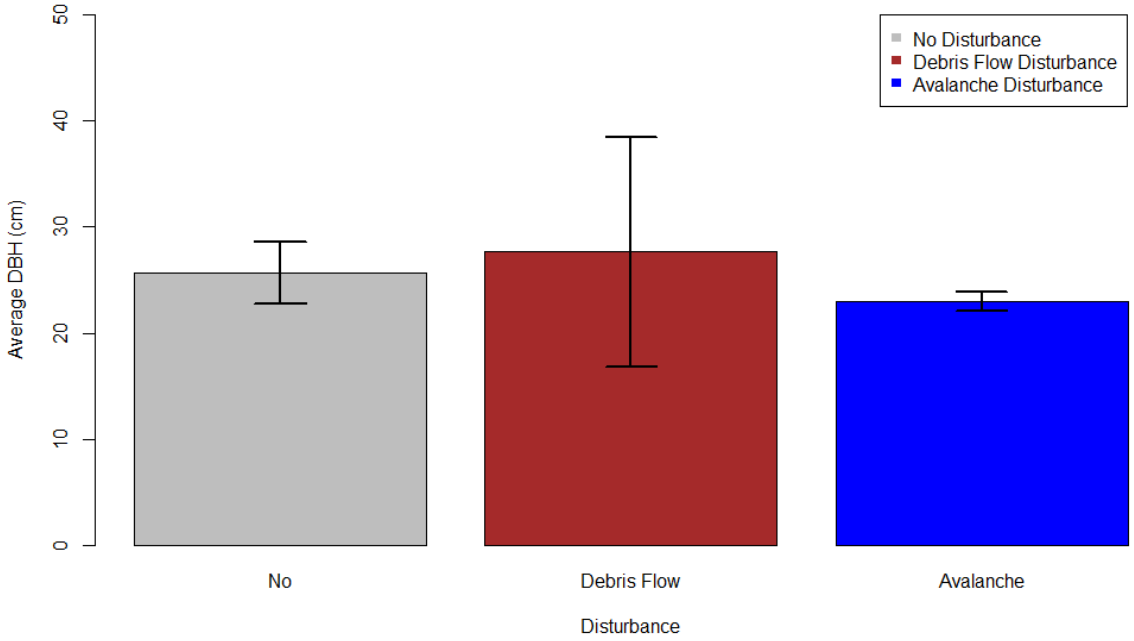

Figure 17: DBH distribution per disturbance.

3.3 Results of dendrochronological analysis

The results of the dendrochronological analysis contain details about the age distribution of the forest plots, as well as the disturbance history of the tracks. The chapter will finish with spatial information about the runouts of past avalanches.

3.3.1 Age distribution

The age of trees varies between 34 and 146 years (Fig. 18). Only in plot number 11 the average tree age is over 100-year. Trees in plot number 11 reached the DBH-height in the year 1868. In average trees in forests without disturbances are older than trees in forest with debris flow and avalanche disturbances. The age difference between forests in debris flow tracks and forests in avalanche tracks is not significant (Fig. 19). The initial growth year at the DBH-level is 1942 in forests without disturbances. Forests in debris flow tracks reached the DBH-level in 1955 and those in avalanche tracks in 1958.

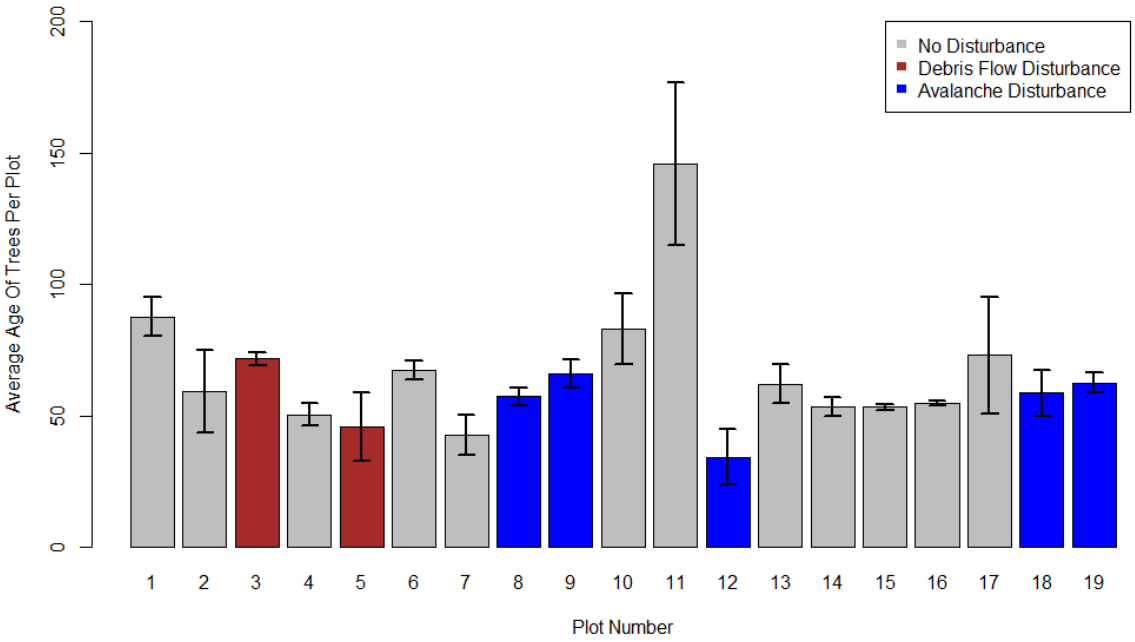

Figure 18: Age distribution per plot.

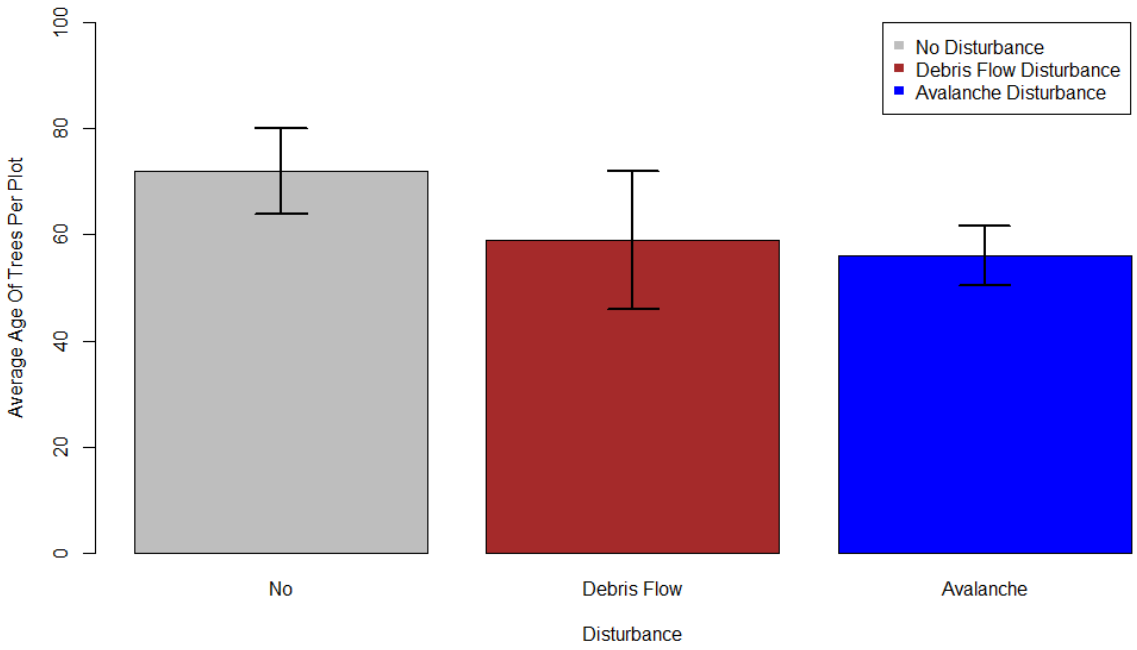

Figure 19: Age distribution per disturbance.

3.3.2 Disturbance history

Scars and growth responses are the basis to detect past events. All responses of the trees per year in one plot are taken together (Fig. 20 and Fig. 21). Due to the different age of the investigated tree, the amount of trees varies over the time.

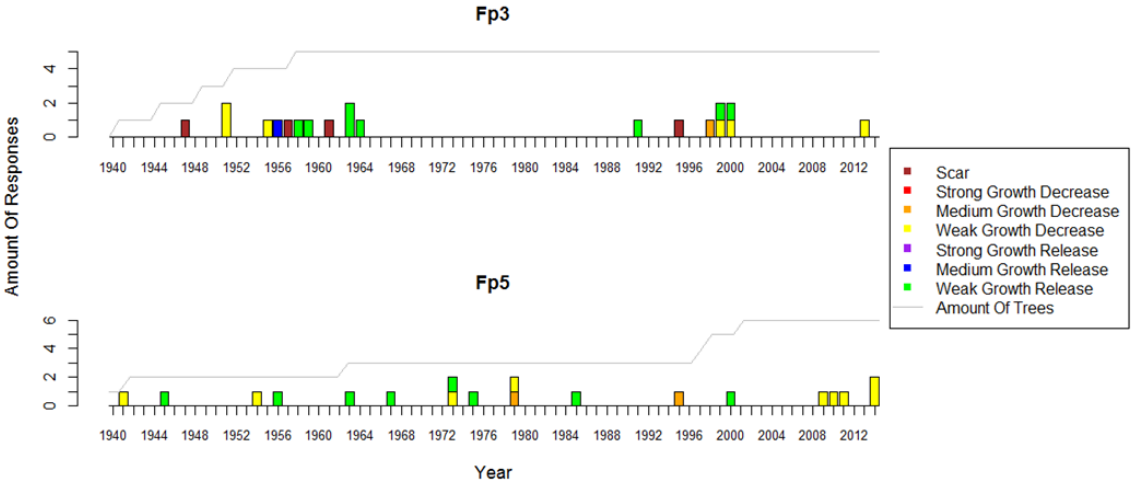

Figure 20: Scars and growth responses in trees of forest plot 3 and 5 (fp3 and fp5) which belong to the debris flow tracks 3 and 4 (df3 and df4).

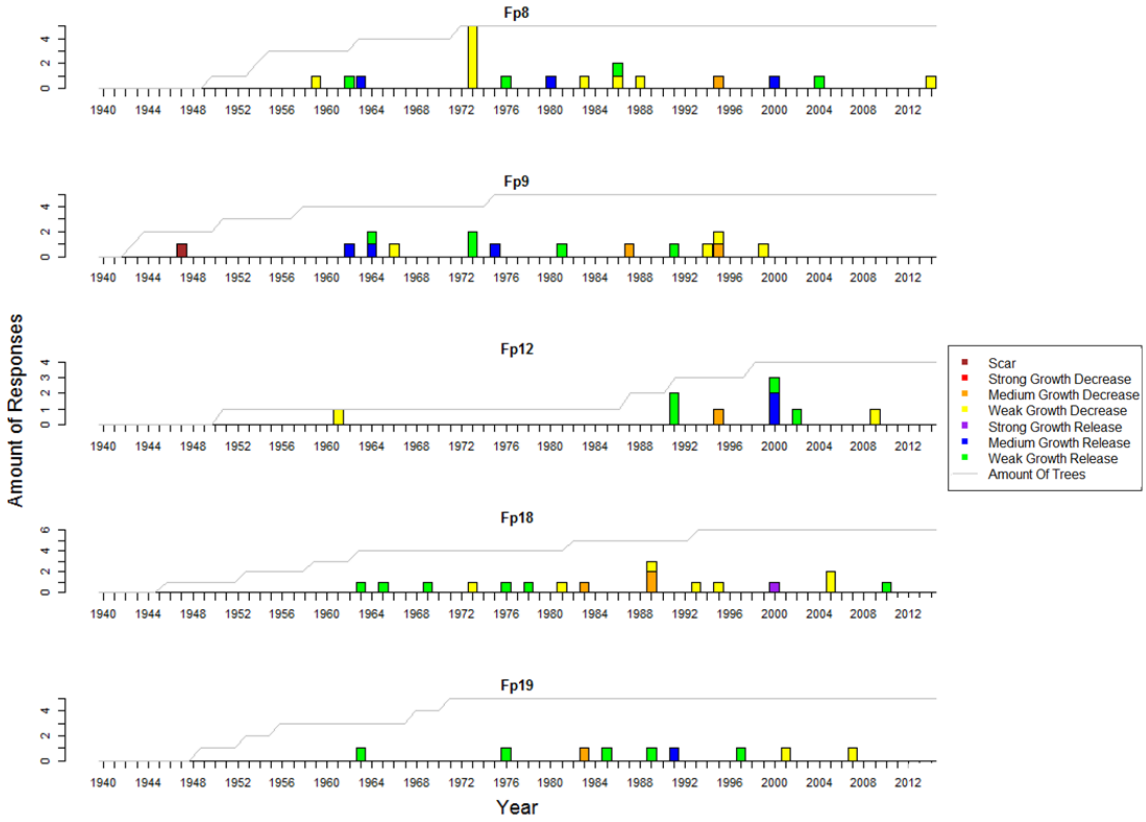

Figure 21: Scars and growth responses in avalanche tracks 6, 7, 8, 16 and 17 (av6, av7, av8, av16 and av17).

The investigation showed that Nevados de Chillán has a rich event history. In the past, many avalanches and debris flow events occured (Table 7). In the years 1995 and 2000, avalanches were released in most of the tracks. With the runout sampling strategy in avalanche track 6 and 9 (av 6 and 9) much more events can be detected compared with the forest structure sampling strategy in the same track (fp 8 and 12).

Table 7: List with all detected past events in the investigation area. Fp3 and fp5 show event years in the debris flow tracks (df3 and df4). Fp8, av6, fp9, fp12, av9, fp18 and fp19 show historic avalanche events in different avalanche tracks (av6, av6, av7, av8, av9, av16 and av17).

Avalanche/Debris flow years	Fp 3	Fp 5	Fp 8	Av 6	Fp 9	Fp 12	Av 9	Fp 18	Fp 19
2014		x							
2012				x			x		
2011				x			x		
2010	x						x		
2005				x				x	
2002							x		
2000				x		x	x	x	
1995	x	x	x	x	x	x	x		
1992				x					
1991				x		x	x		
1989				x				x	x
1986			x	x				x	
1984				x					
1983				x			x		x
1982				x					
1980				x					
1977				x					
1975				x					
1974				x					
1972				x					
1968				x					
1964					x				
1962				x					
1961	x								
1957	x								
1954				x					
1951	x			x					
1947	x								
1945				x					
1942				x					

In different years growth responses are caused by the climate (Table 8). Two different methods show different climate response years. Only the year 1973 was detected as a climate year with both methods.

Table 8: Climate response years detected with different methods.

Method with reference chronology	1964, 1970, 1973, 1999, 2005
Method with IMPACT procedure	1966, 1973, 2006, 2007

In avalanche track 9 (av9) the history of past events is also traced with the indices approach. Historic avalanche years were considered as such with at least three responding trees (Fig. 22,

graph A) and an Index value I > 10% (Fig. 22, graph B). This approach indicates that 1983, 1991, 1995, 2000, 2011 and 2012 were avalanche years (Fig. 22, graph C).

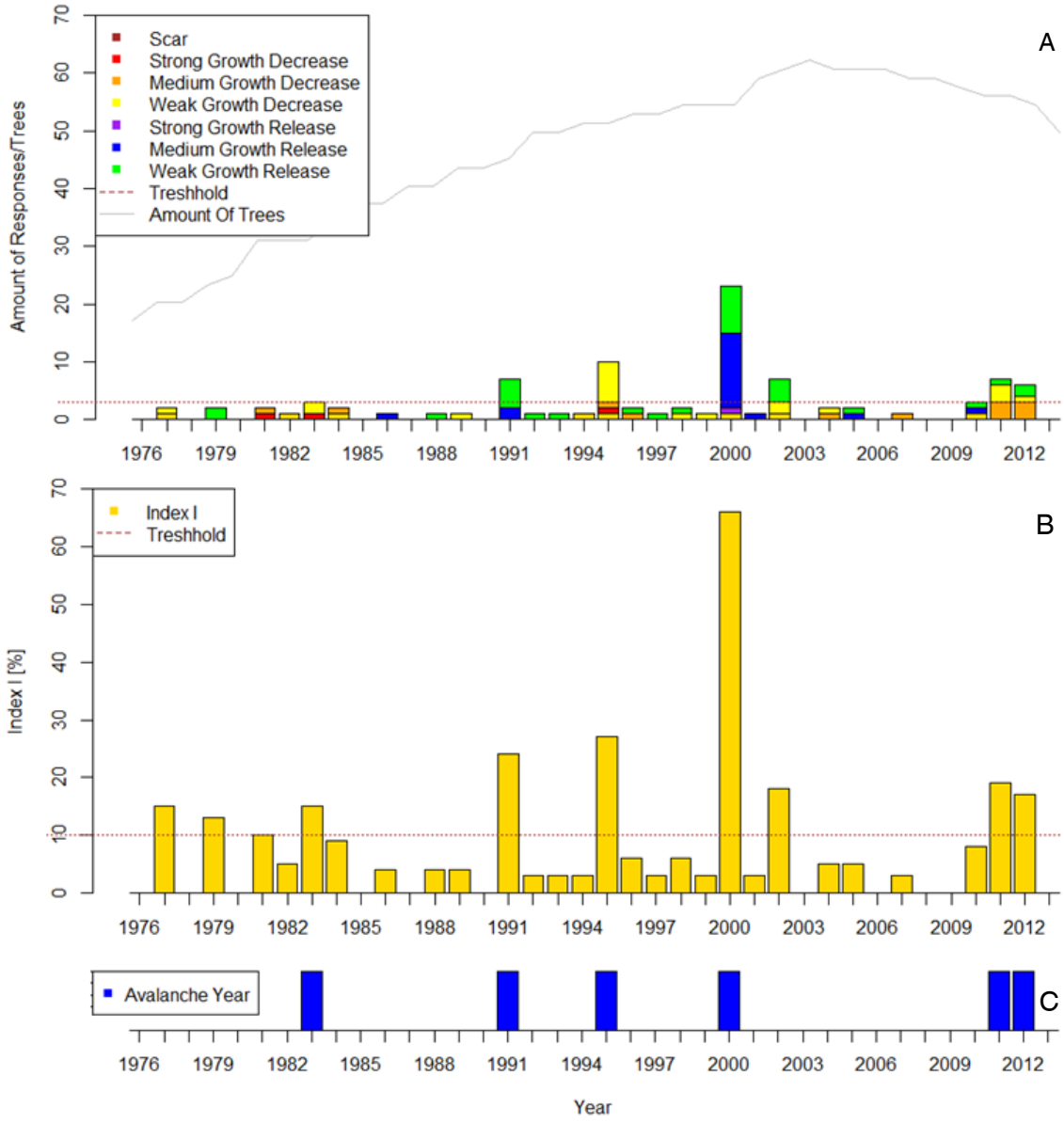

Figure 22: Event-response histogram from avalanche track 9 (av9) (adapted from Corona et al., 2012). Graph A shows the total number of growth disturbances (GD) with a threshold of three responding trees. Graph B displays the index value I with the percentage of responding trees to an event with a treshhold value I of 10% and graph C shows the detected avalanche years.

3.3.3 Runout distances

The combination of trees which show growth responses in the same year allows the reconstruction of runout distances. Several years have the same runout distance and are combined together. For a better overview the runouts of avalanche track 6 (av6) are subdivided in runouts which cross the road or not (Fig. 23 and 24). The avalanche runouts from 1962, 1975 and 1991 also go to the right side of the track (Fig. 24). Trees below the road show a rich

avalanche history. Because all these trees stand close together, below the road there is no spatial differentiation between the runouts. Three different runout distances exist where trees don't reach the road (Fig. 24). In each of the two further runout distances three different avalanche years had the same spatial extent. The avalanche in 2011 has the shortest runout.

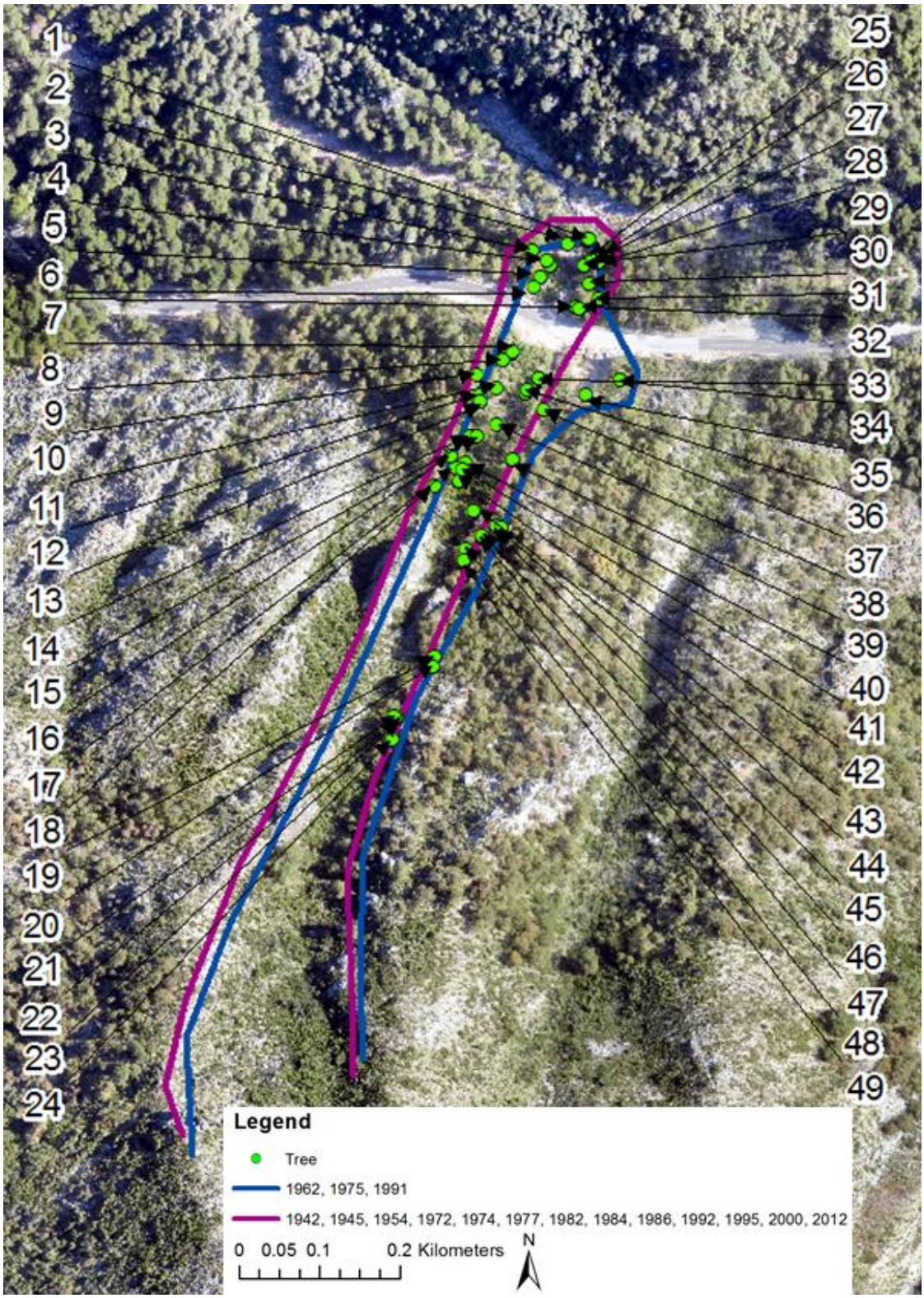

Figure 23: Avalanche track 6 (av6) runouts over the road. These numbers refer to Table 9.

Table 9: Avalanche years in runouts of track 6 (av6).

Tree number	Avalanche years	Tree number	Avalanche years
1	1972, 1982, 1986, 1992, 1995, 2000,2012	26	1942, 1945, 1954, 1972, 1992
2	1991	27	2012
3	1942, 1992	28	1930, 1945,1954, 1972, 1992
4	1974, 1984,1992, 1995	29	1995
5	1977, 1984, 1995	30	2000
6	1975, 1991, 2000	31	1977, 1995, 2000
7	1983, 1995, 2010, 2012	32	1962, 1974, 2000, 2012
8	1974, 1977, 1983, 1995, 2000	33	1974, 1983, 1992, 2000
9	1989, 2000	34	1962, 1975, 1991
10	1930	35	1951,1962
11	1989	36	1995
12	2005	37	1983
13	1995, 2012	38	2000
14	1995	39	1951, 1984, 2000
15	1992, 2000, 2005	40	1974, 2000
16	1974, 1982, 2005	41	2000
17	1962, 1975	42	1942, 1962
18	1974	43	1980, 2000
19	1945, 1951, 1982, 1986, 1991, 1995	44	1974, 1995, 2000
20	2000	45	1954, 2000
21	1968, 1982, 1986, 1991, 1995, 2000, 2005, 2011	46	1968, 1974, 1980, 1982, 1989, 2000, 2011
22	1968, 1983,1986, 1991, 1995, 2000, 2011	47	1962, 1974, 1989, 2000
23	2000	48	1989
24	1983, 1991, 1995, 2000	49	1954, 1991, 2011
25	1995, 1986, 2000		

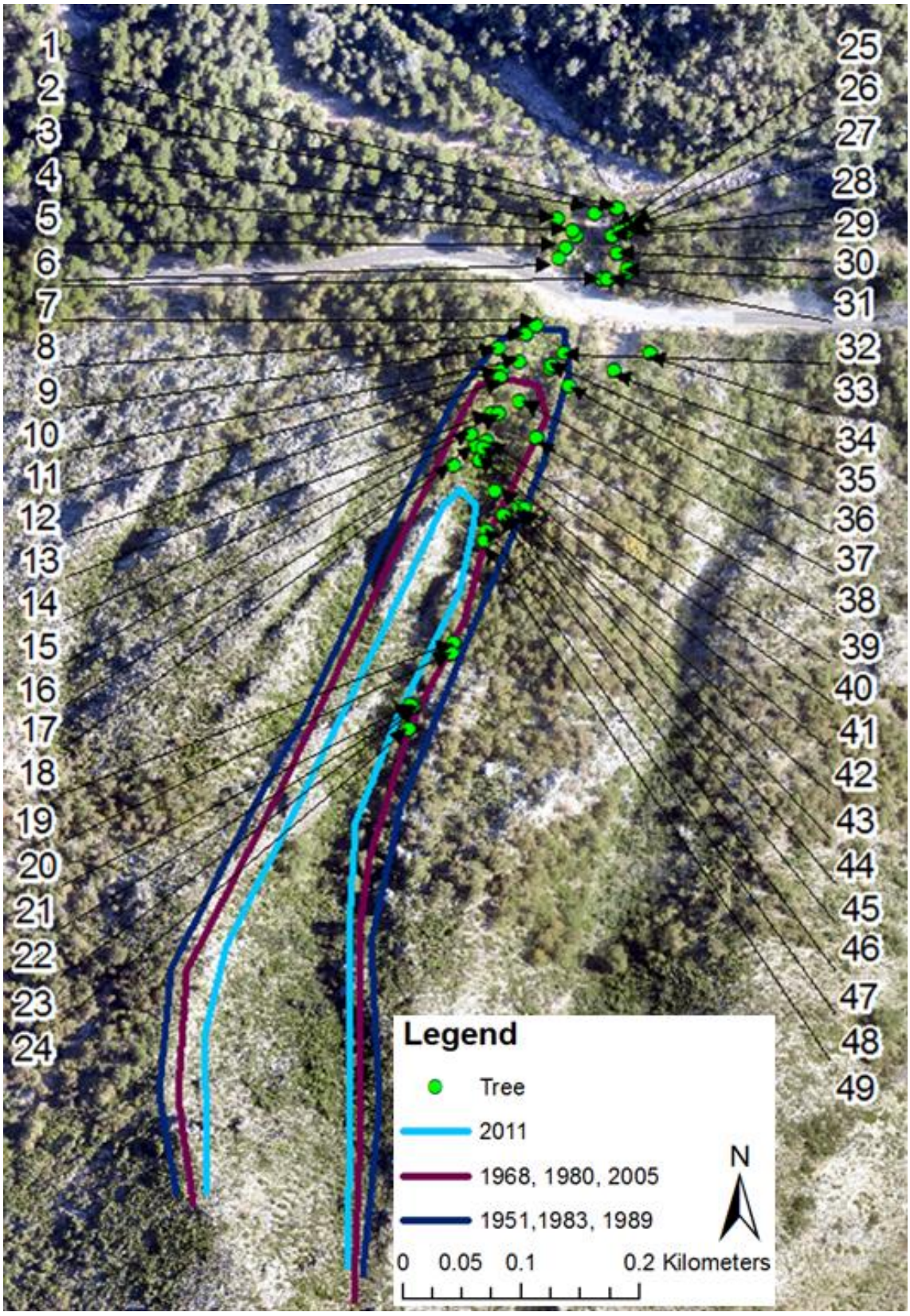

Figure 24: Avalanche track 6 (av6) runouts which do not reach the road. These numbers also refer to Table 9.

In avalanche track 9 (av9) the analysis of the spatial arrangment of responding trees showed, that there are two different release areas which flow in the same runout (Fig. 25). From each release direction there is a short and long runout. The spatial information about the runout distance is used for avalanche simulations.

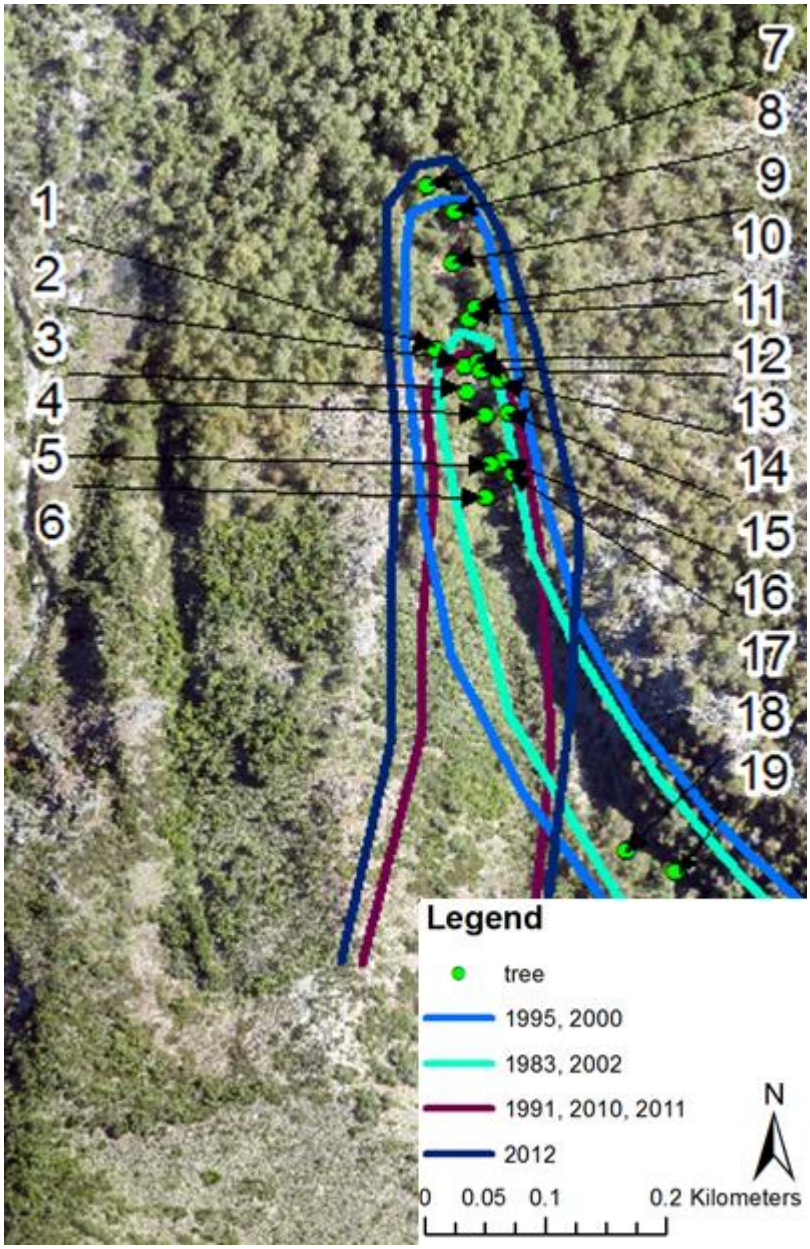

Figure 25: Specific runouts of avalanche track 9 (av9). These numbers refer to Table 10.

Table 10: Avalanche years in runouts of track 9 (av9).

Tree number	Avalanche years	Tree number	Avalanche years
1	1995, 2000	11	2000
2	1991, 1995, 2000	12	2000, 2002, 2010, 2011, 2012
3	1991, 2000, 2002, 2011	13	2000, 2010
4	1991, 2000	14	2000
5	1983, 1995, 2010, 2012	15	2000, 2012
6	1995, 2000, 2002, 2010, 2011	16	1991,1995, 2000
7	2000	17	1991, 2000
8	1995, 2000	18	2000
9	1995	19	1983, 1995, 2000, 2002

3.4 Avalanche simulations with RAMMS

The combination of dendrogeomorphic information with avalanche simulations and the comparison of different input parameters for release areas leads to reliable results of reconstructed past avalanches with their specific extent and location of release areas. Because no documentation of past avalanches exist, release areas and snow release heights[8] were adapted until the avalanche flowed in the right direction. If no specific information about runouts was available, a release height of 0.5 meters gave the best results for 10-year events. In avalanche track 6 and 9 (av6 and av 9) with additional runout information, the release height varies between 0.3 and 0.9 meters. These release heights resulted from different simulations and the runout extent out of dendrogeomorphic informations. For 100-year events in all simulations, a release height of 1.0 meter led to the best results. For avalanche tracks without additional dendrogeomorphic information on the runout, the interpretation of flow directions and runout distances were the main assistance to adapt release areas. The border of forests and the evaluation of the forest structure during fieldwork also helped to adapt the extent of the release area for 10-year events. Additional information about the runout was important for the verification of the flow direction and the spatial extent of runouts. The comparison of the 30 kPa-pressure and the tree destruction approach where the dendrogeomorphic resulted runout distance coincide with the simulated border of tree destrction showed that the tree destruction approach provides better results. The maximal runout distance of 30 kPa-pressure coincides with responding trees only for avalanches with small release areas and a release height of 30 centimeters. For 100-year events, the adaption of release areas is mainly based on information about the flow direction and not on the forest, because it is expected that former unaffected forest would be destroyed. After the evalutation of possible release areas through the avalanche simulation expert Andi Stoffel, release areas were drawn larger depending on the respective

[8] Average release height vertical to the slope.

trend (Lukas Stoffel, personal communication, 21.05.2015). The final release zones are marked in grey (Table 11-27). Release areas resulted to be up to 8 times larger for 100-year events as compared to those of 10-year events. Small avalanches or avalanches where the extent of release areas is limited by the surrounding of forest do not show such significant differences between 10- and 100-year events (av5, av15, av16, av17, av18). In avalanche simulations with a return period of 10-years, 63% of the avalanche tracks reach the road or the walking path (Fig. 26). For the return period of 100-year, 94% of the avalanche tracks reach the road or the walking path (Fig.27). This is an increase of 31%. If the return periods from 10-year events to 100-year events are compared, the spatial extent from the runouts increases around 45%. The maximum pressure at the road and walking path increases around 34% and the flow height around 35%.

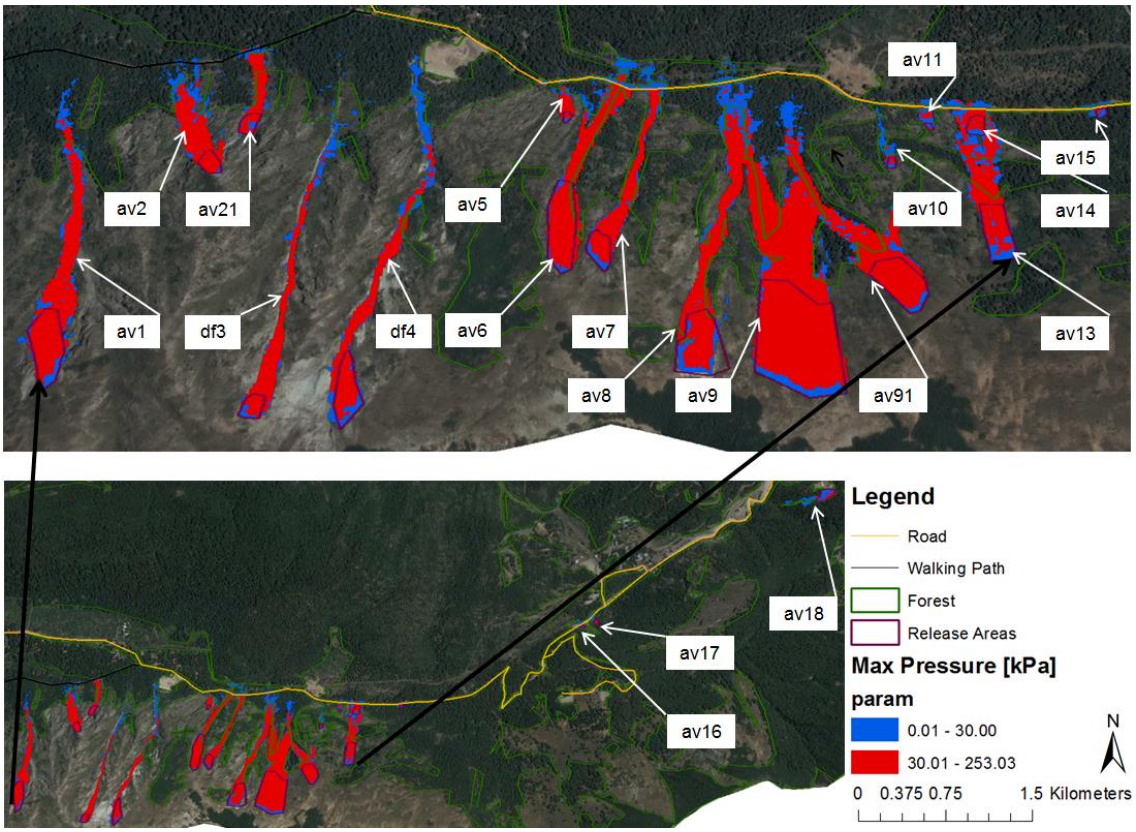

Figure 26: Final release areas (10-year events) with maximum pressure [kPa].

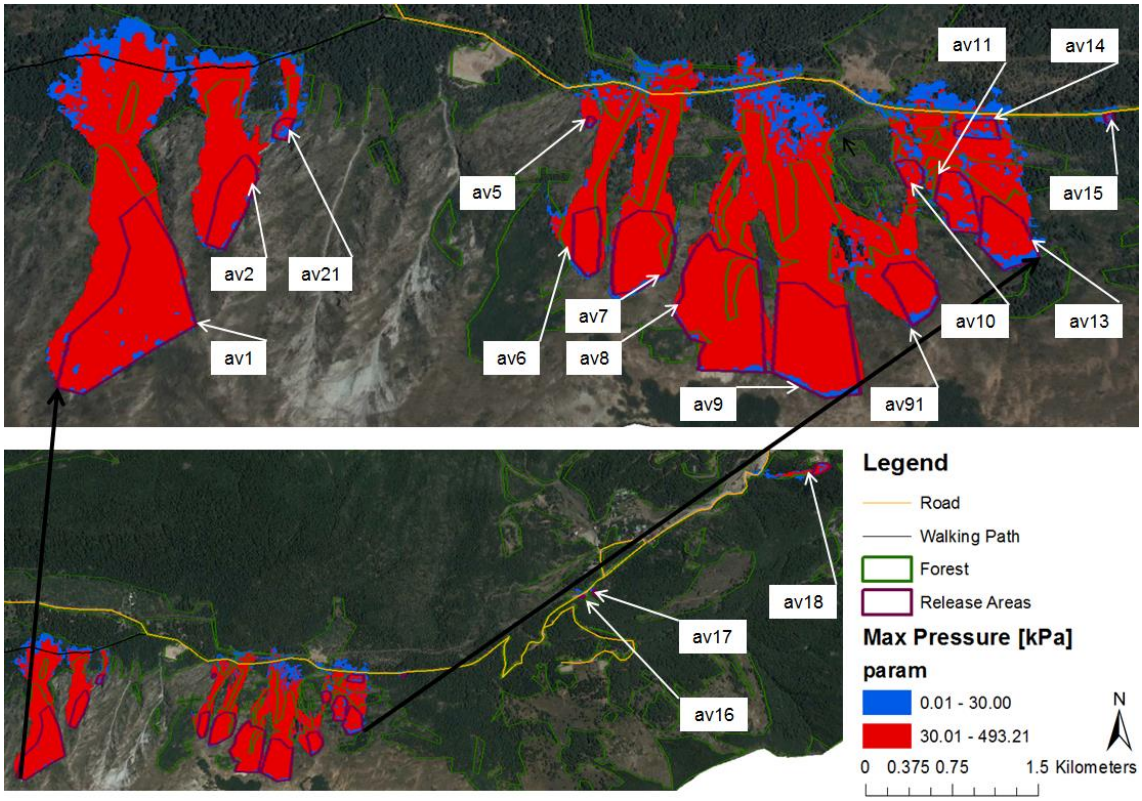

Figure 27: Final release areas (100-year events) with maximum pressure [kPa].

In **avalanche track 1 (av1)** the simulations number 1 to 3 shows different release areas for a 10-years event (Table 11). The release zone of number 3 contains all parts of a possible release area with a slope between 28 and 55 degrees. In simulation number 2 and 3 the release area from number 3 is grouped in two parts with a similar aspect. For a 100-year event the biggest possible release area was selected and the simulations were computed with two different release heigths (0.5 and 1m). The results show that the maximum velocity, flow height and pressure is higher in simulation number 5. The pressure till forest was destroyed by the avalanche, is calculated in each simulation and depending of the forest structure.

Table 11: Input parameters and results of RAMMS simulations in avalanche track one (av1).

Number	Return period [years]	Release area [m²]	Release height [m]	Max velocity [m/s]	Max flowheight [m]	Max pressure [kPa]	Forest destruction
1	10	10425	0.5	23.14	5.36	160.69	no
2	10	9675	0.5	22.08	4.35	146.26	no
3	10	69200	0.5	29.4	9.29	259.35	yes
4	100	79625	0.5	32.76	11.55	322.11	yes
5	100	79625	1	40.56	20.81	493.2	yes

Table 12: Input parameters and results of RAMMS simulations in avalanche track 2 (av2).

Number	Return period [years]	Release area [m²]	Release height [m]	Max velocity [m/s]	Max flowheight [m]	Max pressure [kPa]	Forest destruction
1	10	4800	0.5	28.68	4.61	246.78	no
2	10	2825	0.5	22.8	3.42	155.97	no
3	10	2425	0.5	22.37	2.8	150.19	no
4	100	17425	1	37.35	8.06	418.55	yes
5	100	2425	1	20.33	5.28	124.08	yes

Different simulations in **avalanche track 2 (av2)** show that two different release areas are possible (Fig. 28). Simulation number 1, 3 and 5 show another possible release areas (Table 12). Due to topographical settings (rocky parts with a slope angle steeper than 60°) the release areas are quite small.

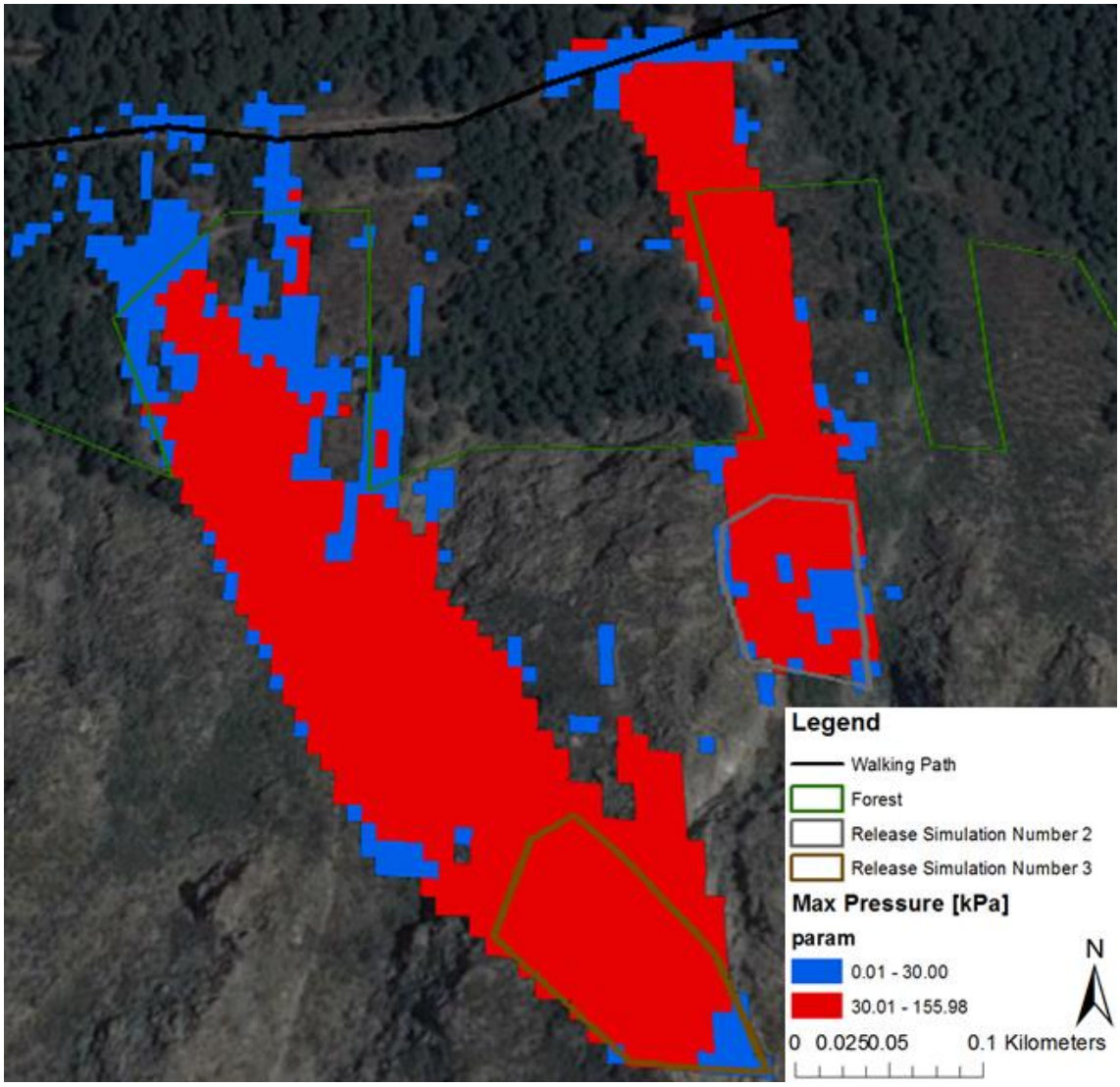

Figure 28: Simulation number 2 (left) and 3 (right) in avalanche track 2 (av2) with their different release areas.

Table 13: Input parameters and results of RAMMS avalanche simulations in debris flow track 3 (df3).

Number	Return period [years]	Release area [m²]	Release height [m]	Max velocity [m/s]	Max flowheight [m]	Max pressure [kPa]	Forest destruction
1	10	46700	0.5	27.97	9.01	234.78	no
2	10	13175	0.5	24.66	5.05	182.46	no
3	10	1775	0.5	22.36	4.18	150.07	no
4	100	42900	0.5	30.2	11	273.78	no
5	100	42900	0.5	48.18	20.32	696.51	yes

In **debris flow track 3 (df3),** where forest plot 3 (fp3) is located, no signs of avalanches are visible. Due to simulation number 1 and 2, signs of past avalanches are expected in the forest plot (Table 13). However, field observations showed that in this track just small avalanches can happen as in simulation number three, which does not affect the forest (Fig. 29). Simulation number 6 represents a possible release area of a 100-year event, which would destroy a lot of forest. Due to different aspect in the release area, a release of simulation number 6 is unlikely. In this track avalanches and debris flows can occur. With RAMMS only avalanches are simulated.

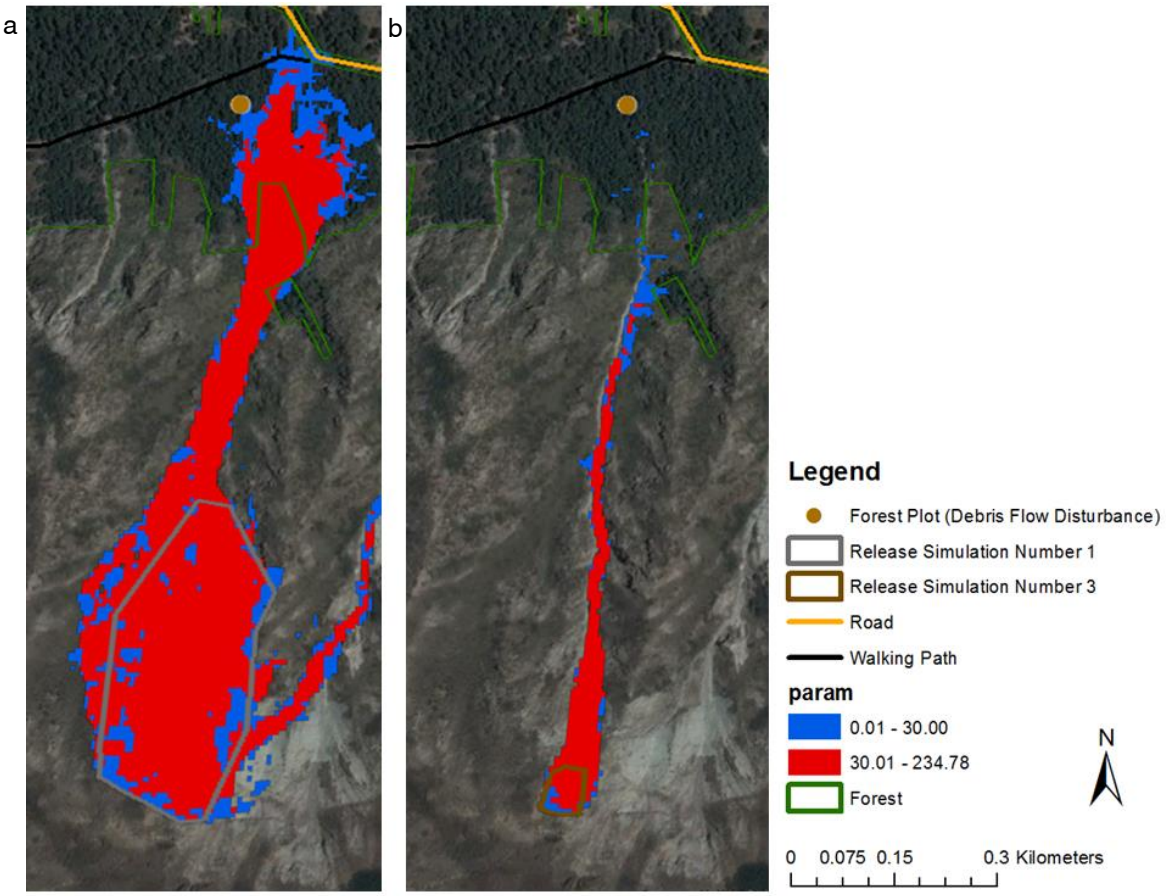

Figure 29: Comparison of simulation number 1 (a) versus simulation number 3 (b) in debris flow track 3 (df3).

As in debris flow track three (df3) before, also for **debris flow track 4 (df4)** past avalanches didn't reach the forest. In this track avalanches and debris flows are possible, but only the avalanches are simulated in RAMMS. Due to rocks with a slope angle > 60 degrees no bigger release areas are possible. In forest plot 5 (fp5) and its surrounding no signs of avalanches are visible. No major event (return period of 100 years) is possible due to the topography. It is expected that in reality, the release area from simulation number 6 would start as three different avalanches (simulation number 2 to 4 as 10-year events) (Table 14). From these three possible 10-year events, the biggest one (number 2) is selected as the most possible one to release (Fig. 30). Due to different aspects and ridges in the release area, a release of simulation number 6 is unlikely.

Table 14: Input parameters and results of RAMMS avalanche simulations in debris flow track 4 (df4).

Number	Return period [years]	Release area [m²]	Release height [m]	Max velocity [m/s]	Max flowheight [m]	Max pressure [kPa]	Forest destruction
1	10	59725	0.5	30.11	9.87	272	yes
2	10	5325	0.5	20.81	3.81	129.96	no
3	10	2375	0.5	22.55	2.75	152.62	no
4	10	2275	0.5	20.18	2.06	122.25	no
5	100	65350	0.5	31.99	8.71	307.13	yes
6	100	65350	0.5	31.99	37.98	21.033	yes

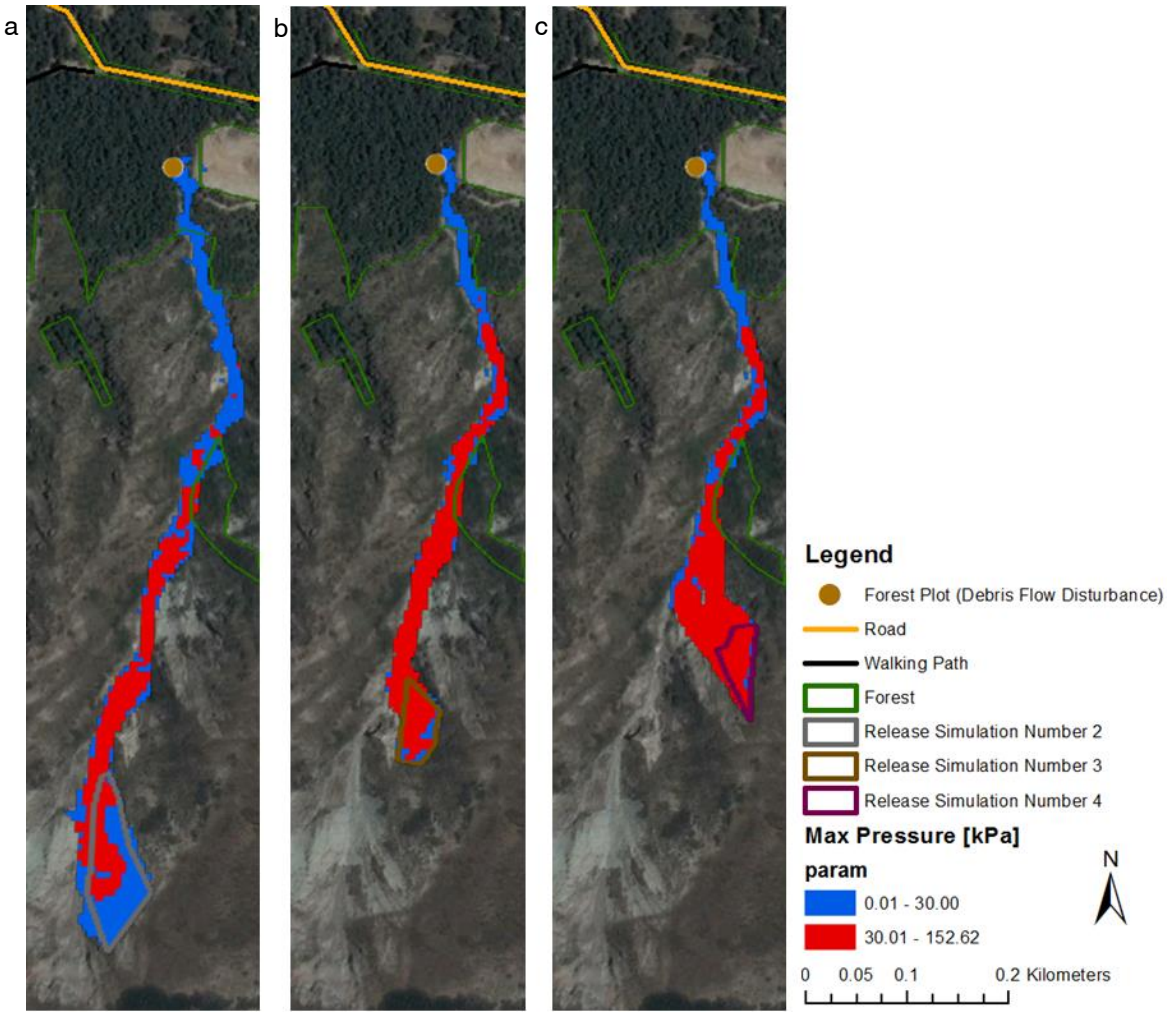

Figure 30: Comparison of simulation number 2 (a), simulation number 3 (b) and simulation number 4 (c) in debris flow track 4 (df4).

In **avalanche track five (av5)** for 100-year events no major release areas are possible, because the flow direction would change (Table 15). The release area is just above the road and the snow would simply slide down to the road.

Table 15: Input parameters and results of RAMMS simulations in avalanche track 5 (av5).

Number	Return period [years]	Release area [m²]	Release height [m]	Max velocity [m/s]	Max flowheight [m]	Max pressure [kPa]	Forest destruction
1	10	500	0.5	17.38	1.13	90.71	no
2	10	1250	0.5	23.17	2.24	161.19	no
3	100	500	1	18.05	1.85	97.78	no

In **avalanche track 6 (av6)** informations for potential avalanche years is available from tree cores (Table 16). In this track, two different approaches were tested to show how much pressure is necessary for trees to respond to avalanches. First the 30 kPa-pressure approach is tested in different runout zones for the specific years (Fig. 31). In simulation number 2, 3 and 4, only the release height is adapted to extend the runout zone of an avalanche with the 30 kPa-pressure approach. A larger release area and higher release heights are drawn to extend the

runout zone and the 30 kPa-pressure zone (simulation number 5). For this approach quite small release areas are necessary.

Table 16: Input parameters and results of RAMMS simulations in avalanche track six (av6). The simulations are differentiated in examples with the 30 kPa-pressure and tree destruction approach.

Number	Return period [years]	Release area [m²]	Release height [m]	Max velocity [m/s]	Max flowheight [m]	Max pressure [kPa]	Forest destruction	approach	avalanche year
1	10	3325	0.9	23.01	1.93	158.88	no		
2	10	1500	0.3	20.81	1.11	129.97	no	30 kPa-pressure	2011
3	10	1500	0.4	22.27	1.36	148.88	no		2005,1980,1968
4	10	1500	0.5	20.922	1.51	131.321	no		1989,1983,1951
5	10	3325	0.7	25.65	2.74	197.41	yes		years over street
6	10	3325	0.9	27.08	3.29	220.07	no		years over street
7	10	4475	0.5	24.51	2.66	180.33	yes	tree destruction	2011
8	10	9125	0.5	28.02	4.08	235.54	yes		2005,1980,1968
9	10	9125	0.8	31.92	5.56	305.82	yes		1989,1983,1951
10	10	12175	0.5	27.63	5.06	229.17	yes		years over street
11	10	15875	1	35.17	7.83	371.13	yes		years over street
12	100	15875	1	35.91	8.01	385.89	yes		years over street

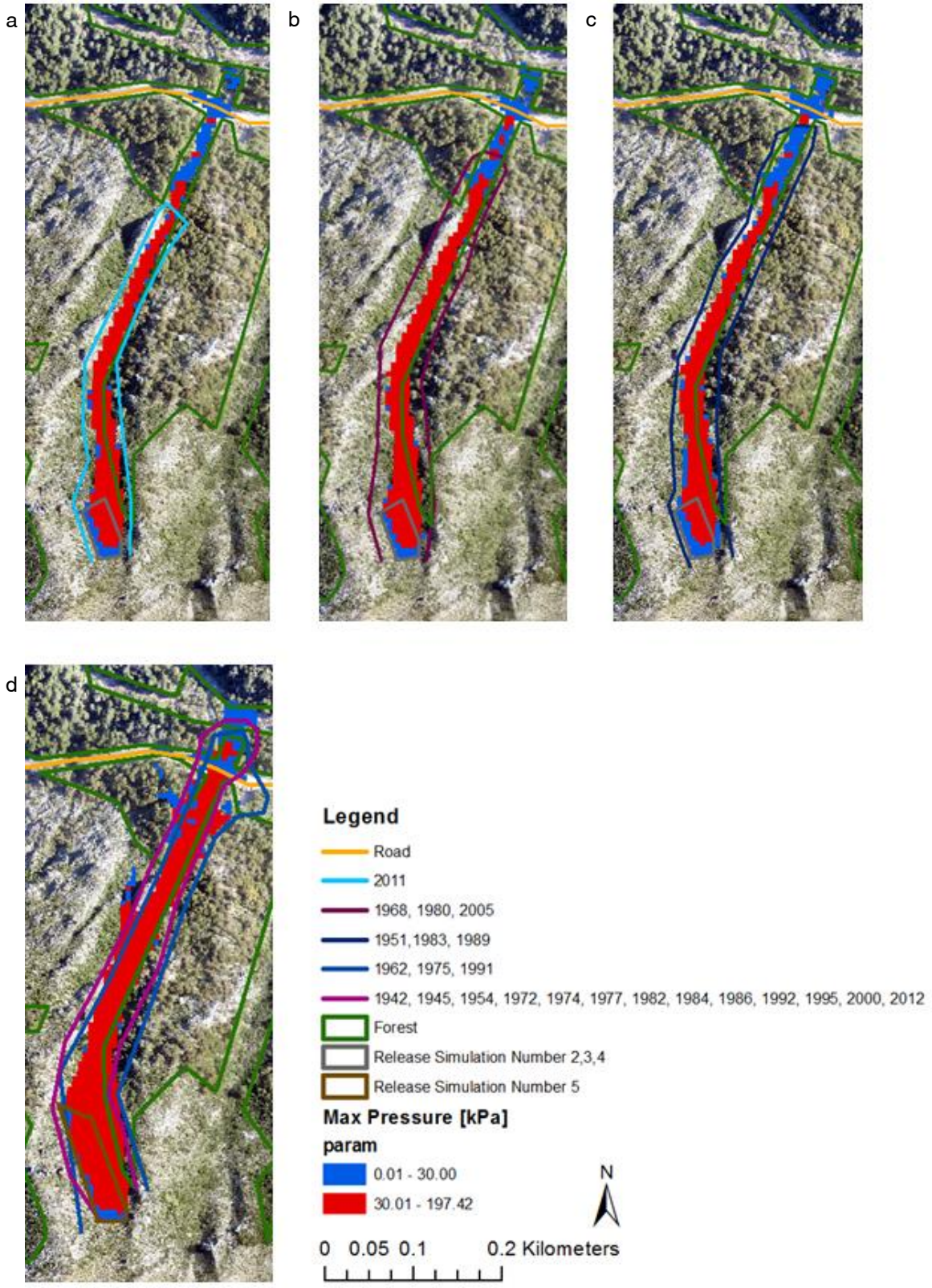

Figure 31: Comparison of different maximum pressures to reach the specific runout distance with the 30 kPa-pressure approach. In avalanche track 6 (av6), simulation number 2(a), 3(b), 4(c) and 5(d) are displayed.

With the tree destruction approach, the most remote tree destruction areas correspond to the runouts of avalanches. Different sizes of release areas and different snow depths were simulated to reach the different runouts (Fig. 32). Simulation number 10 fits best because it

simulates the runouts of the most frequent avalanches. No simulation was able to destroy trees below the road.

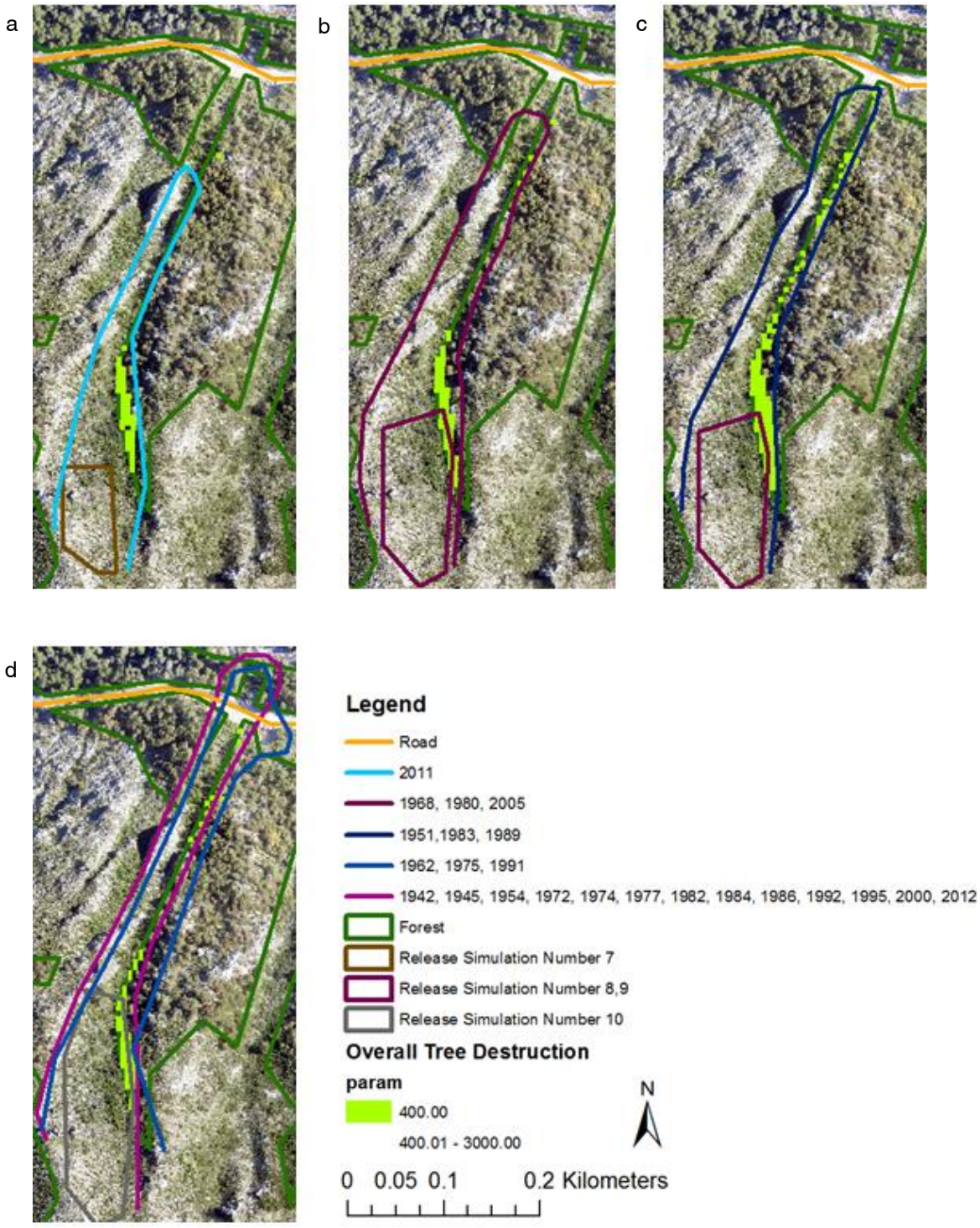

Figure 32: Different release areas and release heights to reach the specific runout distance with the tree destruction approach. In avalanche track 6 (av6) simulation number 7(a), 8(b), 9(c), and 10(d) are displayed from left to right.

The release areas of simulations in **avalanche track 7 (av7)** with a higher return period had a larger extent (Table 17). The release area of simulations with a 10-year return period cannot be

drawn larger, because otherwise forest in places withouth signs of avalanches would be destroyed.

Table 17: Input parameters and results of RAMMS simulations in avalanche track 7 (av7).

Number	Return period [years]	Release area [m²]	Release height [m]	Max velocity [m/s]	Max flowheight [m]	Max pressure [kPa]	Forest destruction
1	10	3750	0.5	20.45	2.29	125.57	no
2	10	1475	0.5	19.51	1.2	114.3	no
3	10	1575	0.5	17.67	1.24	93.72	no
4	10	13625	0.5	28.87	4.72	250.1	yes
5	100	26550	1	35.32	14.14	374.26	yes

The comparison of field observation and avalanche simulations in **avalanche track 8** (av8) shows the best agreement for simulation number two (Table 18).

Table 18: Input parameters and results of RAMMS simulations in avalanche track 8 (av8).

Number	Return period [years]	Release area [m²]	Release height [m]	Max velocity [m/s]	Max flowheight [m]	Max pressure [kPa]	Forest destruction
1	10	2250	0.5	19.47	2.62	113.83	no
2	10	10775	0.5	22.77	6.73	155.6	yes
3	10	29750	0.5	26.93	8.62	217.58	yes
4	100	49575	1	38.21	20.26	438.01	yes

In **avalanche track 9 (av9),** information for potential avalanche years is available from the tree cores (Table 19). The spatial arrangement of the affected trees indicates a release area on the right side where the avalanche flows through the forest. For track 9, both approaches to detect tree response were tested. Again, the 30 kPa-approach worked only for quite small release areas (Fig. 33).

Table 19: Input parameters and results of RAMMS simulations in avalanche track nine (av9). The simulations are differentiated in examples with the 30 kPa-pressure and tree destruction approach.

Number	Return period [years]	Release area [m²]	Release height [m]	Max velocity [m/s]	Max flowheight [m]	Max pressure [kPa]	Forest destruction	approach	avalanche year
1	10	975	0.5	18.48	2.17	102.52	yes		
2	10	1750	0.5	18.94	3.1	107.65	yes		
3	10	8525	0.5	23.01	10.35	158.84	yes		
4	10	375	0.5	14.38	0.69	62.09	no		
5	10	1200	0.5	18.74	1.77	105.44	no		
6	10	1100	0.3	18.14	2.3	98.79	no	30 kPa-pressure	2012
7	10	625	0.4	14.96	1	67.21	no		1991,2010,2011
8	10	1250	0.6	16.22	2.78	79	no		1983, 2002
9	10	1250	0.8	18.31	3.52	100.59	no		1995, 2000
10	10	38200	0.5	29.04	9.41	253.02	yes	tree destruction	2012
11	100	38200	1	38.99	15.51	456.06	yes		1991,2010,2011
12	10	11725	0.5	22.02	10.93	145.53	yes		
13	10	9300	0.5	22.65	7.13	153.94	yes		2002,1983
14	10	10675	1	25.68	10.94	197.91	yes		1995, 2000
15	100	15275	1	27.97	12.32	234.8	yes		

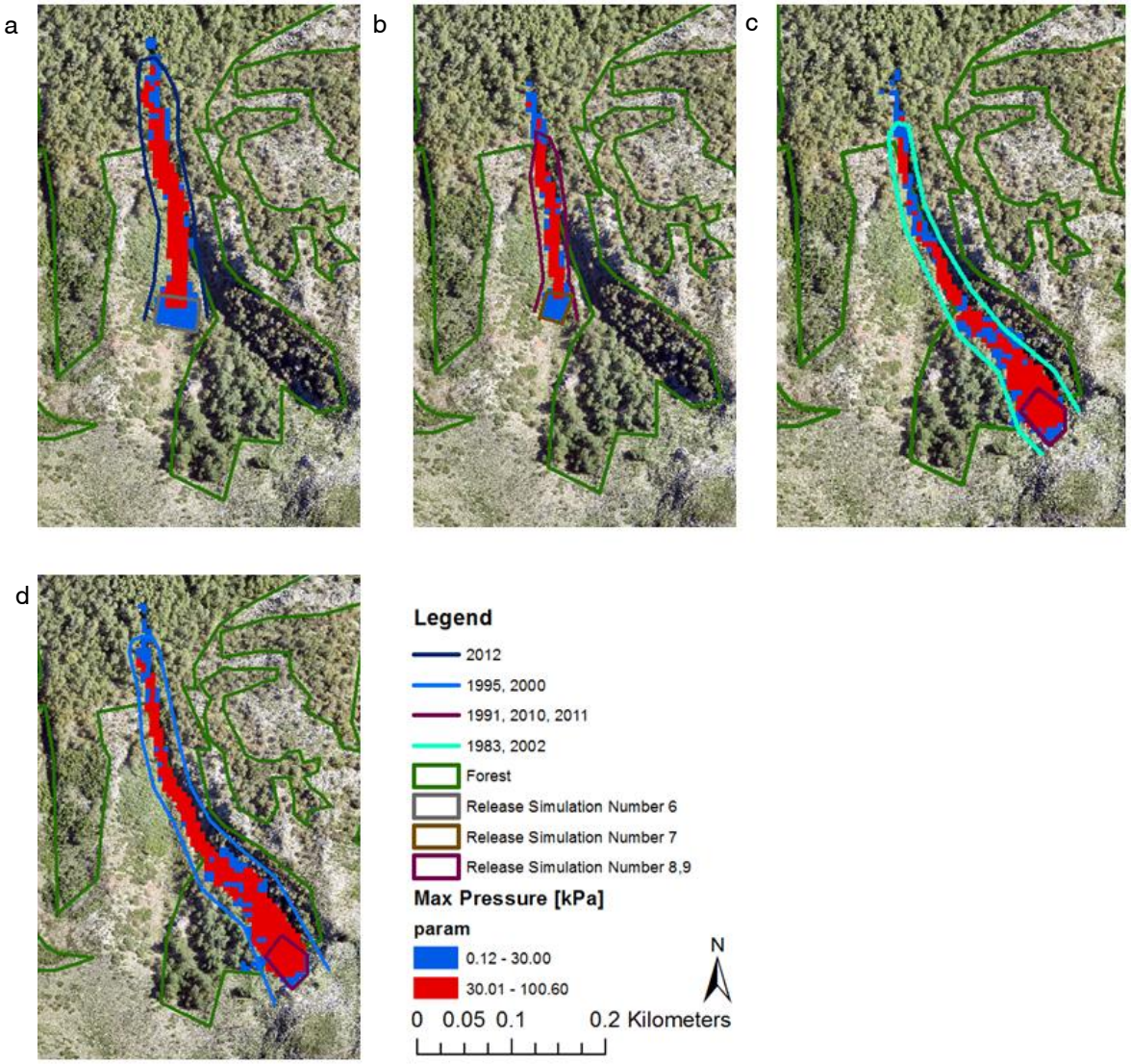

Figure 33: Comparison of different maximum pressures to reach the specific runout distance with 30kPa-pressure approach. In avalanche track 9 (av9) simulation number 6(a), 7(b), 8(c) and 9(d) are displayed from left to right.

Simulations number 10 and 11 produced big release areas with two different runouts in track number 8 and 9 (Fig. 34). Smaller release areas with runouts only in track 9 are possible, but are not strong enough to destroy trees in the observed places.

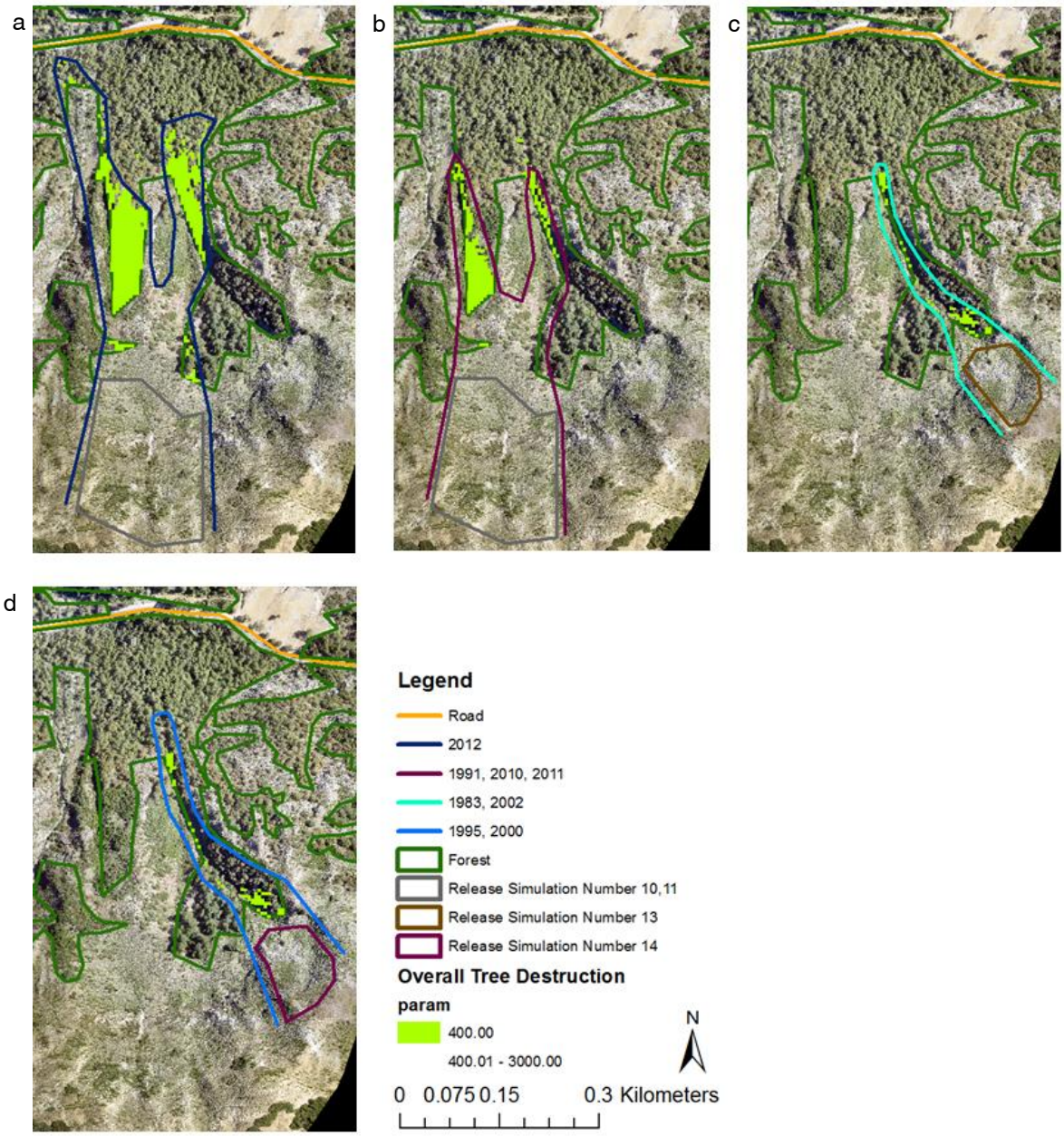

Figure 34: Different release areas and release heights to reach the specific runout distance with the tree destruction approach. In avalanche track 9 (av9) simulations number 10(a), 11(b), 13(c), 14(d) are shown from left to right.

The avalanche in **avalanche track 10 (av10)** was not visible from arial pictures. The snow slides through the forest to the road (Table 20). Release areas in higher parts of the area are not possible because no signs of avalanches are observed in the forest structure and the slope angle is too low.

Table 20: Input parameters and results of RAMMS simulations in avalanche track 10 (av10).

Number	Return period [years]	Release area [m²]	Release height [m]	Max velocity [m/s]	Max flowheight [m]	Max pressure [kPa]	Forest destruction
1	10	575	0.5	12.14	1.45	44.26	no
2	10	725	0.5	16.78	0.85	84.5	no
3	100	3825	0.5	18.74	5.14	105.42	no
4	100	3825	1	25.24	8.52	191.15	yes

The avalanche in **avalanche track 11 (av11)** is also not visible from arial pictures. It is also possible that this runout is caused by avalanche track 13, which could have two different runouts (Table 21). There are no signs of tree destruction visible in the forest. The simulations were done with small snow slides. A big avalanche release from a 100-year event is rather unrealistic because of the knobby terrain in this area.

Table 21: Input parameters and results of RAMMS simulations in avalanche track 11 (av11).

Number	Release area [m²]	Release height [m]	Return period [years]	Max velocity [m/s]	Max flowheight [m]	Max pressure [kPa]	Forest destruction
1	575	0.5	10	14.85	1.24	66.2	no
2	275	0.5	10	13.65	1.5	55.93	no
3	13125	1	100	31.11	10.88	290.36	yes

It was excpected that in **avalanche track 12 (av12),** this avalanche has the same runout as avalanche track number 13. Several simulations did not support this assumption. The avalanches flowed in directions where no signs of former avalanches were detected during field observations. Therefore, no release zone in this area was drawn.

In **avalanche track 13 (av13)** two different release areas above each other are possible (Table 22). It isn't possible to combine these two release zones because in the middle part the terrain is not steep enough and forested. Simulations number 1, 2, 3, 5 and 8 have a release area above this afforested part. All these simulations have one main flow direction and runout. Apart from the main flow direction, the snow in simulation number 8 also flows on a broad range (Fig. 35). To get only one runout, a release area under the forest is drawn (simulation number 4). Field observations and simulations showed that simulation number 5 is the most realistic version. The flow directions of these two simulations are quite similar. The larger release area and release height in simulation number 8 causes a higher flow height and also higher accumulations in the runout. The runout distance is almost the same.

Table 22: Input parameters and results of RAMMS simulations in avalanche track 13 (av13).

Number	Return period [years]	Release area [m²]	Release height [m]	Max velocity [m/s]	Max flowheight [m]	Max pressure [kPa]	Forest destruction
1	10	7500	0.5	22.18	4.94	247.6	yes
2	10	1175	0.5	21.74	1.31	141.89	yes
3	10	400	0.5	17.2	0.91	88.78	no
4	10	2550	0.5	16.72	2.72	83.94	no
5	10	8400	0.5	21.42	3.65	137.7	yes
6	100	17200	0.5	25.81	7.64	199.92	yes
7	100	17200	1	28.23	12.73	239.13	yes

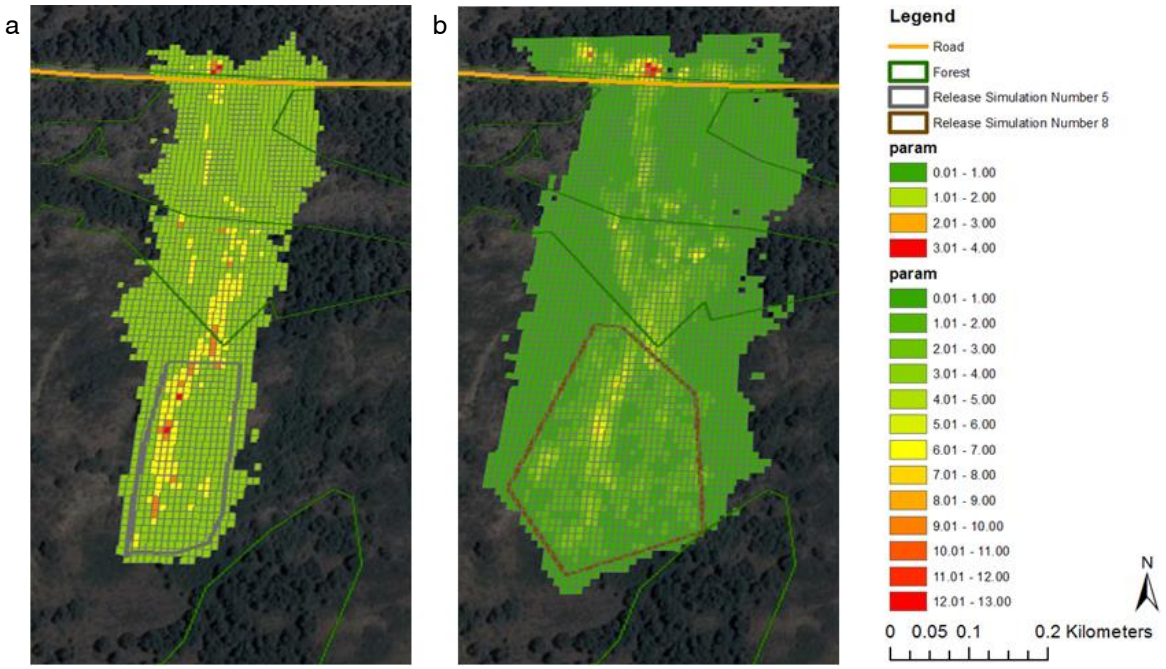

Figure 35: Maximum flow height [m] in simulation number 5 (a, 10 years event) and 8 (b, 100 years event) in avalanche track 13 (av13).

This snow slide in **avalanche track 14 (av14)** was also not visible from the interpretation of arial pictures. From the interpretation of the topography, two different release areas are possible (Table 23). It isn't possible to combine these two release areas because they are diagonal to each other and the middle part is too flat. For a possible 100-year event a larger release area is drawn.

Table 23: Input parameters and results of RAMMS simulations in avalanche track 14 (av14).

Number	Release area [m²]	Release height [m]	Return period [years]	Max velocity [m/s]	Max flowheight [m]	Max pressure [kPa]	Forest destruction
1	2250	0.5	10	18.58	4.45	103.67	no
2	1150	0.5	10	17.28	1.01	89.65	no
3	5475	0.5	100	16.81	4.92	84.86	no

Avalanche track 15 (av15) was not visible from the interpretation of arial pictures. However, there are no signs of avalanche disturbances in the forest. Therefore, only the sliding down of snow from above the road is possible (Table 24).

Table 24: Input parameters and results of RAMMS simulations in avalanche track 15 (av15).

Number	Release area [m²]	Release height [m]	Return period [years]	Max velocity [m/s]	Max flowheight [m]	Max pressure [kPa]	Forest destruction
1	500	0.5	10	14.22	2.11	60.7	no
2	1800	0.5	10	20.58	1.34	127.08	yes
3	500	1	100	15.25	3.7	69.79	no

The release area in **avalanche track 16 (av16)** is restricted by forests and located directly above the road. For different return periods only the release height can be changed (Table 26).

Table 25: Input parameters and results of RAMMS simulations in avalanche track 16 (av16).

Number	Release area [m²]	Release height [m]	Return period [years]	Max velocity [m/s]	Max flowheight [m]	Max pressure [kPa]	Forest destruction
1	325	0.5	10	11.59	0.66	40.31	no
2	325	1	100	12.75	1.18	48.82	no

Also in **avalanche track 17 (av17)** the release area is restricted by forests and located directly above the road. For different return periods only the release height can be changed (Table 26). The maximum pressure for a 10-year return period and for a 100-year return period is slightly different (Fig. 36). As an example which outputs RAMMS can create, a plot with the flow height is shown. Most of the snow is accumulated on the road (Fig. 37).

Table 26: Input parameters and results of RAMMS simulations in avalanche track 17 (av17).

Number	Release area [m²]	Release height [m]	Return period [years]	Max velocity [m/s]	Max flowheight [m]	Max pressure [kPa]	Forest destruction
1	1000	0.5	10	14.87	2.82	66.34	no
2	1000	1	100	17.83	4.58	95.41	no

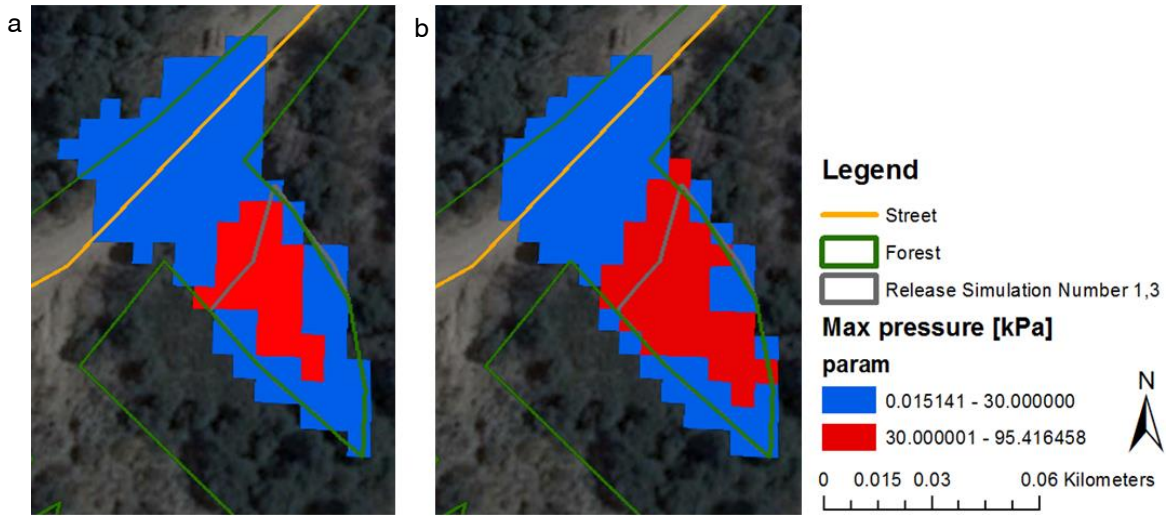

Figure 36: Comparison of the maximum pressure of an event with a 10 (a, simulation number one) and 100-year (b, simulation number three) return period in avalanche track 17 (av17).

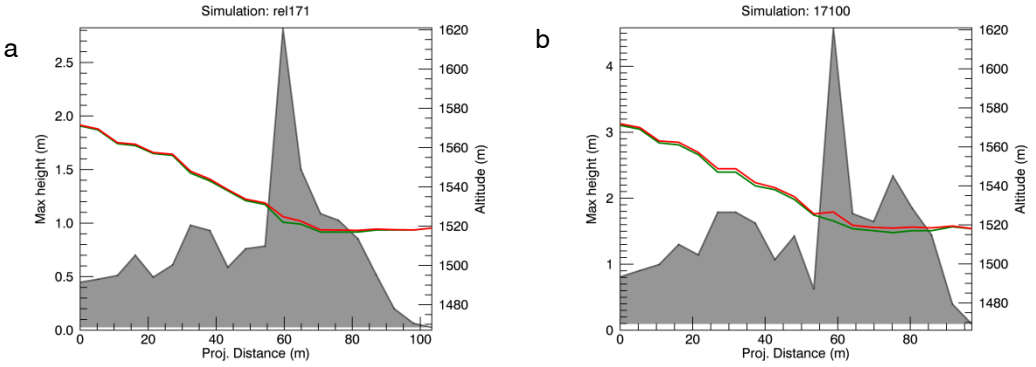

Figure 37: RAMMS profile output: Comparison of flow height [m] in simulation number 1 (rel171,a) and simulation number 3 (17100,b). The green line shows the altitude. The red line displays the altitude plus the maximum flow height. The peak of each plot shows the snow accumulation on the road. The higher release height in simulation number 3 causes a higher maximum snow height on the road.

It was excpected that in **avalanche track 18 (av18)** there would be a side track and this avalanche would have the same runout as avalanche track number 18. However, different avalanche simulations showed that this avalanche just collapses in the channel and doesn't propagate. In simulation number 2 and 3 the release area from number 1 is divided in two different parts (Table 28). The simulations almost doesn't reach the area where the forest plot is. Only simulation number 5 with a return period of 100-year and a release height of 1 meter can reach the road (Fig. 39).

Table 27: Input parameters and results of RAMMS simulations in avalanche track 18 (av18).

Number	Release area [m²]	Release height [m]	Return period [years]	Max velocity [m/s]	Max flowheight [m]	Max pressure [kPa]	Forest destruction
1	5000	0.5	10	19.99	4.25	119.98	no
2	1725	0.5	10	13.51	2.64	54.81	no
3	1000	0.5	10	11	2.06	36.32	no
4	5000	1	100	27.17	7.16	221.53	yes

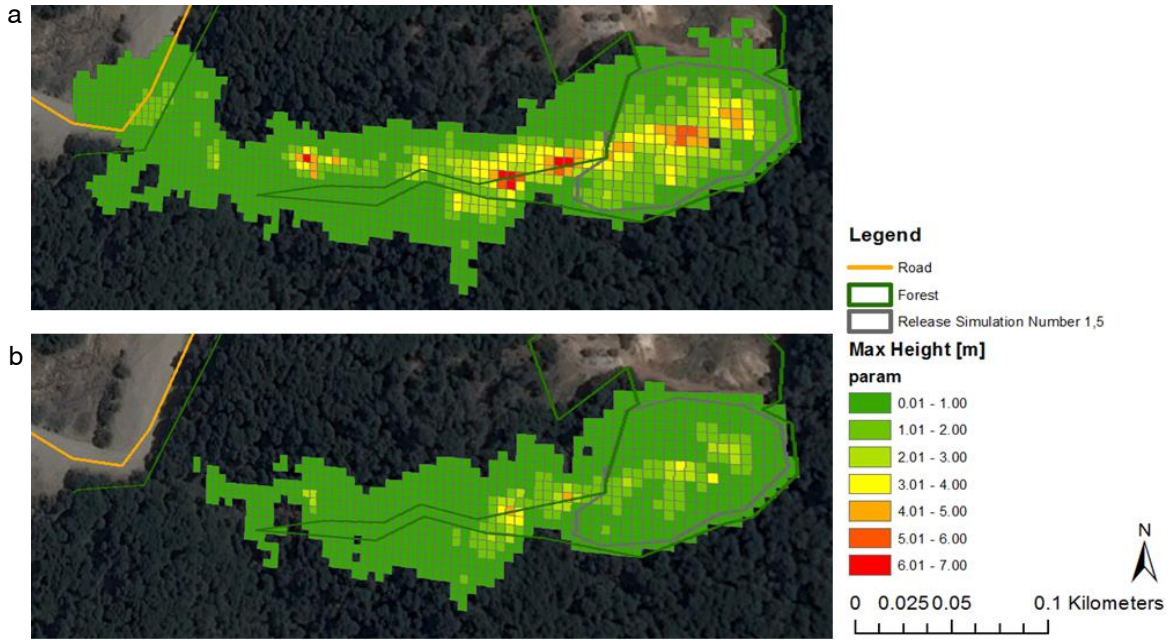

Figure 38: Comparison of the flow height [m] of simulation number 1 (a, 10-year event) and 5 (b, 100-year event) in avalanche track 18 (av18).

The definition of potential release areas to simulate realistic avalanches is specific to each track and depends on the local conditions. According to the avalanche classification used in RAMMS, most of the avalanches with a return period of 10 years are classified as minor/small avalanches (Christen et al., 2010). Depending on the track, the size of 100-year event avalanches varies from very small to large avalanches.

3.5 Influence of forest on avalanches

Avalanches are influenced by forests. To illustrate this influence on avalanches, simulations without forests are conducted. The following figures show the effect of forests. First, the effect of forest for all avalanche tracks is shown, before individual tracks are shown in particular. In specific avalanche tracks the impact of additional afforested parts is tested. In avalanche simulations with a 10-year return period, the spatial extent of runouts in scenarios without forest is 24% larger than in scenarios with forest (Fig. 39). Also the maximum pressure [kPa] and the flow height on the road or walking path increases by 19% and 20%, respectively. In total, 90% of the avalanche tracks reach the road or the walking path. Compared to scenarios with forest, this is a total inrcrease of 27%.

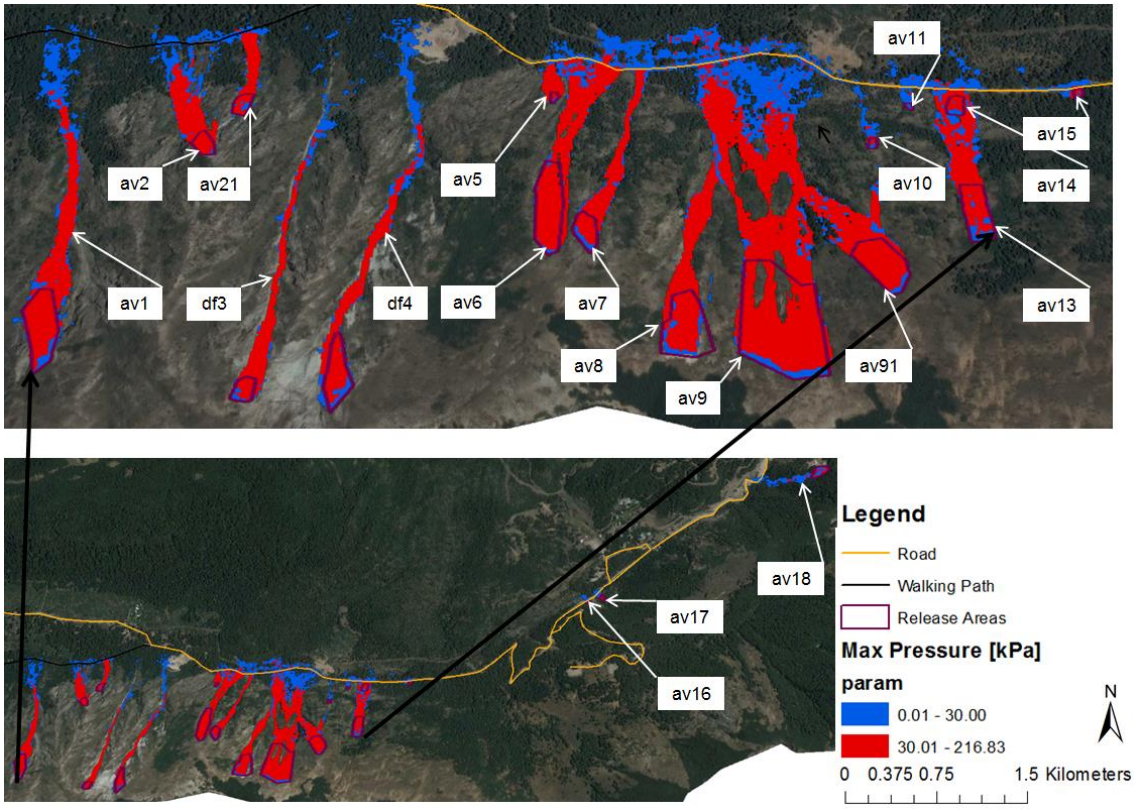

Figure 39: The maximum pressure of avalanches with a 10-year event scenario withouth forest. Hotels and ski stations are located in Termas between avalanche track 17 (av17) and avalanche track 18 (av18).

For 100-year events, the spatial extent of runouts is in average 14% larger in simulations without forest (Fig. 40). The maximum pressure and flow height on the road or walking path increase by 24% and 22%, respectively. With these scenarios all avalanche paths reach the road, which is an increase of 6% compared to simulations with forest. If we compared 10-year events with 100-year events, a slightly stronger influence of scenarios without forest in 100-year events can be seen for the maximum pressure and the flow height on the road or walking path (5 and 2 %, respectively). Also 6% more of the tracks reach the road. The important influence of forest to the runout distance, flow height and maximum pressure is also displayed in two specific tracks. These calculations are made in all avalanche tracks but are only shown in these two best investigated examples.

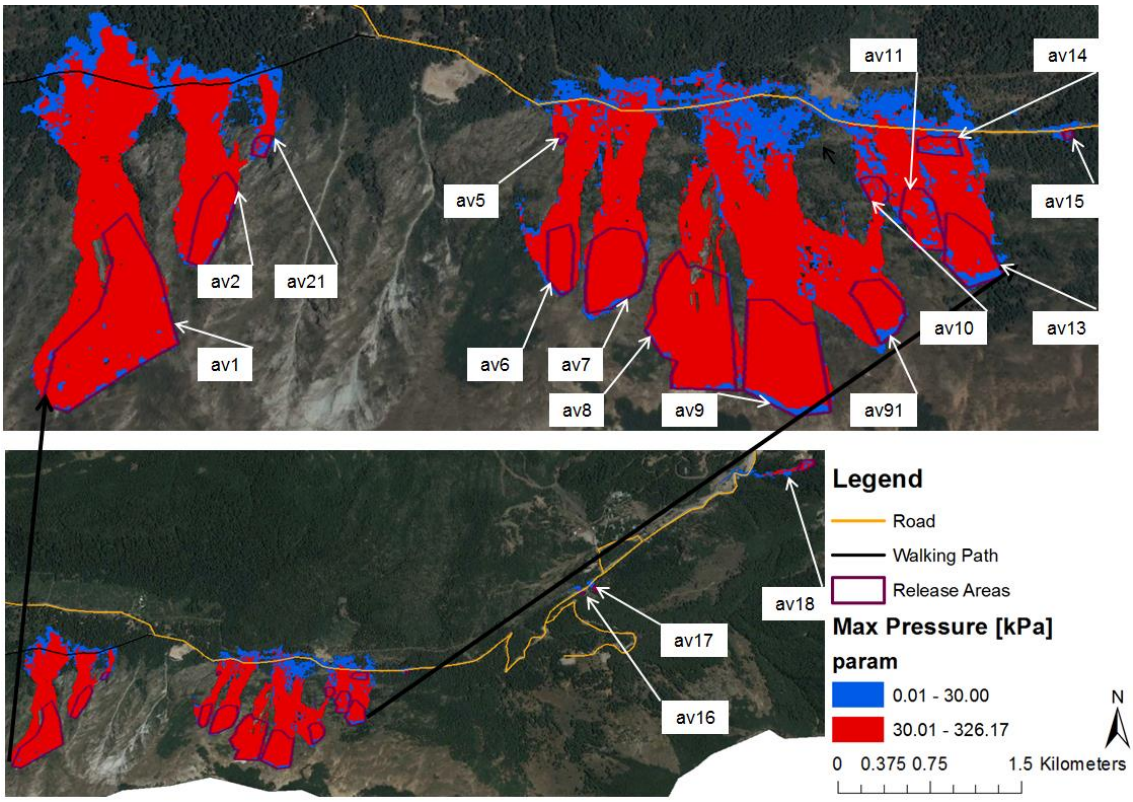

Figure 40: The maximum pressure of avalanches with a 100-year event scenario withouth forest. Hotels and ski stations are located in Termas between avalanche track 17 (av17) and avalanche track 18 (av18).

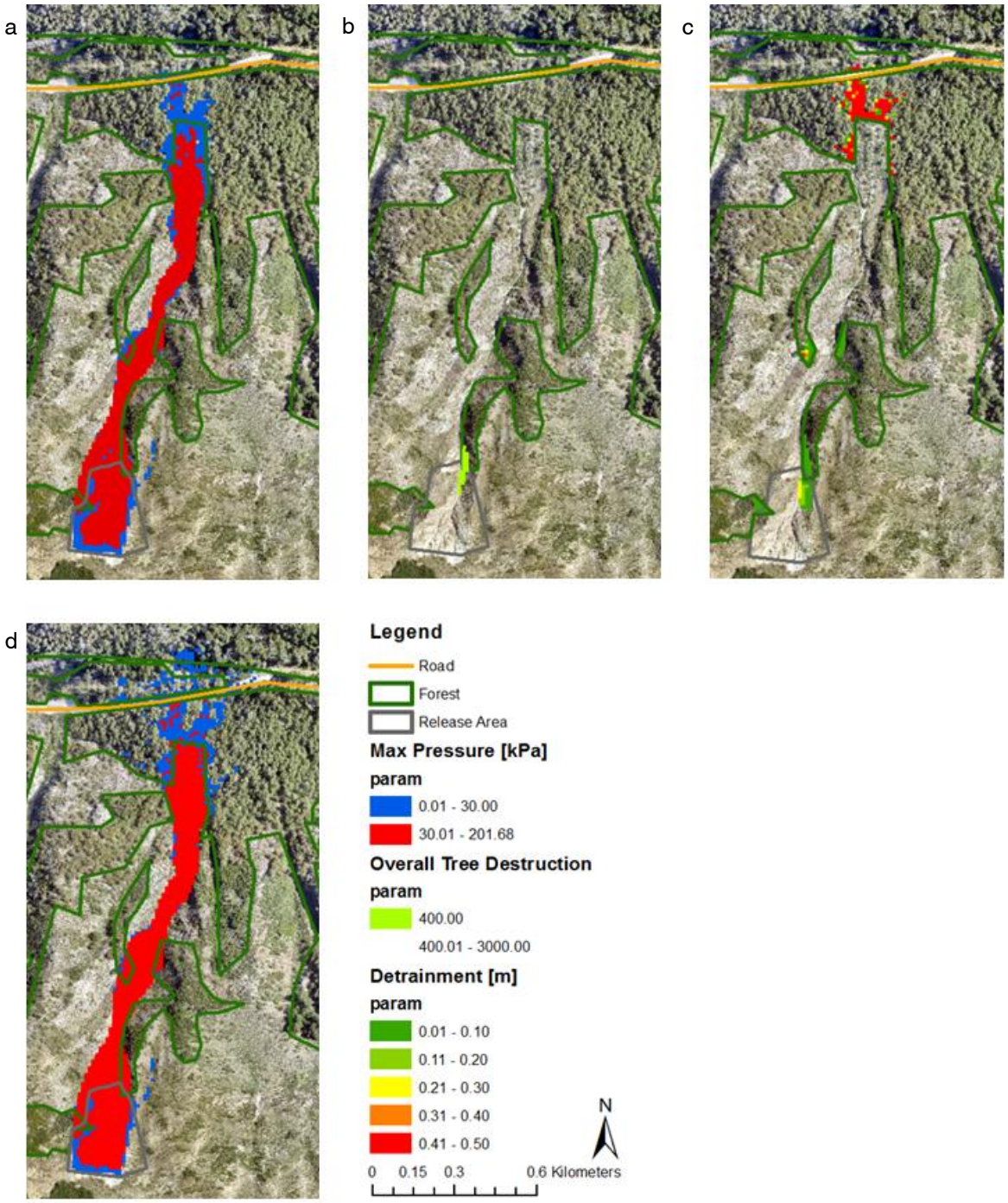

Figure 41: From left to right avalanche simulations in avalanche track 8 (av8) with a 10-year return period: maximum pressure of an avalanche scenario with forest (a), area where forest is destroyed (b), detrainment in the forest (c) and the maximum pressure of an avalanche scenario without forest (d).

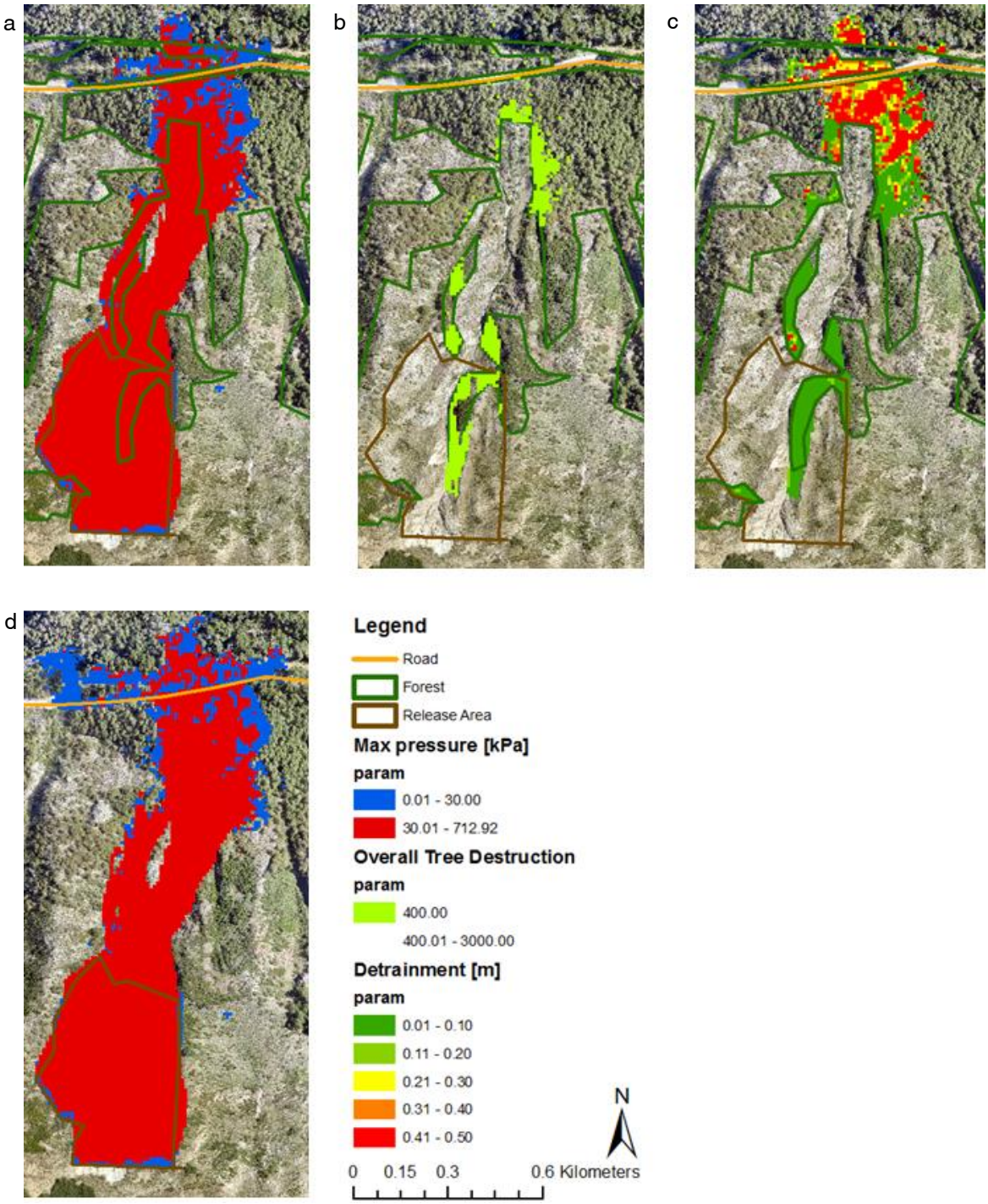

Figure 42: From left to right avalanche simulations in avalanche track 8 (av8) with a 100-year return period: maximum pressure of an avalanche scenario with forest (a), area where forest is destroyed (b), detrainment in the forest (c) and the maximum pressure of an avalanche scenario without forest (d).

The spatial extent of a 10-year return period avalanche scenario in **avalanche track 8 (av8)** without forest is 18% larger and leads to an increase of the maximum pressure on the road of 33%. Also the flow height on the road is 37% higher in scenarios without forest (Fig. 41). In 100-year events, the spatial extent of the runout of an avalanche scenario without forest is 9% larger and the maximum pressure on the road is 33% higher in this specific track (Fig. 42). The flow

height on the road is 11% higher in scenarios without forest. The same trends can be observed in avalanche track 9 (av91).

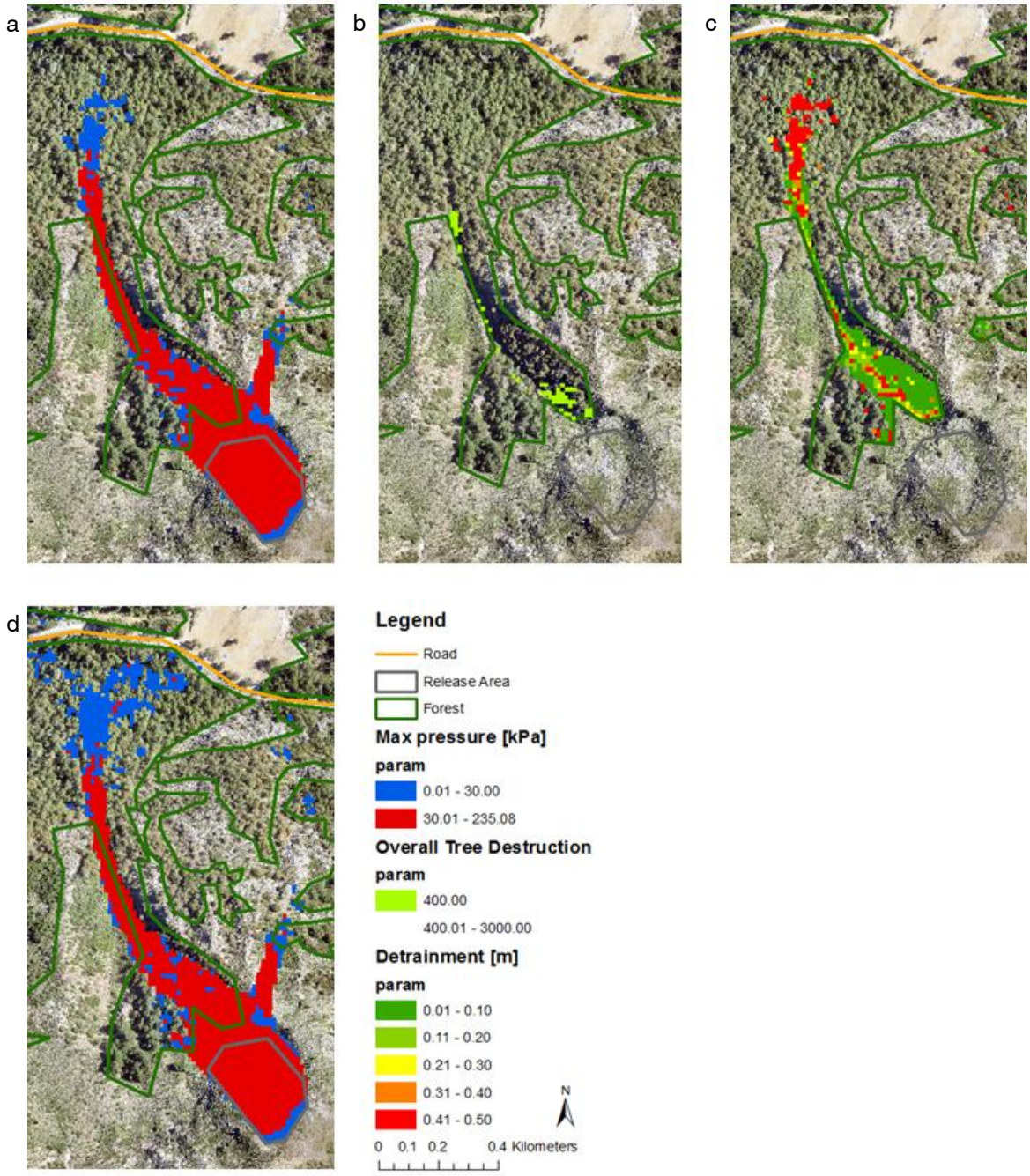

Figure 43: From left to right avalanche simulations in avalanche track 9 (av91) with a 10-year return period: maximum pressure of an avalanche scenario with forest (a), area where forest is destroyed (b), detrainment in the forest (c) and the maximum pressure of an avalanche scenario without forest (d).

For a 10-year event in **avalanche track 9 (av91),** the spatial extent of an avalanche scenario without forest is 19% larger. The runouts with and without forest don't reach the road. For a 100-year return period, the spatial extent of an avalanche scenario without forest is 23% larger and only an avalanche simulation without forest reaches the road.

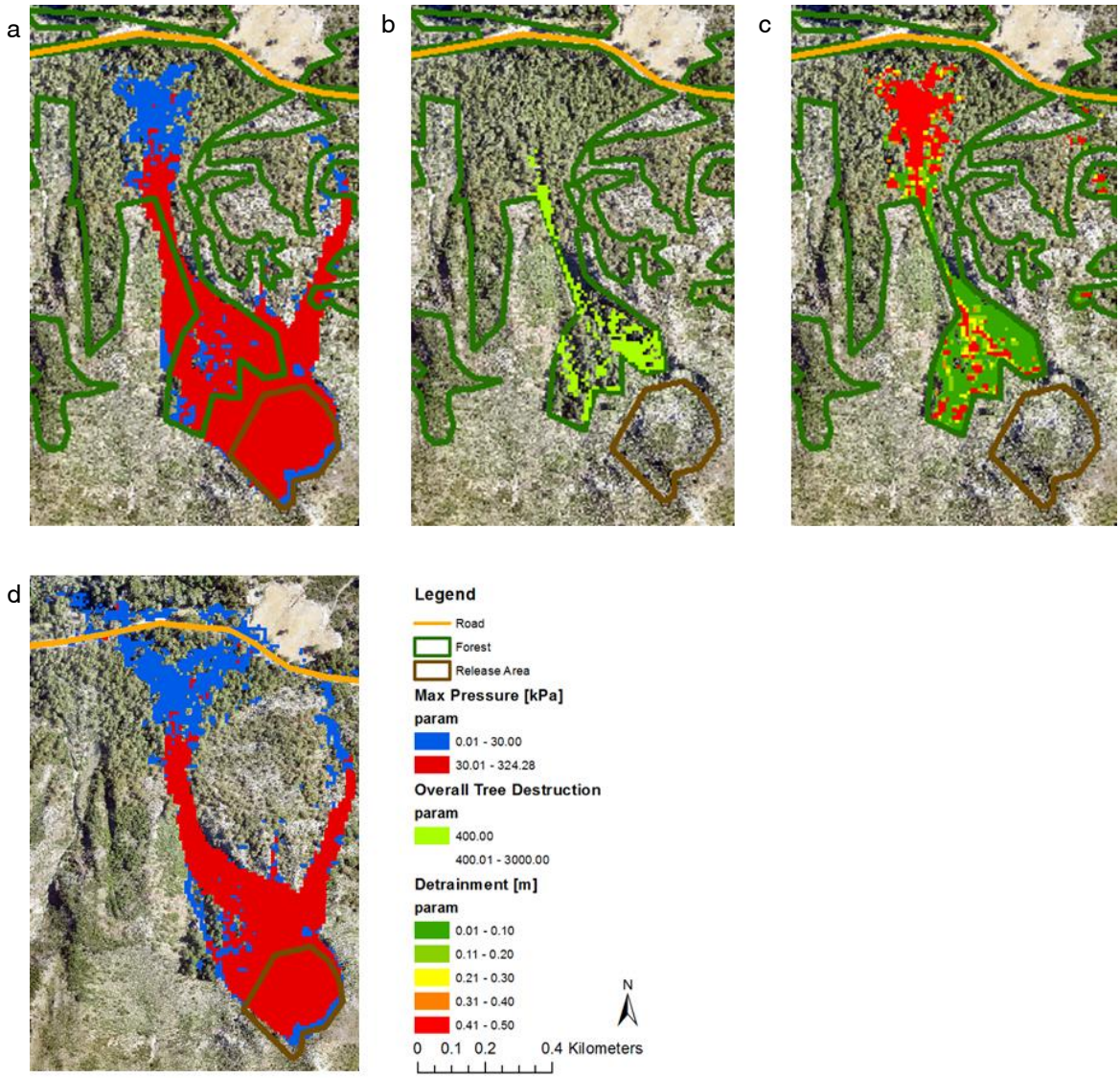

Figure 44: From left to right avalanche simulations in avalanche track 9 (av91) with a 100-year return period: maximum pressure of an avalanche scenario with forest (a), area where forest is destroyed (b), detrainment in the forest (c) and maximum pressure of an avalanche scenario without forest (d).

3.5.1 Afforestation

The effect of possible afforestations and their impact on avalanches is shown in two avalanche tracks which often release and afforestations would have the biggest impact. The assumption is that the newly grown forest has the same diameter as the old forest. Afforestations lead to a reduction of the maximum pressure on the road. The maximum pressure from a simulation in **avalanche track 6 (av6)** with additional afforestation is reduced by 24 % (Fig. 45). The avalanches can still reach the road and the runout extent is 5 % smaller. The flow height on the road remains the same. In avalanche track 6 (av6) only simulations with a 10-year return period were done.

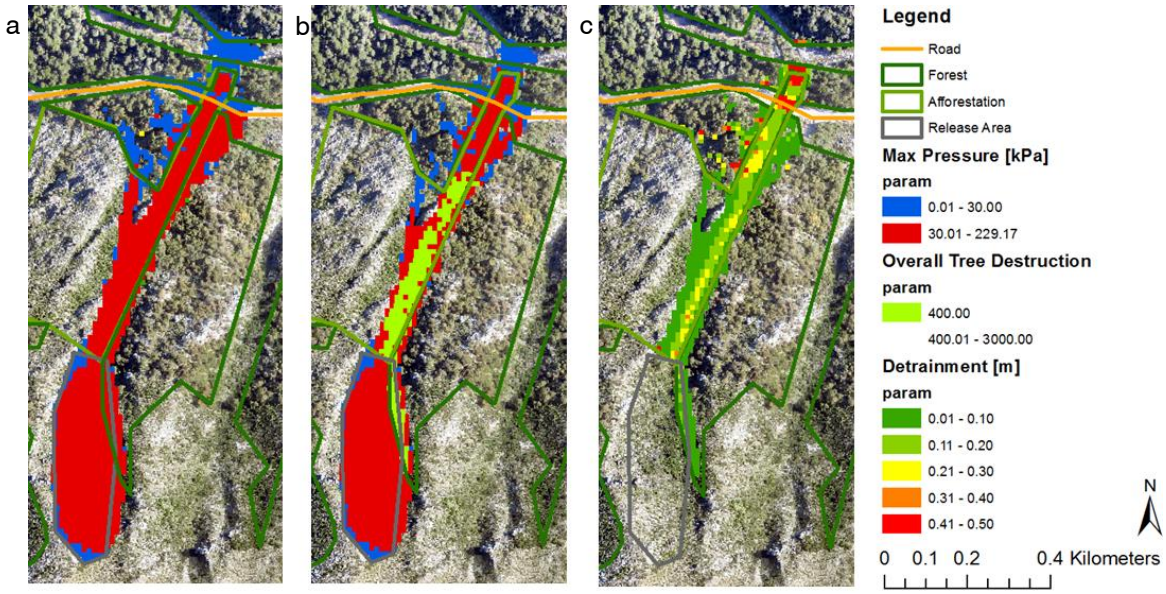

Figure 45: From left to right impact of additional afforestation in avalanche track 6 (av6) with a 10-year return period: maximum pressure in an avalanche simulation without additional forests (a), maximum pressure and overall tree destruction in an avalanche simulation with additional forest (b), detrainment in an avalanche simulation with additional forest (c).

With a 10-year event in **avalanche track 7 (av7)** no tree destruction happens with additional forests (Fig. 46). The detrainment leads to a slightly smaller runout zone (5%) and also to a decrease of the maximum pressure (7%) on the road. Because in the past only two events happened, a simulation with a return period of 100-year was conducted as well. Tree destruction and the detrainment in the additional forest lead to a reduction of the maximum pressure by 14%. The spatial extent almost remains the same (1% smaller) and the flow height is 6% lower on the road for scenarios with additional afforestation (Fig. 47).

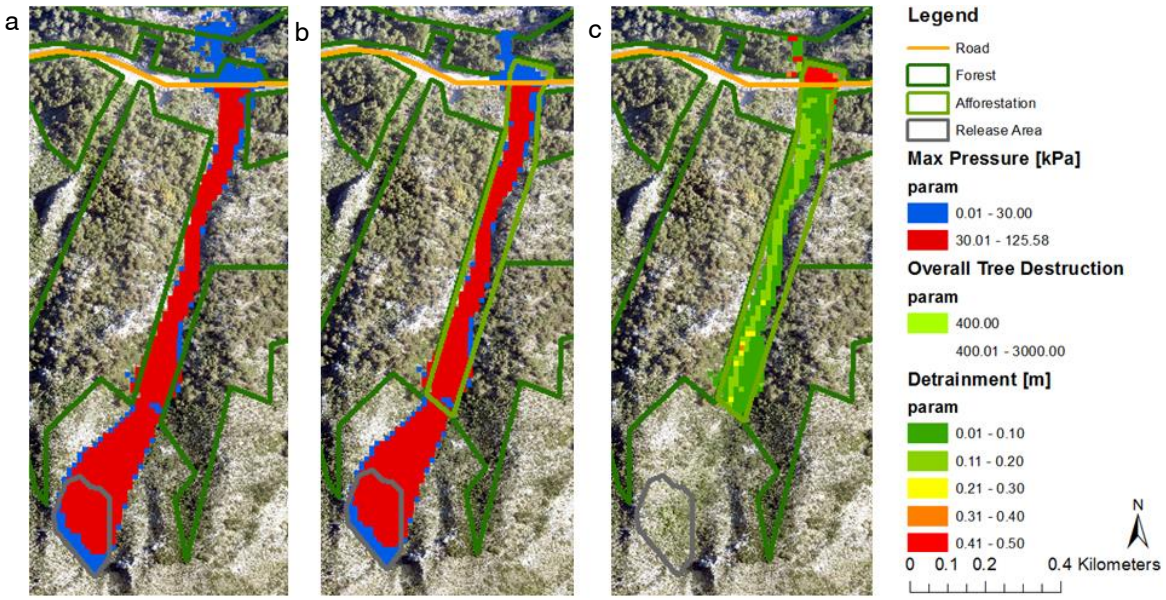

Figure 46: From left to right impact of additional afforestation in avalanche track 7 (av7) with a 10-year return period: maximum pressure in an avalanche simulation without additional forests (a), maximum pressure and overall tree destruction in an avalanche simulation with additional forest (b), detrainment in an avalanche simulation with additional forest (c).

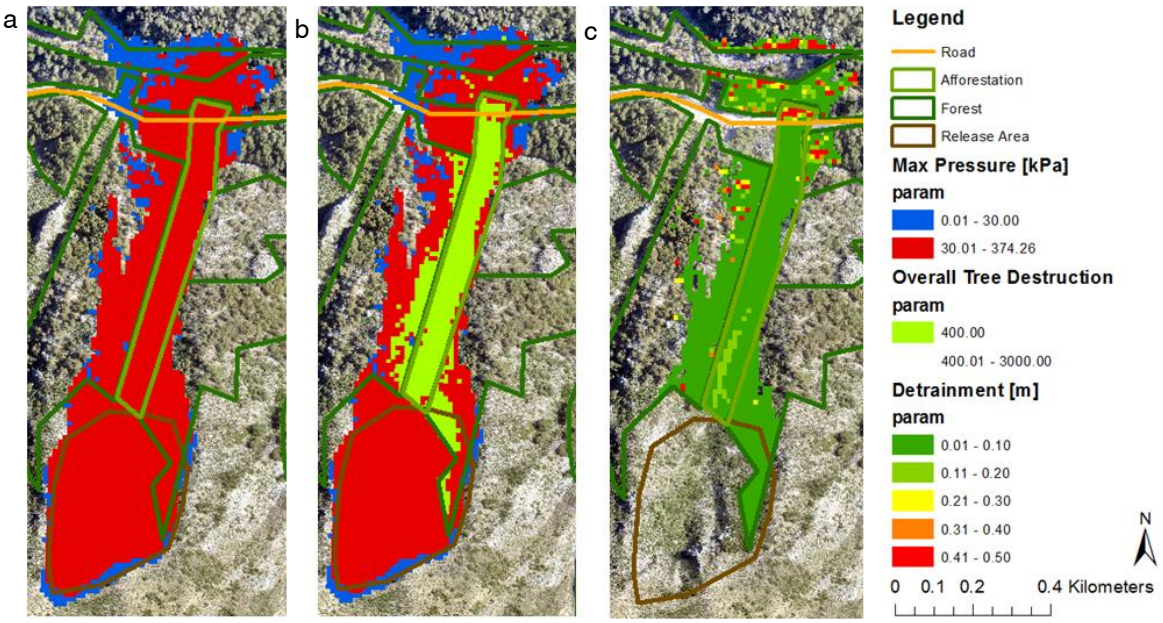

Figure 47: From left to right impact of additional afforestation in avalanche track 7 (av7) with a 100-year return period: maximum pressure in an avalanche simulation without additional forests (a), maximum pressure and overall tree destruction in an avalanche simulation with additional forest (b), detrainment in an avalanche simulation with additional forest (c).

4 Discussion

The forest structure in Nevados de Chillán is influenced by debris flow and avalanche disturbances and plays an important role for risk reduction. The slope between Las Trancas and Las Termas has a rich event history with frequent avalanche and debris flow events which are able to reach the street. The spatio-temporal patterns of avalanches was reconstructed with dendrogeomorphic approaches. Release areas are defined through the combination of avalanche simulations with dendrogeomorphic information. To analyse the growth anomalies first the geomorphic processes was identified with remote sensing data.

The analysis of remote sensing data showed that different disturbances are present in the investigation area. Avalanches, mud avalanches, landslides, debris flows and rockfalls are disturbances which were detectable with remote sensing data. The available satellite images and aerial photographs had a limited resolution. The best available data were Google Earth images and a recent drone image for one part of the study area. The amount and accuracy of detected disturbances could have been increased if high resolution LiDAR (Light Detection And Ranging) images were available. LiDAR is already an often used tool in disturbance mapping (e.g. van den Eeckhaut et al., 2007; Scheidl et al., 2008), but their cost hindered their utilization in our study. Avalanches were detected as the most frequent and spatially most distributed natural disturbance in the investigation area. For the identification of avalanche track, the spatial extent and structure of forests helped to detect possible transition and runout zones. The release areas were mainly determined via topographic criteria such as slope angle and aspect. In case of missing information regarding the extent of avalanche, the interpretation of remote sensing data only allowed a rough definition of avalanche-affected areas. Field observations showed that the area above Las Termas is directly influenced by vulcanic activity and hot steam is released at several locations. Because the conditions for avalanches are different here due to the influence of the volcano, the new category for mud avalanches was build.

Beside avalanches, landslides are a further category of mass movement processes and were subdivided in two categories. Through the analysis of remote sensing data, two areas were detected as possible landslide areas. The verification in the field subsequently showed that these were pits or human induced deposit areas from the construction of the new road. These places are still in use and their shape is changing. As soon as all construction work will end, these areas are planned to be stabilized (Hector Araya, Road Service, personal communication, 19.02.2015). During the fieldtrip to the study area, another type of landslides was detected. This is related to the pavement and enlargement of the road between Las Trancas and Las Termas which results in up to 6 meter steep walls in the upslope direction of the road without stabilizing vegetation. It is foreseen that these slopes are prone to collapsing during heavy rain periods. To protect these walls from landslides the angle of the walls is planned to adapt in the future and bioengineering measures are carried out (Sanjay Dektova, EPIC Project Nepal, personal

communication 18.02.2015). These landslides are only a temporal risk due to the construction of the road. Historical records indicate that landslides are major hazards on the lower flanks and valleys (Dixon et al., 1999).

For debris flows only the initiation zone and transport zone are visible on remote sensing data. In the investigation area two debris flow tracks were detected. The deposition zone of these debris flows is located in the forest and is not visible via remote sensing data. The extent of the deposition zone is based on field observations. An interaction of disturbances in the same area could only be confirmed between debris flows and avalanches in track 8 (av8). Here both disturbances have the same starting zone, but a different flow direction and runout zone. The forest structure plot in this area shows that the forest is only influenced by avalanches. In track 3 and 4, debris flows were detected as the main disturbances via remote sensing data, but the occurance of small avalanches is also possible. Besides debris flows rockfall also occur in Nevados de Chillán. Remote sensing data only allowed detecting of rockfall activity in open areas. Further disturbances in the area are forest fires which were not detectable through the interpretation of remote sensing data. The presence of charcoal in several old trees of the area points to the occurrence of forest fires. Aravena et al. (2003) report that wildfires in Chile are mostly human-set fires. Naturally induced fires by lightning and volcanic eruptions are possible, but compared to the frequency of human-induced fires quite rare. The opening of grazing land by burning of forest patches was a common practice in the study area some 100 years ago and the forests in the investigated slopes are post fire-forests (Francisco Castillo[9], personal communication, 12.02.2015). A further disturbance which is detectable with remote sensing data was the lava flow from volcanic eruptions. Here it is not possible to distinguish between the different lava flows from different event years. The disturbances with the highest damage potential in the area are volcanic eruptions. The hazard zone and impact of the Nevados de Chillán volcano on the region are already addressed in works by SERNAGEOMIN[10] (SERNAGEOMIN, 2015). Disturbances on a broader scale like earthquakes and their consequences are not considered in this thesis.

In our study area the structure of the forest is mainly influenced by avalanche and debris flow disturbances. It was possible to verify that the canopy density and tree density is lower in disturbed forests. In debris flow tracks the canopy density is higher than in avalanche tracks. Field observations confirmed these findings. The runouts of debris flow tracks are still afforested and no mature trees were killed during recent debris flows events at the investigated tracks. In avalanche-disturbed forests, several trees are broken or tilted. These trees are not present anymore in the prevailing layer and were not counted for the canopy density. This is confirmed other studies which show that the tree density of larger trees is lower in forests which are influenced by avalanches. The density of short stems can even be higher in avalanche tracks

[9] Head of the regional CONAF–office (Corporación Nacional Forestal; in English: National Forest Corporation).
[10] Servicio Nacional de Geología y Minería, in English: Chilean Autorithy of Geology and Mining.

(Bebi et al., 2009). Observations in the European Alps have shown that avalanches lead to favorable conditions for the germination of larch and spruce. In the investigated forest, stem sprout could be observed nearby the avalanche tracks. These stems often do not reach a DBH of 8 centimeters and are therefore not counted in our study design. No extended regeneration is observed in the avalanche-influenced *Nothofagus spp.* forests. Tree density in the investigation area is higher in avalanche-disturbed forests than in forests affected by debris flows. In the field, trees with several stems were observed. The fact that tree density seems to be lower in avalanche paths compared to control sites in avalanche-unaffected forests is also supported by a study with *Nothofagus pumilio* forests in Argentina (Mundo et al., 2007). For the DBH-distribution, no difference between disturbed forest and control plots could be found. Therefore, the hypothesis that avalanche-disturbed forests have smaller diameters has to be rejected for the study area. The findings of other studies that avalanche-disturbances lead to trees with smaller diameters cannot be confirmed (Bebi et al., 2009). *Nothofagus obliqua* is in disturbed as well as in control plots the most frequent tree species. The occurence of a specific tree species in the investigation area depends rather on environmental aspects and local climate than on the occurence of disturbances. *Nothofagus dombeyi* trees prefer humid locations and can be found in plots close to the river. In warm, north-exposed slopes, mainly *Nothofagus obliqua* trees exist. In the highest forest structure plot (fp19) *Nothofagus pumilio* is present, which prefer dry sites at higher altitudes (Pflanzelt et al., 2008). Avalanches and debris flows can eliminate whole forest stands. In these places the germination ages can be used to date previous destructive events (Stoffel and Corona, 2014) and it is shown that trees in avalanche and debris flow tracks are younger. The age is measured at DBH-level and is based on the assumption that all trees reach the DBH-level with the same age. Lower tree ages in avalanche-disturbed sites could also be confirmed in a study with *Nothofagus pumilio* forests in Argentina (Mundo et al., 2007). Tree heights are significantly smaller in avalanche tracks because higher trees are more susceptible to avalanche damages (Bebi et al., 2009). In all these findings, only the result that trees are smaller in avalanche tracks is significant. In our investigation area there are two debris flow-disturbed forest plots, five avalanche-disturbed forest plots and twelve control plots. Higher number of forest structure plots in each track and in other places would strengthen these results. Similar research designs and investigations should be carried out in other investigation areas to confirm our results. Out of LiDAR data, important forest parameters such as canopy height and canopy density can also be extracted (Suárez et al., 2005). The availability of this data in future could help to enlarge the quality of data.

The application of dendrogeomorphic methods made possible to reconstruct the spatial and temporal history of avalanches and debris flow events at our study area. All these events occur frequently. The comparison of the obtained results with local information, sample size and criticism of the used methods are discussed in the following section. Local stakeholders recorded that in 1995, 2000, 2005, 2006 and 2011 avalanches occured and hit the road at several tracks (Gustavo Aldea, personal communication, 25.02-8.03.2014). Except for 2006, all

avalanche years could be confirmed with dendrogeomorphic techniques. For the comparison between historic events with dendrogeomorphically detected events, information about the location of the track and the spatial extent of the runout would be extremely helpful.

Two different sampling strategies applied during two fieldtrips to the study area lead to different precision regarding the detection of former events. For the forest structure sampling strategy, in each forest structure plot usually five trees were cored with the main purpose of detecting the age structure of the forest. Besides, avalanche-affected trees were cored in the runouts of track 6 and 9 (av6 and av9) with the runout sampling strategy, where all avalanche affected trees were cored in the runout. The results show that in disturbance-affected forest plots between two and six past event years can be detected. In contrast 23 and 8 event years were detected in avalanche tracks 6 and 9 (av6 and av9), respectively. These differences in the number of detected event years are caused by different sampling strategies and sample sizes. The trees in the forest structure plots were cored perpendicular to the slope at DBH-level. Trees in avalanche track 6 and 9 (av6 and av9) were cored nearby visible scars and some cross-sections were taken. Previous events are most easily dateable through cross-sections (Stoffel and Bollschweiler, 2008). Due to the protective function of the forest only few cross-sections from dead trees were obtained. For the sample size in each forest structure plot, five increment cores from five different trees were in most cases available to detect avalanche and debris flow disturbances. In avalanche track 6 and 9 (av6 and av9), 121 and 73 cores, respectively were available for detecting disturbance events. Other studies have found that an optimal sample size of 100 disturbed trees seems to produce the most accurate results. Above this value no more events are replicated (Corona et al., 2012). The finding that the sample size influences the number of detected past events can be confirmed if we compare the amount of events in avalanche track 6 (av 6). In this track, trees with the forest structure sampling strategy (fp8) and also the runout sampling strategy (av6) were cored. Two events were detected in forest plot 8 (fp8) compared to 23 past events with the runout sampling strategy. It is expected that the avalanche years detected with the forest structure sampling strategy can also be found in the collected trees of the runout sampling strategy. This holds true for the year 1995 and 1986, as with both strategies an avalanche year was detected. To detect more avalanche events in the forest structure plots the runout sample strategy should therefore be adapted and trees with visible scars should be cored nearby the scar, as well the sample size should be at least ten trees with visible damage (Butler and Sawyer, 2008).

In avalanche track 9 (av9) avalanches are detected with the expert as well with the indices approach. Both approaches show the same avalanche years except for 2010, which is only detected with the expert approach. This shows that the criteria used to detect an avalanche or debris flow year with the expert approach are well set. The determination of these criteria can strongly influence the amount of detected avalanches. According to Stoffel and Corona (2014), at least three to five strong growth disturbances are necessary to date a disturbance. Schläppy

et al. (2013) demonstrated that both approaches lead to the same results. The results of the indices approach depend on the optimal thresholds of responding trees per sampled trees and vary according to the sample size (Butler and Sawyer, 2008). In the literature, indices threshold values between 10% and 40% are used (e.g. Dubé et al., 2004; Reardon et al., 2008). In this work the Index value was set to 10%. Corona et al. (2012) illustrated that flexible thresholds would provide more reliable results. In our study the threshold for minimum number of responding trees is set to three trees. These values range between two and ten trees in the literature (Stoffel et al., 2013). A combination of geomorphic and climatic effects leads to late event responses (Strunk 1997). In short successive avalanche years it is not possible to exclude that an avalanche year is caused by late event responses. To prevent that late responses are taken for an avalanche year, the detection of past events should not be based only on a single indicator (Stoffel and Corona, 2014). In this case beside of scars, growth releases and reductions are used to detect past events. According to Corona et al. (2012), on average 40% of the documented avalanche events are recorded with dendrogeomorphic techniques. Missing responding trees in the field and the fact that several avalanches leave no response in trees show that not all avalanches can be detected dendrogeomorphic methods. With these techniques it is also not possible to get information on wether avalanches occur several times per year. Although not all avalanche years can be detected, trees provided important information about the spatial and temporal extent of avalanches and debris flows in the investigationa area.

The combination of avalanche simulations with historic records, evidence from tree-ring data and comparison of avalanche simulations with different input parameters allows to define reliable release areas. Dendrogeomorphic information is a valuable source to define the flow direction and runout distance of avalanches. These informations are also important for the recalculation of release areas. The combination of runout distances from simulated avalanches with information from responding trees showed that the tree destruction approach produces the best results. For that the computed maximum extent of tree destruction in RAMMS is combined with the outermost responding trees in the runout. The extent of the release area and the release height were adapted untill the simulated extent of tree destruction coincide with the occurance of responding trees. The 30kPa-pressure approach requires avalanches with a small spatial extent of the release area, so that the responding trees coincide with the extent of 30kPa- pressure. In reality such small release areas are not expected to release. It is not possible to define a required impact pressure that trees respond to avalanches. Scars in trees are caused by the mechanical impact of debris and tilting of small trees is possible until the end of the runout. This investigation showed that the best agreement is reached when the spatial arrangement of responding trees coincides with the calculated tree destruction. Another study showed that runout distances are often underestimated and tree- ring data suggests larger lateral extents of the avalanche in the runout (Corona et al., 2012). Variable runout distances of different event years are simulated in avalanche track 6 and 9 (av6 and av9) with RAMMS.

Different release areas and release heights were tested and minimal differences in the input parameters were necessary to reach the specific runout extent. The differences in the input parameters are quite small. The results of the simualtions showed that it is limited possible to simulate different runouts which are nearby. No strict line of the extent of tree destruction and maximum pressure of 30kPa can be seen and individual pixels are dispersive. Dendrogeomorphic information is valuable for the definition of the flow direction and the general runout extent, but with the RAMMS simulations it is difficult to simulate the specific runout extent of different avalanche years in the same track. The definition of release areas from avalanches without additional dendrogeomorphic information is mainly based on the interpretation of the flow direction and forest extent and structure. Several avalanches are indicated by observations from local stakeholders. Information on the flow height on the road and spatial extent would significantly improve the value of such information and help to verify the accuracy of the simulations. It is suggested that these parameters should be recorded in the future in order to improve avalanche simulations. A drone flight during an avalanche episode in the Austral winter 2015 is planned to obtain more information about the spatial extent of release areas, as well as release heights. In this study the adaption of release areas for 100-year events is mainly based on the interpretation of flow directions. It is expected that in these extreme scenarios a lot of forest would be destroyed. The comparison of 10-year and 100-year events shows that 100-year events have a runout extent that is larger by 45% and 31% more avalanches reach the road and also the flow height and maximum pressure on the road is higher. This can be explained by the fact that the less frequent 100-year events have larger release areas, a higher release depth and also different friction parameters.

The comparisons of avalanche simulations with and without forest along their way show that forests indeed have an important influence on the spatial extent of runouts. According to the hypothesis it was possible to confirm that forests are able to reduce the runout zone of avalanches. Without forest, more tracks reach the road or the walking path with a higher maximum pressure and flow height. The comparisons between simulations with and without forest also include small avalanche tracks where the snow only slides to the road. If these small tracks would not be included in the comparison, the influence of forest would be even higher. There are some avalanche tracks (av6, av7 and av8) where avalanches do not cross the forests to reach the road (unforested channels). In these cases the influence of the forest is limited to the edges of the track which are afforestated. These avalanches occur frequently and for that reason no forest can regenerate between avalanche events. In avalanche track 6 and 7 (av6 and av7) the potential of additional afforestation is evaluated. In these tracks the destruction of trees and snow detrainment behind stems is currently not enough to reduce the energy of the avalanche to stop before it reaches the road. The simulations with additional afforestation are based on the assumption that additional forest has the same diameter and structure composition as the neighboring forest. It can be assumed that during the time the new forest needs to reach the same diameter as the neighboring forest, no avalanches will affect the

forest. Since these avalanches release quite frequently, additional artificial defense constructions would need to be installed in order to prevent the avalanche from releasing. Another possibility would be the plantation of trees in the avalanche track assuming that these trees would tolerate the snow pressure exerted by avalanches through leaning and bending. According to Kajimoto et al. (2004), small trees with a height of less than 5 meters can tolerate these snow pressures. This possibility takes into account that avalanches can release while trees survive the avalanche by leaning and bending. The release areas of the avalanches in this study are all below or nearby the treeline. The slope where these avalanches occur is mostly north-exposed and summers are dry and hot. Within these conditions, the growth of new afforested trees in the avalanche track would require a lot of effort (Pflanzelt et al., 2008). Simulations where the release area is also afforested, a release of the avalanche is still possible. This is a restriction of the avalanche simulations with the new RAMMS module is shown. In reality in afforested areas no avalanche should release. For the management in broadleaved forests, a crown coverage > 50% and absence of gap length > 50 meter (slope angle steeper than 35°) is necessary so that avalanches do not release in forest areas (Frehner et al., 2005). For really small (<5000m^3) and snow slides to the road, RAMMS simulations overestimate the runout distance. Investigations showed that snow temperature and snow density also have an influence on the runout distance of small and medium sized avalanches. These processes should also be incorporated in the model for the future (Vera Valero et al., 2012).

Climate scenarios in the investigated region for the year 2100 foreseen an increase of the temperature between two and over five degrees. For the precipitation, a reduction between 25 and 90% is expected (CONAMA, 2006). The scenarios lead to the assumption that in the future the snow cover duration will be shorter. Investigation in the European Alps showed that due to global warming, fewer situations with favorable conditions for avalanche releases in the forest are expected (Teich et al., 2012). For open unforested terrains, the impact of climate change on avalanche frequency is expected to be rather small (Latenser and Schneebeli, 2002). Due to climate warming more wet snow avalanches will release in the European Alps and replace dry snow avalanches (Martin et al., 2001). It is expected that also in the investigation area in Nevados de Chillán, avalanches will still occur along the winter season. However more investigation will be necessary to verify this assumption. The effect of climate change to other mass movements show, that sediment supply for debris flow may increase. The rockfall intensity is expected to increase in the fututure and in a case study in the European Alps, a decrease of shallow landslides has been shown (Stoffel and Huggel, 2012). Future mass movement predictions are afflicted with high uncertainties.

Nevados de Chillán is undergoing high economic development (Pflanzelt et al., 2008). New tourist facilities and accommodations have been built. Based on the provided data, a hazard map should be established to channel the construction activity in areas where no hazard risks exist. Hazard maps provide information about the type of risk, intensity and probability of

occurance of a dangerous event (Heinimann et al., 1998). For the preparation of a hazard map, detailed information about the present hazard are necessary and is under progress at the moment. At the moment, housing construction activities are dispersive and houses have been built in areas endangered by avalanches and debris flows. Construction activity should be concentrated in Las Trancas and Las Termas in areas with no avalanche and debris flow danger. The information about past events and the knowledge about the extent of release areas and runout zones are an important contribution for risk management.

For areas with a lack of information, the combination of dendrochronological information with avalanche simulations contribute to a better knowledge about the spatio-temporal pattern of past avalanche events. Further studies should focus on debris flow and rockfall simulations and the ability of connecting with dendrochronogical information. Furthermore the approach should be tested in other investigation areas.

5 Conclusion

This study showed that avalanches are the most important disturbance in the research area and the structure of the forest is influenced by avalanches and debris flows. Both disturbances lead to a reduction of canopy density, tree density and tree age, but had no effect on the DBH distribution of trees. Tree height is significantly reduced in avalanche-disturbed forests, but higher in forests disturbed by debris flow compared to not disturbed forests. Increment cores provided valuable information to detect past avalanche and debris flow events. Because spatial information on avalanches was missing, the used method of combining dendrogeomorphic information with avalanche simulations leads to reliable results. The spatial extent of affected trees in specific years could be combined with specific runout distances. Because of missing snow data, possible release areas were drawn with the help of different simulations, where release area and snow depth had to be calibrated based on topographic information, forest occurence and local observations. The approach of combining dendrogeomorphic information with avalanche simulations should be tested in other areas where data about the specific runout of past avalanches are available. These suggested release areas and spatial extents of the events have to be better verified through observations of such events in future. Our findings reveal that forests in avalanche tracks reduce the impact pressure and flow height on the road and walking path, as well as lead to a smaller runout extent. Simulations without forest resulted in more tracks reaching the road or the walking path, larger spatial extent of the runout, higher maximum pressure and flow height. For 100-year events the same results can be confirmed and even all observed avalanche tracks would reach the street or walking path if there is no forest in the investigation area. Additional afforestations in selected tracks would reduce the impact pressure but do not completely stop the avalanche before it reaches the road. Higher temperatures and lower precipitation may reduce the relative importance of risks by snow avalanches compared to risks of other disturbances like debris flow and rockfall in the future.

Acknowledgments

I would like to thank Peter Bebi and Alejandro Casteller for supervision and enable me to work on this project. I am grateful to Sandra Häfelfinger and Noémie Augustin for their constructive comments on earlier versions of the thesis.

6 List of references

6.1 Bibliography

Alestalo, J. (1971). Dendrochronological interpretation of geomorphic processes. Fennia 105:1–139.

Aravena, J.C., Le Quesne, C., Jiménez, H., Lara, A., and Armesto, J.J. (2003). Fire history in central Chile: Tree-ring evidence and modern records. Fire and climatic change in temperate ecosystems of the Western Americas, Springer: 343-356.

Arbellay, E., Stoffel, M., and Bollschweiler, M. (2010). Wood anatomical analysis of Alnus incana and Betula pendula injured by a debris-flow event. Tree Physiology: tpq065.

Arbellay, E., Stoffel, M., and Decaulne, A. (2013). Dating of snow avalanches by means of wound-induced vessel anomalies in sub-arctic Betula pubescens. Boreas 42(3): 568-574.

Bartelt, P. and V. Stöckli (2001). The influence of tree and branch fracture, overturning and debris entrainment on snow avalanche flow. Annals of Glaciology 32(1): 209-216.

Bartelt, P., Bühler, Y., Christen, M., Deubelbeiss, Y., Salz, M., Schneider, M., Schumacher, L., (2013) . User Manual v1.5 Avalanche. Davos WSL Institute for Snow and Avalanche Research SLF 110p.

Bebi, P., Kienast, F., and Schönenberger, W. (2001). Assessing structures in mountain forests as a basis for investigating the forests' dynamics and protective function. Forest Ecology and Management 145(1): 3-14.

Bebi, P., Kulakowski, D., and Rixen, C. (2009). Snow avalanche disturbances in forest ecosystems—State of research and implications for management. Forest Ecology and Management 257(9): 1883-1892.

Bollschweiler, M., Stoffel, M., Ehmisch, M., and Monbaron, M. (2007). Reconstructing spatio-temporal patterns of debris-flow activity using dendrogeomorphological methods. Geomorphology 87(4): 337-351.

Bollschweiler, M., Stoffel, M., and Schneuwly, D.M. (2008). Dynamics in debris-flow activity on a forested cone—a case study using different dendroecological approaches. Catena 72(1): 67-78.

Bollschweiler, M. and Stoffel, M. (2010). Tree rings and debris flows: recent developments, future directions. Progress in Physical Geography.

Brang, P., Schönenberger, W., Frehner, M., Schwitter, R., Thormann, J. J., & Wasser, B. (2006). Management of protection forests in the European Alps: an overview. Forest Snow and Landscape Research, 80(1), 23-44.

Bräker O.U. 1981. Der Alterstrend bei Jahrringdichten und Jahrringbreiten von Nadelhözern und sein Ausgleich. Mitt. Forstl. Bundes-Vers.anst. Wien 142: 75–102.

Burrows, C., and Burrows, V. (1976). Procedures for the study of snow avalanche chronology using growth layers of woody plants, Institute of Arctic and Alpine Research Occasional Paper 23, University of Colorado. 212.

Butler, D. R. (1987). Teaching General Principles and Applications of Dendrogeomorphology. Journal of Geological Education 35(2): 64-70.

Butler, D. and Sawyer, C. (2008). Dendrogeomorphology and high-magnitude snow avalanches: a review and case study. Natural Hazards and Earth System Science 8(2): 303-309.

Casteller, A., Christen, M., Villalba, R., Martinez, H., Stöckli, V., Leiva, J., and Bartelt, P. (2008). Validating numerical simulations of snow avalanches using dendrochronology: the Cerro Ventana event in Northern Patagonia, Argentina. Natural Hazards and Earth System Science 8(3): 433-443.

Casteller, A., Villalba, R., Araneo, D., and Stöckli, V. (2011). Reconstructing temporal patterns of snow avalanches at Lago del Desierto, southern Patagonian Andes. Cold Regions Science and Technology 67(1): 68-78.

Christen, M., Kowalski, J., and Bartelt, P. (2010). RAMMS: Numerical simulation of dense snow avalanches in three-dimensional terrain. Cold Regions Science and Technology 63(1): 1-14.

Comisión Nacional del Medio Ambiente (CONAMA) (2006). Estudio de la variabilidad climàtica en chile para el siglo XXI informe final. Figuras de Sección 5: Cambios Climáticos Regionales para fines del siglo XXI Santiago: Departamento de Geofísica Facultad de Ciencias. Físicas y Matemáticas Universidad de Chile.

Cordero, D., Casteller, A., Podvin, K., Buchholz, A., and Jiménez, M.C. (2014). Ecosystems Protecting Infrastructure and Communities (EPIC): Chile Baseline Report.

Corona, C., Saez, J.L., Stoffel, M., Bonnefoy, M., Richard, D., Astrade, L., and Berger, F. (2012). How much of the real avalanche activity can be captured with tree rings? An evaluation of classic dendrogeomorphic approaches and comparison with historical archives. Cold Regions Science and Technology 74: 31-42.

Dalgaard, P. (2008). Introductory Statistics with R, Second Edition, Springer: 108-111.

de Quervain, M., 1978. Wald und Lawinen. In: Proceedings of the IUFRO Seminar Mountain Forests and Avalanches, Davos, Switzerland, pp. 219–231.

Dixon, H.J., Murphy, M.D., Sparks, S.J., Chavez, R., Naranjo, J.A., Dunkley, P.N., Young, S.R., Gilbert, J.S., and Pringle, M.R. (1999). The geology of Nevados de Chillán volcano, Chile. Revista geológica de Chile 26(2): 227-253.

Donoso, C. (1993). Bosques templados de Chile y Argentina. Variación, estructura y dinámica. Ecología forestal. Santiago de Chile 1.

Dubé, S., Filion, L., and Hétu, B. (2004). Tree-ring reconstruction of high-magnitude snow avalanches in the northern Gaspé Peninsula, Québec, Canada. Arctic, Antarctic, and Alpine Research 36(4): 555-564.

ESRI (Environmental Systems Research Institute), 2013: ArcGIS 10.2, Redlands, California (1995–2013).

Feistl, T. (2015). Vegetation effects on avalanche dynamics. Dissertation, Technische Universität (TU), München.

Föhn, P. (1993): Lawinen - kurzfristige Gefahrenbeurteilung (Prognose). In: Naturgefahren, Forum für Wissen, WSL, 1993.

Frehner, M., Wasser, B., Schwitter, R. (2005). Nachhaltigkeit und Erfolgskontrolle im Schutzwald. Wegleitung für Pfl egemassnahmen in Wäldern mit Schutzfunktion, Vollzug Umwelt. Bundesamt für Umwelt, Wald und Landschaft, Bern, 564 p.

Freiberg, H.-M. (1984). Entwicklung von Böden und Vegetation an südchilenischen Vulkanen. Biogeographica 19: 211-222.

Friedman, J.M., Vincent, K.R., and Shafroth, P.B. (2005). Dating floodplain sediments using tree-ring response to burial. Earth Surface Processes and Landforms 30(9): 1077-1091.

Grissino-Mayer, H., Holmes, R., and Fritts, H. (1997). International tree-ring data bank program library manual. Tucson, Arizona, Laboratory of Tree-Ring Research, University of Arizona.

Heinimann, H. R., Hollenstein, K., Kienholz, H., Krummenacher, B., Mani, P., (1998). Methoden zur Analyse und Bewertung von Naturgefahren. Unwelt-Materialien Nr. 85. Naturgefahren. Ed. Bundesamt für Umwelt, Wald un dLAndswchaft (BUWAL), Bern, 248p.

Holmes, RL. COFECHA – Computer-assisted quality control in tree-ring dating and measurement, Version 6.06 (1983) Tree Ring Bull 43: 69-78.

Hupp, C.R., Osterkamp, W., and Thornton, J.L. (1987). Dendrogeomorphic evidence and dating of recent debris flows on Mount Shasta, northern California.

Jakob, M., Hungr, O., and Jakob, D.M. (2005). Debris-flow hazards and related phenomena, Springer.

Kajimoto, T., Daimaru, H., Okamoto, T., Otani, T., and Onodera, H. (2004). Effects of snow avalanche disturbance on regeneration of subalpine Abies mariesii forest, northern Japan. Arctic, Antarctic, and Alpine Research 36(4): 436-445.

Keller M. (Red), 2010: «Schweizerisches Landesforstinventar – Anleitung für die Feldaufnahmen der Erhebung 2010», Eidg. Forschungsanstalt WSL., Birmensdorf,1–213.

Kulakowski, D., and Veblen, T.T. (2002). Effects of fire and spruce beetle outbreak legacies on the disturbance regime of a subalpine forest in Colorado. Journal of Biogeography 30(9): 1445-1456.

Laternser, M. and Schneebeli, M. (2002). Temporal trend and spatial distribution of avalanche activity during the last 50 years in Switzerland. Natural Hazards 27(3): 201-230.

Leiva, J. C., Martinez, H., Casteller, A., Novello, V., Bruce, R.H., Corvalan, E., Videla, V. H., Montepeluso, M. S.: Sistema de Control y Manejo de Vialidad Invernal de la Ruta Nacional 7, Etapa I 2006/7, Tercer Trimestre, Expediente 11334/05 DNV, Mendoza, 26 pp., 2007.

Luebert, F. and Pliscoff, P. (2006). Sinopsis bioclimática y vegetacional de Chile, Editorial Universitaria.

Lundström, T., Heiz, U., Stoffel, M., and Stöckli, V. (2007). Fresh-wood bending: linking the mechanical and growth properties of a Norway spruce stem. Tree physiology 27(9): 1229-1241.

Lundström, T., Stoffel, M., and Stöckli, V. (2008). Fresh-stem bending of silver fir and Norway spruce. Tree physiology 28(3): 355-366.

Maggioni, M. and Gruber, U. (2003). The influence of topographic parameters on avalanche release dimension and frequency. Cold Regions Science and Technology 37(3): 407-419.

Margreth, S. 2008. Protect: Beurteilung der Wirkung von Schutzmassnahmen gegen Naturgefahren . Arbeitsanleitung Lawinen. WSL Institute for Snow and Avalanche Research, SLF Davos.

Martin, E., Giraud, G., Lejeune, Y., and Boudart, G. (2001). Impact of a climate change on avalanche hazard. Annals of Glaciology 32(1): 163-167.

Mundo, I.A., Barrera, M.D., and Roig, F.A. (2007). Testing the utility of Nothofagus pumilio for dating a snow avalanche in Tierra del Fuego, Argentina. Dendrochronologia 25(1): 19-28.

Munter, W. (1999). 3x3 Lawinen: Entscheiden in kritischen Situationen.
Agentur Pohl and Schellhamer, Garmisch-Partenkirchen. ISBN 3-00-002060-8.

Olschewski, R., Bebi, P., Teich, M., Hayek, U.W., and Grêt-Regamey, A. (2012). Avalanche protection by forests—A choice experiment in the Swiss Alps. Forest policy and Economics 17: 19-24.

Pfanzelt, S., Grau, J., and Rodríguez, R. (2008). A VEGETATION MAP OF NEVADOS DE CHILLAN VOLCANIC COMPLEX, BIO-BIO REGION, CHILE CARTOGRAFIA DE VEGETACION DEL COMPLEJO VOLCANICO NEVADOS DE CHILLAN, REGION DEL BIO-BIO, CHILE. Gayana Bot 65(2): 209-219.

Potter, N. (1969). Tree-ring dating of snow avalanche tracks and the geomorphic activity of avalanches, northern Absaroka Mountains, Wyoming. Geological Society of America Special Papers 123: 141-166.

R Development Core Team. R: A language and environment for statistical computing, Version 0.98.507 (2009-2013) Vienna, Austria: R Foundation for Statistical Computing.

Reardon, B., Pederson, G., Caruso, C., and Fagre, D. (2008). Spatial reconstructions and comparisons of historic snow avalanche frequency and extent using tree rings in Glacier National Park, Montana, USA. Arctic, Antarctic, and Alpine Research 40(1): 148-160.

RINNTECH. TSAP-Win, Version 4.64 (2002-2009): RINNTECH Heidelberg.

Rubner, K. (1910). Das Hungern des Cambiums und das Aussetzen der Jahrringe, Ludwig-Maximilians Universität München, 19p.

Salm, B. (1982). Lawinenkunde für den Praktiker: eine allgemeinverständliche, auf wissenschaftlicher Basis beruhende Einführung für Tourenfahrer, Tourenleiter, Verantwortliche von Sicherheitsdiensten und allgemein Interessierte, Verlag Schweizer Alpen-Club.

Scheidl, C., Rickenmann, D., and Chiari, M. (2008). The use of airborne LiDAR data for the analysis of debris flow events in Switzerland. Natural Hazards and Earth System Science 8(5): 1113-1127.

Schweingruber, F. H.: Dendroökologische Holzanatomie. Paul Haupt, Bern, Stuttgart, Wien, 472 pp., 2001.

Shigo, A. L. (1984). Compartmentalization: a conceptual framework for understanding how trees grow and defend themselves. Annual review of phytopathology 22(1): 189-214.

Shroder, J. F. (1978). Dendrogeomorphological analysis of mass movement on Table Cliffs Plateau, Utah. Quaternary Research 9(2): 168-185.

Stoffel, M. (2006). A review of studies dealing with tree rings and rockfall activity: the role of dendrogeomorphology in natural hazard research. Natural Hazards 39(1): 51-70.

Stoffel, M., Bollschweiler, M., and Hassler, G.R. (2006). Differentiating past events on a cone influenced by debris-flow and snow avalanche activity–a dendrogeomorphological approach. Earth Surface Processes and Landforms 31(11): 1424-1437.

Stoffel, M. and Bollschweiler, M. (2008). Tree-ring analysis in natural hazards research? an overview. Natural Hazards and Earth System Science 8(2): 187-202.

Stoffel, M. and Huggel, C. (2012). "Effects of climate change on mass movements in mountain environments." Progress in Physical Geography 36(3): 421-439.

Stoffel, M., Butler, D.R., and Corona, C. (2013). Mass movements and tree rings: A guide to dendrogeomorphic field sampling and dating. Geomorphology 200: 106-120.

Stoffel, M. and Corona, C. (2014). Dendroecological dating of geomorphic disturbance in trees. Tree-ring research 70(1): 3-20.

Strunk, H. (1997). Dating of geomorphological processes using dendrogeomorphological methods. Catena 31(1): 137-151.

Suárez, J.C., Ontiveros, C., Smith, S., and Snape, S. (2005). Use of airborne LiDAR and aerial photography in the estimation of individual tree heights in forestry. Computers & Geosciences 31(2): 253-262.

Teich, M., Bartelt, P., Grêt-Regamey, A., and Bebi, P. (2012). Snow avalanches in forested terrain: Influence of forest parameters, topography, and avalanche characteristics on runout distance. Arctic, Antarctic, and Alpine Research 44(4): 509-519.

Tiri, R. (2009). Interaktionen zwischen verschiedenen Baumeigenschaften und Lawinen. Master thesis, unpublished.

Van Den Eeckhaut, M., Poesen, J., Verstraeten, G., Vanacker, V., Nyssen, J., Moeyersons, J., Van Beek, L., and Vandekerckhove, L. (2007). Use of LIDAR-derived images for mapping old landslides under forest. Earth Surface Processes and Landforms 32(5): 754-769.

Veblen, T.T., Hadley, K.S., Nel, E.M., Kitzberger, T., Reid, M., and Villalba, R. (1994). Disturbance regime and disturbance interactions in a Rocky Mountain subalpine forest. Journal of Ecology: 125-135.

Vera Valero, C., Feistl, T., Steinkogler, W., Buser, O., and Bartelt, P. (2012). Thermal temperature in avalanche flow. Proceedings, 2012 International Snow Science Workshop.

Westing, A. H. (1965). Formation and function of compression wood in gymnosperms. The Botanical Review 31(3): 381-480.

Winter, L.E., Brubaker, L.B., Franklin, J.F., Miller, E.A., and DeWitt, D.Q. (2002). Initiation of an old-growth Douglas-fir stand in the Pacific Northwest: a reconstruction from tree-ring records. Canadian Journal of Forest Research 32(6): 1039-1056.

6.2 Online sources

Colorado Geological Survey (2015) Access 3.07.2015, http://coloradogeologicalsurvey.org/geologic-hazards/rockfall/definition/

UNESCO (2011). Access 24.03.2015, http://www.unesco.org/new/en/natural-sciences/environment/ecological-sciences/biosphere-reserves/latin-america-and-the-caribbean/chile/corredor-biologico-nevados-de-chillan-laguna-del-laja/

SERNAGEOMIN (2015). Access 17.09.2015, http://www.sernageomin.cl/